Vol. 50 • No. 1

January 2007

Microwave Journal

Radar/Antennas

Use of Military Antenna Technology in Modern Communications

Design of a Non-symmetric Ground λ/4 Slot Antenna

Integrated Short Backfire Antennas

horizon house®
Founded in 1958

w.mwjournal.com

Microwave Journal

JANUARY 2007 VOL. 50 • NO. 1

FEATURES

NOTE FROM THE PUBLISHER

15 East Meets West

Carl Sheffres, Publisher, Microwave Journal

A look at what *Microwave Journal* has planned for 2007, including this year's MTT-S IMS event in Honolulu, HI

COVER FEATURE

24 The Use of Broadband Military Antenna Technology in Modern Communications Systems

Chris Walker, European Antennas Ltd.

Use of military antenna technology for design variations applied to traditional spiral and bi-conical broadband antenna structures for commercial communications systems

TECHNICAL FEATURES

66 Memory Effect Minimization and Wide Instantaneous Bandwidth Operation of a Base Station Power Amplifier

Jeonghyeon Cha, Ildu Kim, Sungchul Hong and Bumman Kim, Pohang University of Science and Technology; Jong Sung Lee and Han Seok Kim, Samsung Electronics Co. Ltd.

Introduction to a matching topology used to minimize the memory effect and extend the instantaneous bandwidth in a next generation base station power amplifier

86 Dual-band Assembly of Integrated Short Backfire Antennas

H.D. Hristov and R. Feick, Universidad Técnica Federico Santa María; R.J. Urumov and G.S. Kirov, Technical University of Varna

Description of a dual-frequency assembly of two short backfire antennas, including one large for low frequencies and one small for high frequencies

110 Broadband Design of a Small Non-symmetric Ground λ/4 Open Slot Antenna

Wen-Shan Chen and Kuang-Yuan Ku, Southern Taiwan University of Technology

Investigation of the broadband design of a small size, λ/4 open slot antenna with a bandwidth of 94 percent and an overall size of 35 × 30 × 0.8 mm

122 The Requirements and Procedures for Testing WiMAX Equipment

Jan E. Prochnow, Rohde & Schwarz

Explanation of the three techniques used to achieve high data throughput in mobile radio communication systems

50 Years of Publishing Excellence

Microwave Journal (USPS 396-250) (ISSN 0192-6225) is published monthly by Horizon House Publications Inc., 685 Canton St., Norwood, MA 02062. Periodicals postage paid at Norwood, MA 02062 and additional mailing offices.

POSTMASTER: Send address corrections to *Microwave Journal*, PO Box 3256, Northbrook, IL 60065-3256 or e-mail mwj@omeda.com. Subscription information: (847) 291-5216. This journal is issued without charge upon written request to qualified persons working in that part of the electronics industry, including governmental and university installation, that deal with VHF through light frequencies. Other subscriptions are: domestic, $120.00 per year, two-year subscriptions, $185.00; foreign, $200.00 per year, two-year subscriptions, $370.00; back issues (if available) and single copies, $10.00 domestic and $20.00 foreign. Claims for missing issues must be filed within 90 days of date of issue for complimentary replacement.

Microwave Journal

FEATURES

TECHNICAL FEATURES

134 A Triple-band Polygonal Slot Antenna for WiMAX Applications

Wen-Shan Chen and Bao-Hung Kao, Southern Taiwan University of Technology

Experimental study of a printed polygonal slot antenna fed by a 50 Ω microstrip line with two narrow strips for three-band operation

144 A 60 GHz Millimeter-wave CMOS RFIC-on-chip Dipole Antenna

H.R. Chuang, S.W. Kuo, C.C. Lin and L.C. Kuo, National Cheng Kung University

Discussion of the design, fabrication and on-wafer measurement of a 60 GHz millimeter-wave CMOS RFIC-on-chip dipole antenna with an integrated microstrip via-hole balun

TECHNICAL NOTE

154 A Low Profile Multi-band U-shaped Aperture-coupled Microstrip Antenna with a Coil

Yong-Woong Jang, Keukdong College; Hyun-Chul Go, AMC Centurion Korea Co. Ltd.

Description of an alternative design technique that combines an L-shaped probe-fed, U-slot patch antenna with a coil for use in GSM, PCS, IMT-2000 and WLL applications

PRODUCT FEATURES

160 6 × 6 mm Quad-band RF Transmit Modules for High Efficiency EDGE Operation

TriQuint Semiconductor Inc.

Introduction to a multi-mode GSM/GPRS/EDGE quad-band radio frequency transmit module for next generation mobile handsets

172 Perfectly Calibrated Ports for EM Analysis

Sonnet Software Inc.

Port calibration designed to enhance high frequency design methodology in the field of radio frequency integrated circuit design

178 High Frequency Circuit Material for Base Station Applications

Rogers Corp., Advanced Circuit Materials Division

Development of a replacement product for PTFE woven glass circuit material providing superior mechanical and thermal properties for base station antenna applications

DEPARTMENTS

16 . . .Ask Harlan
19 . . .Coming Events
20 . . .Workshops & Courses
37 . . .Defense News
41 . . .International Report
45 . . .Commercial Market
50 . . .Around the Circuit
180 . . .Catalog Update
184 . . .New Products
190 . . .Microwave Metrics
192 . . .The Book End
194 . . .Ad Index
198 . . .Sales Reps

Our November cover included the image of a MEMS chip, which was manufactured by WiSpry. We apologize for not giving them proper attribution for the image.

THIS MONTH ON THE WEB

Visit www.mwjournal.com for the latest industry news and exclusive on-line articles

IEEE Radio and Wireless Symposium
January 7–12, 2007
Long Beach, CA

A complete wrap-up of all news, information and product announcements at this year's IEEE Radio and Wireless Symposium, including a detailed look at the new products on display at RWS 2007.

JTRS/SINCGARS Ultra-broadband (30 to 2000 MHz) Airborne Blade Antenna for Sub-sonic Aircraft and Helicopters

By Joseph R. Jahoda
Chief Technology Officer
Astron Wireless Inc.

A white paper introducing "HESA™ Technology," a unique and proprietary set of advanced techniques providing high efficiency, sensitivity and accuracy in Astron's miniaturized and standard DF antenna systems.

RF Component Industry Review: July–September 2006

Strategy Analytics reports that almost 60 percent of leading suppliers of RF components reported significant profits in Q3. The majority of RF component suppliers reported strong profits in the third quarter of 2006, due in large part to the continued strength in demand for cellphone components.

STRATEGYANALYTICS
INSIGHTS FOR SUCCESS

EAST MEETS WEST

As I write this, I've just returned from the Asia Pacific Microwave Conference (APMC) in Yokohama, Japan. Having never been to Japan, this was a new experience for me. While I enjoyed the cultural differences that Japan offers, I was also struck by the similarities between East and West.

The big news in Japan all week wasn't about the national economy, education or politics. It was all about Dice-K. As in Daisuke Matsuzaka, the 26 year-old pitching phenom of the Seibu Lions. This was the final week of negotiations with the Boston Red Sox, and all talk revolved around the potential deal. When I mentioned to anyone that I was from Boston, they would immediately exclaim, "Matsuzaka!" My Japanese representative, Mr. Ishii, could recite the Sox lineup as well as any diehard fan. When the deal was culminated at the end of the week, we all celebrated the victory. It seems that when it comes to baseball, it is indeed a small world.

The theme of this year's MTT-S IMS event is "Microwaves Across the Pacific," and like the sport of baseball, our industry has truly become global. Microwave Week is certainly an international event, with attendees and exhibitors representing nearly 30 countries last year. This year, more than 30 percent of the submitted papers came from Asia, and all indications are that we will have the largest Asian attendance in the history of the conference. There has been a good deal of promotion targeted to the Asia Pacific engineering community, including at the recent APMC, which had representatives from both *Microwave Journal* and MTT-S.

There has been much debate about the show being in Honolulu. However, there's no debating the fact that the MTT-S IMS is the premier industry event of the year. The technical conference is second to none, and offers the opportunity to become current on all of the latest technologies being advanced worldwide. The exhibition is the largest of its kind, bringing together the latest products available, many of which will be debuted at the show. And the event remains the optimum networking environment, where old friendships are renewed and new relationships are established.

I traveled far to attend the APMC, and it was well worth the trip. I saw some old friends and I made some new ones. We talked about business, baseball and many other things. I expect that we'll continue those conversations in June in Honolulu. I hope that you'll join us.

Best wishes for the New Year.

Carl Sheffres
Publisher

PS: *Watch for the newly redesigned Microwave FLASH email newsletter, which now features weekly updates on the IMS conference and exhibition, as well as travel and entertainment information. You can subscribe to the newsletter at www.mwjournal.com.*

Ask Harlan

How it works: Harlan has selected one question from his "Ask Harlan" column to be featured in the magazine. Please visit www.mwjournal.com/askharlan to provide an answer to this month's featured question (see below). Harlan will be monitoring the responses and will ultimately choose the best answer to the question. Although all of the responses to the featured question will be posted on our web site, we plan to publish the winning answer in the March issue. All responses must be submitted by **February 7, 2007**, to be eligible for the participation of the January question.

The winning response will win a free book from Artech House, along with an "I Asked Harlan!" t-shirt. In addition, everyone who submits a legitimate response will be sent an "I Asked Harlan!" t-shirt.

November Question and Winning Response

The November question was submitted by Subhash Janakiraman from Icon Systems Inc.:

Dear Harlan,

I am trying to test an RF communication link inside an enclosed chamber which is free from RF leakage. I want to emulate a test in the same set up in such a way that the receiver and transmitter are 30 metres apart. I thought calculating the signal strength at this distance and attenuating the transmit power accordingly will justify my testing. Is that true? Am I justified to introduce that attenuation to account for the distance despite the fact that there is no free space loss? Can you point me to a link to calculate the attenuation in the transmit power due to varying distances?

The winning response to the November question is from Melanie Barclay of Scientific Research Corp.:

If I name these variables as follows: Received Power = Pr Transmitter Power = Pt Transmitting Antenna Gain = Gta Spreading Loss = Ls Atmospheric Loss = La Receiving Antenna Gain = Gra then the following equation is true: Pr = Pt + Gta – Ls – La + Gra. Notice that there are two losses in the equation above: Spreading Loss and Atmospheric Loss. Spreading Loss is defined as being related to distance, as: Ls(dB) = 32.4 + 20log(base 10)(distance in km) + 20 log(base 10)(frequency in MHz). It appears that you will want to consider this in determining the total losses related to distance. That leaves atmospheric loss (attenuation). The best way to determine the atmospheric loss is to refer to a chart, rather than an equation. I referred to page 14 of a book from Artech House by David Adamy called *EW 101: A First Course in Electronic Warfare*. Figure 2.3 in this book is a graph of atmospheric attenuation (in dB) per kilometer of transmission path. This graph has frequency (GHz) on the X-axis, and Atmospheric Loss (dB per km) on the Y-axis. You will have to look at the graph and find where the line is at the frequency you are transmitting.

Harlan's response:

I don't think the measurement will be valid since the antennas will be too close. You can add the estimated loss due to range, but the loss due to the distorted antenna patterns will have an unknown effect. There is a good discussion of link propagation along with the various factors that affect it in *Introduction to RF Propagation*, J. Seybold, Wiley, 2005, ISBN#0-471-65596-1.

This Month's Question of the Month

(answer on-line at www.mwjournal.com/askharlan)

John McFarland from SNC has submitted this month's question:

Dear Harlan,

Can you explain why the polarization sense of a circularly polarized plane wave changes when it bounces off a reflecting surface? For instance, Right Hand Circular Polarization (RHCP) turns into Left Hand Circular Polarization (LHCP) when undergoing a single bounce off a reflector. The sense of the polarization is defined by the sense (CW/CCW) of rotation of the composite wave (vector sum of the H and V waves) as viewed in the direction of its propagation. When the incident wave undergoes two bounces—say off a dihedral corner reflector—it changes back to the originally incident sense, e.g., RHCP undergoing two bounces will propagate back to the transmitter as RHCP. I know this is what happens from experience, but I have never been able to explain why.

If your response is selected as the winner,
you'll receive a free book of your choice from Artech House.
Visit the Artech House on-line bookstore at www.artechhouse.com
for details on hundreds of professional-level books in microwave engineering and related areas
(maximum prize retail value $150).

STAFF

Publisher: Carl Sheffres
Associate Publisher: Edward Johnson
Editor: Harlan Howe, Jr.
Managing Editor: Keith W. Moore
Technical Editor: Frank M. Bashore
Associate Technical Editor: Dan Massé
Staff Editor: Jennifer DiMarco
Editorial Assistant: Barbara Walsh
Consulting Editor: Howard I. Ellowitz
Consulting Editor: Peter Staecker
Consulting Editor: Dan Swanson
Web Editor: Stephen Heiser
Traffic Manager: Edward Kiessling
Traffic Administrator: Ken Hernandez
Director of Production & Distribution: Robert Bass
Multimedia Designer: Eli Conner
DTP Coordinator: Janet A. MacDonald

EUROPE

Deputy Publisher: Michel Zoghob
European Editor: Richard Mumford
Office Manager: Eugenie Hardy

CORPORATE STAFF

Chairman: William Bazzy
CEO: William M. Bazzy
President: Ivar Bazzy
Vice President: Jared Bazzy

Executive Editorial Office:

685 Canton Street, Norwood, MA 02062
Tel: (781) 769-9750
FAX: (781) 769-5037
e-mail: mwj@mwjournal.com

European Editorial Office:

46 Gillingham Street, London SW1V 1HH, England
Tel: Editorial: +44 207 596 8730 Sales: +44 207 596 8740
FAX: +44 207 596 8749

www.mwjournal.com

Printed in the USA

CALL FOR NOMINATIONS

IEEE Joseph F. Keithley Award in Instrumentation and Measurement
by January 31, 2007
www.ieee.org/portal/pages/about/awards/sums/keithley.html

CALL FOR PAPERS

European Microwave Week
by February 25, 2007

FEBRUARY

International Solid-state Circuits Conference (ISSCC 2007)
February 11–15, 2007 • San Francisco, CA
www.isscc.org/isscc/

3GSM World Congress
February 12–15, 2007 • Barcelona, Spain
www.3gsmworldcongress.com

Satellite 2007
February 19–22, 2007 • Washington, DC
www.satellite2007.com

MARCH

Military Technologies Conference
March 27–28, 2007 • Boston, MA
http://mtc07.events.pennnet.com

CTIA Wireless 2007
March 27–29, 2007 • Orlando, FL
www.ctiawireless.com

RF & Hyper Europe 2007
March 27–29, 2007 • Paris, France
www.rfhyper.com

International Wireless Communications Expo (IWCE 2007)
March 28–30, 2007 • Las Vegas, NV
www.iwceexpo.com

APRIL

IEEE Radar Conference 2007
April 17–20, 2007 • Waltham, MA
www.radar2007.org

JUNE

IEEE MTT-S International Microwave Symposium and Exhibition
June 3–8, 2007 • Honolulu, HI
www.ims2007.org

IEEE Radio Frequency Integrated Circuits Symposium (RFIC 2007)
June 3–8, 2007 • Honolulu, HI
www.rfic2007.org

69th ARFTG Conference
June 7–8, 2007 • Honolulu, HI
www.arftg.org

WCA 2007
June 11–14, 2007 • Washington, DC
www.wcai.com/events.htm

JULY

IEEE EMC Symposium
July 8–13, 2007 • Honolulu, HI
www.emc2007.org

OCTOBER

European Microwave Week (EuMW 2007)
October 8–12, 2007
Munich, Germany
www.eumweek.com

Association of Old Crows (AOC)
October 28–31, 2007
Orlando, FL
www.crows.org

NOVEMBER

Antenna Measurement Techniques Association (AMTA)
November 4–9, 2007 • St. Louis, MO
www.amta.org

DECEMBER

Asia-Pacific Microwave Conference (APMC)
December 11–14, 2007 • Bangkok, Thailand
www.apmc07.com

WORKSHOPS & COURSES

PRACTICAL RF AND MICROWAVE DESIGN

■ **Topics:** This intensive, five-day course provides acceleration through the RF design learning curve by presenting a comprehensive introduction to RF and microwave design theory, techniques and measurements. Although the course includes necessary theoretical aspects, great emphasis is placed upon the practicalities of RF engineering. For more information, visit www.conted.ox.ac.uk.
■ **Site:** Summertown, Oxford, UK
■ **Dates:** January 22–26, 2007
■ **Contact:** University of Oxford Continuing Education, +44 (0) 1865 286958 or e-mail: anthony.santiago@conted.ox.ac.uk.

MAKING ACCURATE LOW LEVEL ELECTRICAL MEASUREMENTS

■ **Topics:** This course provides users with a detailed understanding of how to make accurate low level electrical measurements. Users will learn what constitutes a low level measurement, the limitations of these measurements, sources of measurement error, and techniques to eliminate these errors. Additional topics include selecting the proper product for a desired measurement and understanding the basics of how to communicate with an instrument from a PC.
■ **Site:** Irvine, CA
■ **Dates:** February 13–14, 2007
■ **Contact:** For more information, visit www.keithley.com.

PHASED ARRAY ANTENNAS AND ADAPTIVE TECHNIQUES

■ **Topics:** This five-day course presents an in-depth look at the hardware and software that comprise adaptive phased array systems. The objective is to present the student with the diverse spectrum of technologies and algorithms available and to show how they fit together into a design. The principles of phased array antennas are covered first, followed by the details of the underlying hardware. For more information, visit www.pe.gatech.edu.
■ **Site:** Denver, CO
■ **Dates:** February 13–16, 2007
■ **Contact:** Georgia Institute of Technology, Professional Education, PO Box 93686, Atlanta, GA 30377 (404) 385-3500.

PRACTICAL ANTENNA DESIGN

■ **Topics:** The course covers the important and timely issues involving modern antenna design and theory. Developed specifically for engineers and designers who work with radar and radio communications, this workshop will give participants the understanding of antenna theory and techniques, the skills to analyze, design and measure various antennas, and the knowledge of antenna measurements. For more information, visit www.conted.ox.ac.uk.
■ **Site:** Summertown, Oxford, UK
■ **Dates:** February 2007
■ **Contact:** University of Oxford Continuing Education, +44 (0) 1865 286958 or e-mail: anthony.santiago@conted.ox.ac.uk.

THE ENTREPRENEURIAL ENGINEER

■ **Topics:** This short course is an efficient and memorable introduction to the personal, interpersonal, business and organizational skills necessary to help engineers of applied science and mathematics perform at high levels in today's increasingly opportunistic organizations and enterprises. For more information, visit http://online.engr.uiuc.edu/shortcourses/tee/index.html.
■ **Site:** Archived on-line course.
■ **Dates:** Archived on-line for anytime viewing.
■ **Contact:** University of Illinois at Urbana-Champaign, 117 Transportation Bldg., 104 S. Mathews Avenue, Urbana, IL 61801 (217) 333-0897 or e-mail: deg@uiuc.edu.

PCB DESIGN TECHNIQUES FOR EMC AND SIGNAL INTEGRITY

■ **Topics:** This course will assist practicing engineers who are responsible for PCB designs and system-level products. Disciplines include PCB layout, logic design, regulatory compliance and EMC. For more information, visit http://epdwww.engr.wisc.edu.
■ **Site:** For location information, please visit url.
■ **Dates:** For date information, please visit url.
■ **Contact:** University of Wisconsin Madison, Department of Engineering Professional Development, 432 North Lake Street, Madison, WI 53706 (800) 462-0876.

THE USE OF BROADBAND MILITARY ANTENNA TECHNOLOGY IN MODERN COMMUNICATIONS SYSTEMS

For many years, military applications have required broad bandwidth communication links, incorporating antennas that have a similar broadband capability. Often the antennas must operate over a frequency range of several octaves. Consequently, antenna structures that have multi-octave capability have been designed and manufactured and these techniques are now proving very useful in designing antenna products for modern commercial communications systems. This article considers the evolution of commercial communications systems, particularly the increasing demand for new frequency bands before focussing on two types of antenna—spiral and bi-conical—that merit particular consideration.

MODERN COMMUNICATIONS REQUIREMENTS

Many communication systems are required to provide coverage in the 900 MHz frequency range. As networks have evolved, additional bands have been utilised at 1700 to 2200 MHz for DCS, PCS and UMTS capabilities. In addition to these frequencies, coverage is often required for TETRA (approximately 400 MHz), wireless LAN and wireless local loop (approximately 2500, 3500 and 5500 MHz). To satisfy all of these requirements, it is necessary for the antennas to provide effective coverage from 400 MHz to 6 GHz.

In some applications, this may be accomplished by a series of individual antennas each assigned to a specific portion of the band. To avoid many antenna types being required and for a more discreet appearance, however, it is often preferable to provide coverage over the entire frequency range from a single antenna. Furthermore, there are additional benefits of using just one antenna. Apart from general aesthetics, it can aid in obtaining the planning authorization for the antennas siting, where avoiding a proliferation of antennas cluttering the otherwise clean lines of a new building can satisfy architectural requirements.

Antenna requirements will include a multiband capability that may be fixed or mobile access point or base station, as most modern equipment is designed to be multi-functional. This multi-functionality is part of the appeal of many modern systems. The professional user will need the equipment to work without having to adjust its operating mode. The transition between operating bands is, therefore, required to be seamless for both the access point and the subscriber. If a subscriber in a given system is to be mobile, then the antenna radiation pattern will be omni-directional so that coverage is assured, regardless of the orientation of the subscriber with respect to the adjacent access points. In a fixed system, the subscriber antenna may be required to be directional, oriented towards the nearest base

CHRIS WALKER
European Antennas Ltd.
Newmarket, UK

station for optimum performance. Base stations can be deployed in a number of configurations. Sometimes an omni-directional base station is required and is placed in the centre of a coverage area. In other scenarios, a cluster of sector antennas may be deployed at a single location with each covering a sector of the area around the base station. Systems typically employ sector angles ranging from 30° to 180°. The polarisation used in systems also varies. It may either be a linear vertical, horizontal or 45° slant, or even circular, each having advantages which vary according to the system protocols and architecture. Further system benefits may be obtained through the use of additional antennas. The provision of spatial diversity, polarisation diversity, adaptive antennas, or multiple-input, multiple-output (MIMO) antenna configurations all serve to increase the statistical likelihood that a link can be maintained with acceptable signal-to-noise ratio for successful operation. The scope of this article is to consider the performance of a single antenna system, rather than looking at the further benefits that might be obtained by combining several antennas.

SPIRAL ANTENNAS

The spiral antenna has long been used in military applications for direction finding systems and for general threat detection. ***Figure 1*** shows a typical 2 to 18 GHz, cavity-backed spiral antenna and ***Figure 2*** shows an electromagnetic simulation performed on such an antenna, indicating the field strengths present on various parts of the structure. In these applications, the antennas generally have requirements for a uniform pattern shape, with respect to amplitude and phase from one antenna to another. Also, the main beam should exhibit a smooth curve without any points of inflection, which is said to be monotonic. A typical radiation pattern for such an antenna is shown in ***Figure 3***. It is generally more important in these applications to control the beam shape and match the performance of the antenna from unit to unit than to maximise the gain of the antenna. For many commercial com-

▲ *Fig. 1 A 2 to 18 GHz cavity-backed spiral antenna.*

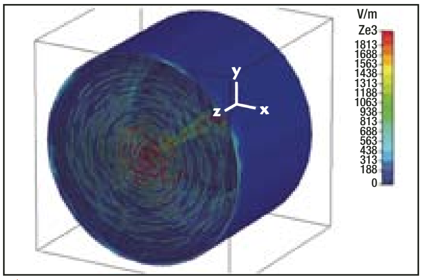

▲ *Fig. 2 Electromagnetic simulation of a cavity-backed spiral antenna.*

munication systems, it is more important to fill efficiently an area with a signal than to produce a very precise beam shape. The spiral radiating structure used in this example is very much suited to this mode of operation, but no longer needs to be used in conjunction with a cavity loaded with an absorber. Two types of antenna can then be created using this type of structure: a bi-directional structure where the spiral is allowed to radiate freely into space in both directions normal to its plane, or a higher gain, uni-directional structure, where a reflector plate is positioned close to the spiral such that the radiation in one direction is reflected and the forward gain is therefore enhanced. ***Figure 4*** shows a bi-directional spiral antenna. Note the additional proprietary features used to extend the frequency coverage. An electromagnetic simulation of a similar type of antenna is shown in ***Figure 5***. The radiation characteristics for a bi-directional spiral antenna such as this are shown in ***Figure 6***. It can be seen that when the polarisation is left-hand circular in a forward direction, it is right-hand circular in the opposite direction. Thus, in a transition region in between, it will be linear. Such a pattern

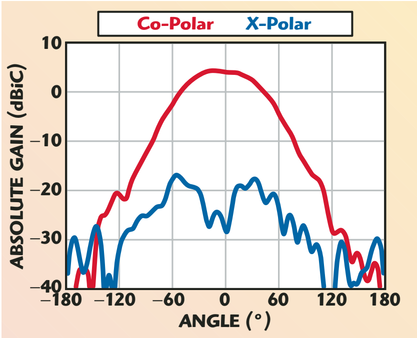

Fig. 3 Typical radiation pattern for a cavity-backed spiral antenna.

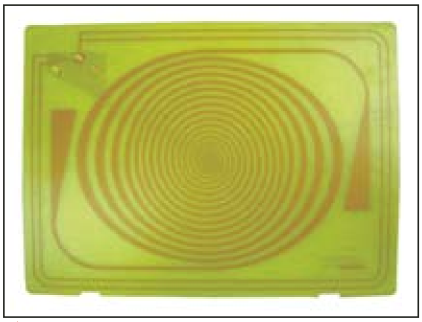

Fig. 4 A bi-directional spiral antenna.

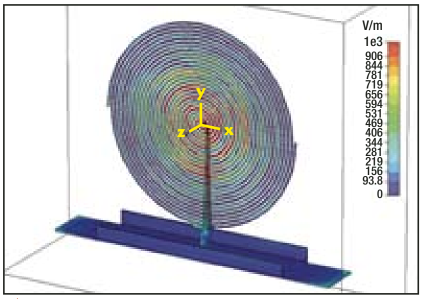

Fig. 5 Electromagnetic simulation of a bi-directional spiral antenna.

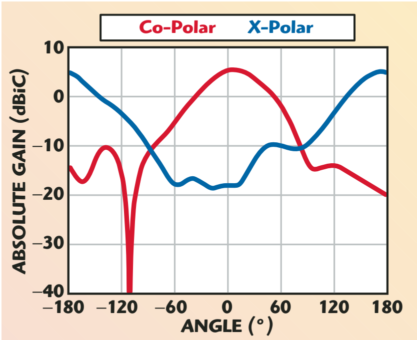

Fig. 6 Typical radiation pattern for a bi-directional spiral antenna.

is an advantage in many deployments. For example, if an antenna is to be placed in a corridor or hall, then a bi-directional antenna of this type is ideally suited. Sometimes, a more directional antenna is desired while retaining its broadband properties. This would typically be for a deployment in the corner of the area to be covered, such as a large hall or atrium. In this case, the reflector plate serves to increase the gain in the forward direction. ***Figure 7*** shows a typical radiation pattern for such a uni-directional low profile spiral antenna. Depending upon the size of spiral selected, it is possible to provide coverage across the band between 400 MHz and 6 GHz. These antennas are used in systems where all the communication bands are required to be transmitted or received by a single antenna, either when originally installed or at some time in the future.

BI-CONICAL ANTENNAS

Bi-conical antennas can be designed to operate effectively over a

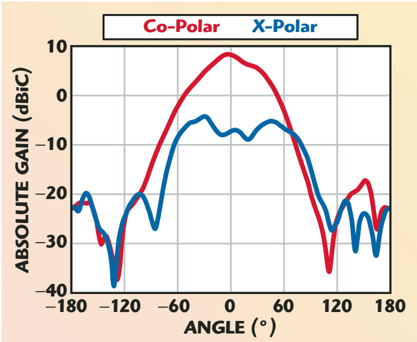

▲ *Fig. 7 Typical radiation pattern for a uni-directional spiral antenna.*

▲ *Fig. 8 A bi-conical antenna.*

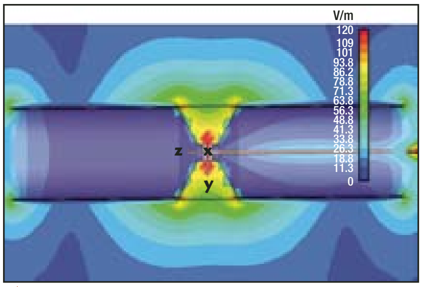

▲ *Fig. 9 Electromagnetic simulation of a bi-conical antenna.*

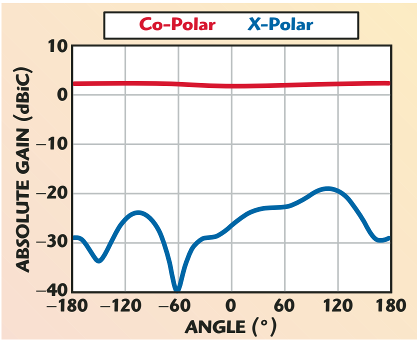

▲ *Fig. 10 Typical radiation pattern for a bi-conical antenna.*

large frequency range. These antennas produce a linearly polarised signal and exhibit extremely low azimuth ripple, meaning that the omni-directional characteristics are excellent. Depending upon the degree of input return loss degradation that can be tolerated, the effective bandwidth of such a structure is in the region of two octaves. This will depend upon the extent to which the structure has been miniaturised by the choice of transition region from a cone to a cylinder, or if an entirely conical section has been used. ***Figures 8*** and ***9*** show a bi-conical antenna and its electromagnetic simulated results, respectively. ***Figure 10*** shows its measured performance and the very low ripple in the azimuth pattern can clearly be seen. Although the high power handling capability is not always important in commercial communications systems, the small size of these structures makes them very attractive in this application. For example, a product capable of covering the whole frequency band from 800 MHz to 2.2 GHz can be packaged in a structure of 32 mm diameter by 225 mm long. It is possible to achieve wider bandwidths, but a compromise has to be made in terms of the diameter of the product. A larger diameter could extend the frequency of operation. These antenna structures retain their radiation pattern characteristic over this very wide frequency range. This makes them suitable for microcell and picocell applications where the antennas can be employed to provide a signal boost (in a railway station, for example). Antennas with this kind of radiation pattern would be the most effective for a central deployment.

CONCLUSION

There is an increasing demand for new frequency bands to be added to modern communications networks. As these new frequency bands become available for commercial use, system antennas have to be upgraded to cover these additional frequencies. If an existing antenna was not originally designed with sufficient bandwidth, it will not maintain its performance over these wider frequency ranges. However, design variations, applied to traditional spiral and bi-conical broadband antenna structures, have resulted in commercial products that are well suited to these requirements, using technology originally developed for military applications. ■

Chris Walker *received his BSc degree in theoretical physics from Cambridge University in 1982. He has worked with EEV, Litton and CPI, developing vacuum tubes for radar and communication systems. He joined European Antennas, part of Cobham Antennas Division of Cobham plc, in 1998, where he has been involved in the design and manufacture of directional flat panel antennas, base station sector antennas and omni-directional antennas within the range from 250 MHz to 40 GHz for military and commercial applications within satellite, data, WiMAX, WLAN, telemetry, security, surveillance and broadcast systems. He is presently technical director of European Antennas Ltd. with responsibility for assessment, modeling and development of antennas for future technologies.*

Northrop Grumman Expands Radar Role in Missile Testing

In the fall, Northrop Grumman-developed C-band radar for the US Navy participated in the successful test of the Ground-based Midcourse Defense (GMD) system, marking the first time a Navy Strategic Systems Program radar has been used by the US Missile Defense Agency (MDA) to optimize data collection and enhance mission success. The GMD test occurred on September 1, 2006, and involved launching a ground-based interceptor from Vandenberg Air Force Base, CA.

This test adds to Northrop Grumman's ongoing success using this extremely mobile radar, year-round, to collect data on Navy ballistic missile tests in both Pacific and Atlantic test ranges. As a trusted supplier of transportable large-dish radars, Northrop Grumman has demonstrated the ability to rapidly relocate large radar systems worldwide to remote land locations and aboard sea-based platforms on demand.

The GMD test is one such example of the company's ability to bring a radar on-line to a sea-based platform in a short time frame. Within three weeks of a request for additional assets, Northrop Grumman—under the direction of the US Navy Strategic Systems Program Office—relocated the Navy Mobile Instrumentation System (NMIS) C-band radar from Cape Canaveral, FL, to California, and installed the radar system aboard the Navy ship USNS Pathfinder. The ship was then positioned approximately 600 miles off the coast of California to track the interceptor flight.

"This disassembly, ground transport, reassembly and installation of the Northrop Grumman-developed radar aboard the USNS Pathfinder within a three week window demonstrates Northrop Grumman's ability to respond to rapid real-world situations requiring high performance discriminating radars," said Frank Moore, vice president of the Northrop Grumman Missile Defense Division. "The valuable data collected from this additional radar asset will further enhance MDA's ability to thoroughly analyze system performance and build confidence in future flight tests."

The radar successfully tracked the GMD interceptor from the point it broke the horizon, throughout separation and intercept. Data is being combined with information from other sensors to provide a thorough analysis to MDA of all aspects of the test to make adjustments to ensure future mission success.

The NMIS C-band radar is an instrumentation radar used normally for data collection and Navy missile testing, under contract to Navy SSP. The company has also developed mechanically steered radars to support major US weapons test and evaluation programs for the US Navy, where Northrop Grumman is a major provider of block upgrades.

Raytheon Achieves Satellite Communications Milestone

Raytheon Co.'s Navy Multiband Terminal (NMT) is the first advanced, next-generation satellite communications (SATCOM) system to successfully log on to and communicate with the US Government's Milstar SATCOM system, using low and medium data rate waveforms. The system will provide naval commanders and sailors with greater data capacity, as well as improved protection against enemy intercept and jamming. Raytheon has also demonstrated that its NMT is fully compatible with existing submarine and shore antennas, an important life-cycle cost-savings objective of the NMT program.

This achievement follows Raytheon's earlier success in developing the first Software Communications Architecture (SCA)-compliant SATCOM system to validate the advanced extended data rate communications waveform. This waveform provides highly protected and high speed communications with the Department of Defense's (DoD) new Advanced Extremely High Frequency satellite constellation planned for operation in 2010. Raytheon's non-proprietary, SCA implementation of these waveforms meets the DoD's vision to make them available for future developments, significantly reducing costs. "Raytheon's designers logged more than 13,000 hours onboard ships and submarines collecting data to understand what matters most to the Navy," said Jerry Powlen, vice president of Network Centric Systems Integrated Communications Systems. "These achievements demonstrate Raytheon's ability to continue to provide the Navy with the most reliable, affordable and user friendly advanced SATCOM capability."

With more than 500 Navy SATCOM systems currently fielded, Raytheon's NMT solution builds on the company's extensive experience and innovative solutions in naval communications. NMT, which replaced several existing SATCOM systems developed and maintained by Raytheon during the last 20 years, is expected to be installed in more than 300 ships, submarines and shore stations.

The Navy's communications program office, which reports to the Navy's program executive office for command, control, communications, computers and intelligence, is responsible for developing and delivering NMT capabilities to the fleet.

"Our NMT SATCOM design features over 95 percent commonality of parts," said Powlen. "For our customer, that means it can share a significant percentage of parts between ships, subs and shore stations, without additional investment and logistic costs. In fact, our total life-cycle design even reduces the number of personnel needed to operate and maintain the system, while minimizing the training needed to support it. We consider these critical features for the future."

Lockheed Martin's Compact Kinetic Energy Missile Successful in Flight Test

Lockheed Martin successfully conducted a guided test flight of its Compact Kinetic Energy Missile (CKEM) against a main battle tank recently at Eglin Air Force Base, FL. All objectives for this test were achieved. In addition to demonstrating CKEM's capability against an armored target, the test also gathered missile performance and lethality data. This flight was the last of three guided flight tests for the year. The key advantages of the CKEM system are its deployability and tremendous overmatch in lethality, which defeats all projected future armored combat vehicles. The CKEM weapon system also provides increased countermeasure effectiveness and survivability while allowing the soldier to engage the toughest and most sophisticated armored targets.

"This test demonstrated the efficacy of CKEM against a difficult target—an up-armored tank—at long range," said Loretta Painter, CKEM Advanced Technology Demonstration (ADT) program manager at the US Army Research and Development Command (RDECOM), Aviation and Missile Research, Development and Engineering Center (ARMDEC), Redstone Arsenal, AL. "This test collected target effects data to characterize the lethality of CKEM and validates what CKEM could provide to the warfighter."

"Another successful CKEM test bodes well for our soldiers because it means we are well positioned in being able to develop this tremendously lethal, hit-to-kill technology," said Rick Edwards, vice president-Tactical Missiles for Lockheed Martin Missiles and Fire Control. "We have a long history of successful designing, developing and producing hit-to-kill missile systems. CKEM will expand the battle space, provide increased mutual support and defeat all known threat countermeasures." The remaining flight test planned is designed to demonstrate CKEM's ability to fill current lethality gaps against enhanced reactive armor. CKEM will be particularly effective in bridging the Army's capability gaps identified for the Infantry Brigade Combat Team and the Stryker Brigade Combat Team by ensuring lethality overmatch at both close and extended ranges. CKEM is the next generation kinetic-energy anti-tank missile. It is less than 60 inches long and weighs less than 100 pounds, yet has an extended range for direct fire, line-of-sight engagements and provides the Infantry Brigade Combat Teams, Stryker Brigades and Future Combat System platforms overwhelming lethality overmatch against all potential target sets. ■

Triumvirate Awarded Multi-role in R&D

On behalf of the armed forces of Italy and Sweden, FMV, Swedish Defence Materiel Administration, has awarded Saab Microwave Systems AB, Selex Sistemi Integrati S.p.A and Elettronica S.p.A the second phase of a three-phase research and development programme supporting the development of the next generation of microwave multi-function, multi-role systems—Multi-role Active Electronically Scanned Antenna (M-AESA).

The programme will be fully financed by the two countries and the three participating companies will exploit the potential of AESA technologies in future defence electronic systems and aim to achieve the product vision of a true multi-role electronics package capable of active and passive sensing, jamming and special communications. It will not only support this vision but also contribute, in the shorter term, to the development of multifunction radar and EW systems.

The introduction of M-AESA technology, comprising digital beam forming, will greatly increase the performance of future microwave systems. Its benefits include the ability to detect, track and identify small targets in complex environments and to detect, track, identify and jam emitter and communication threats, thus providing the possibility of designing flexible multipurpose electronics in advanced platforms. The multipurpose electronics include functions from radar and electronic warfare, as well as communications.

MEAD Consortium Explores MEMS Technology

QinetiQ, acting as the prime and in partnership with 21 other organisations from industry, academia and the UK defence supply chain, has formed the MEMS Applications for Defence (MEAD) consortium. Its remit is to take a new approach to developing MEMS technology for defence purposes in a UK Ministry of Defence (MoD)-backed project worth £3.2 M over three years. Initially, the consortium will road map the technology, explore exploitation routes and investigate novel MEMS approaches for use in two defence application areas.

Firstly, the MoD has a requirement for deployable, unattended sensor networks, and QinetiQ will lead this area. Here the need is for small, lightweight, minimal cost military grade sensors that remove the need for expert placement, alignment and recovery. Typically these sensors fall into four groups: robust, low noise, high sensitivity acoustic microphones; orientation sensors; seismic sensors; and magnetic sensors.

Secondly, there is a need to indicate the presence of explosives, so the MEAD consortium will investigate techniques for sampling air and detecting compounds that warn of the proximity of an explosive device. Smiths Detection will lead this research package. As part of its remit the consortium will also research the potential failure modes of MEMS devices.

Ed Swindle, MoD Research Acquisition Organisation, stated: "This is a great opportunity for the MoD to foster innovation and co-operation across a broad supply base to access leading-edge technology and accelerate its application in a new generation of MEMS devices that address real defence needs. This new partnership model is a key element in the continued process of defence research competition."

Remodelling of Paris Command and Control Centre

The French armaments directorate (DGA) is completely restructuring the information and communication systems of the Paris Strategy Centre, in a project known by the French abbreviation OE SIC PSP. The associated contract worth around €70 M has been awarded to EADS Defence & Security Systems and Thales, along with their partners INEO and Cegelec, and covers the implementation of a programme for remodelling the information and communication systems of the French High Command of the Paris Strategy Centre (PSP).

The two-phase project is due to be realized over six years, with a potential five-year contract extension for maintenance. The new system will offer a combined and open command centre for the military and the secret services and be capable of implementing an Information Management policy that promotes the transmission of information and operational efficiency.

The PSP system will enable France to supply a joint staff Operational Headquarters, thus meeting the aims of the European Union. From 2007 on, the new system will provide a highly reconfigurable network architecture and enable the command centre to have an initial capacity level at its disposal that will promote cooperation using a modernized information system that synergizes with the existing one.

Innos Supports UK Nanotechnology NoE

Innos is providing integration engineering support and prototyping services for the UK Framework 6 Network of Excellence SiNANO Project. The consortium is funded by the European Union, with the Engineering and Physical Sciences Research Council (EP-

SRC) providing additional access to the Innos fabrication facility to the different UK academic partners—the UK Universities of Warwick, Southampton, Cambridge and Newcastle. The underlying principle of the project is to explore different technology routes and achieve very high speed, silicon-based nanoscale devices, which can be adopted in the future engineering of ICs.

Each partner in the SiNANO project provides the different areas of expertise required in developing these advanced devices using basic materials science, from the design and fabrication through to characterisation and device modelling. The research will aim to enhance device performance and integration.

In order to support the four main UK partners Innos has set up an internal task force led by Riccardo Varrazza, commercial integration engineer at the company's Southampton headquarters. "Achieving the production of IC components at nanometric dimensions could herald a revolution in IC technology, involving the integration of nanoscale CMOS and emerging post-CMOS logic and memory devices," said Varrazza. "Together with SiNANO we are committed to enhance device performance and integration, to meet the ever increasing demands of communications and computing."

Alcatel-Lucent: Leader in Comms Solutions

Alcatel and Lucent Technologies have completed their merger transaction and begun operations as the world's leading communication solutions provider. The new company, Alcatel-Lucent, with one of the largest global R&D capabilities in communications and the broadest wireless, wireline and services portfolio, is incorporated in France, with executive offices located in Paris. The company trades on Euronext Paris and the New York Stock Exchange under a new common ticker.

With a worldwide presence in 130 countries, 79,000 employees (after completion of the Thales transaction) and balanced revenues across all regions, Alcatel-Lucent has strong customer relationships with the 100 largest telecommunications operators in the world. The company will have four geographic regions: Asia-Pacific, Europe and North, Europe and South, and North America.

There will be five Business Groups: the Wireline Business Group, the Wireless Business Group and the Convergence Business Group (addressing the needs of the carrier market), the Enterprise Business Group and the Service Business Group. ■

IEEE Begins Wireless Communications Standard for Power Systems

Wireless data communications offers many benefits in power systems, but it also presents security, reliability and other concerns. In order to help the industry address the potential of this technology, the IEEE has begun work on a new standard to create functional, performance, security and on-site testing practices for wireless technologies in power system operations. The standard, IEEE P1777,™ "Using Wireless Data Communications in Power System Operations," will focus on newer technologies, such as WiFi, Bluetooth, Zigbee, WiMAX and cellular phones. In addition to the practical aspects of wireless use, it also will address the dissemination of information on the uses, benefits and concerns of wireless technologies in the industry. IEEE P1777 will evaluate the potential of wireless technologies in power systems to determine where they are viable alternatives to wire systems and what further development they need in order to meet robustness, security and reliability and other requirements. The standard will explore the potential uses of wireless technologies at many levels of power system operations, including substations, underground vaults, transmission and distribution circuits, generation and distributed generation plants, and customer electrical and metering equipment. IEEE P1777 is sponsored by the IEEE Power Engineering Society.

The IEEE Standards Association, a globally recognized standard-setting body, develops consensus standards through an open process that brings diverse parts of an industry together. These standards set specifications and procedures based on current scientific consensus. The IEEE-SA has a portfolio of more than 870 completed standards and more than 400 standards in development. For information on IEEE-SA, visit http://standards.ieee.org/.

RFID-based Strategies for Aerospace and Defense Supply Chains

Aerospace and defense companies are increasingly looking for ways to gain competitive advantage through the enhanced management of supply chains and assets. By 2011, the A&D Radio Frequency Identification (RFID) market is expected to realize revenue in excess of $2 B. One area that shows particular promise for the use of RFID in an A&D manufacturing environment is "MRO": maintenance, repair and overhaul. "MRO supply chain is about safety and security, as well as efficiency," says ABI Research director Michael Liard. "A&D companies have evolved a new supply chain equation: maintenance strategy + supply side strategy = supply chain strategy. RFID can fulfill many MRO event requirements by enabling real-time track-and-trace and unique identification." Given the one-off equipment maintenance and supply chain management focus of most A&D organizations, an integrated MRO supply chain strategy with linkage between in-line equipment performance and supplier capability is critical. An integrated MRO supply chain can improve service performance in a manufacturer's storeroom by simplifying inventory, purchasing, and other business processes. Integrated supply allows the centralization of all sourcing, procurement, receiving, internal distribution and service to one supplier. The full benefit of integrated supply is achieved when all MRO supply chain functions are outsourced, thereby allowing a plant to better focus on its core competencies. "Integrated MRO strategies based on RFID tagging can deliver marked efficiencies to the processes of locating parts, tools and materials, and to producing the significant amounts of documentation required to meet regulations in the aerospace and defense industry," notes Liard. "RFID is an enabling technology that can facilitate a shift from corrective to predictive maintenance strategies." The new ABI Research study, "The RFID Aerospace and Defense Market," provides an assessment of the opportunities business benefits of RFID in A&D markets. It forms part of the company's RFID Research Service, which includes research reports, research briefs, market data, on-line databases, ABI insights and analyst inquiry support.

ZigBee Emerges as the Wireless Mesh Network of Choice

In-Stat believes that because of the clarity of the ZigBee standard, the organizational strength of the ZigBee Alliance and the involvement of several of the world's largest semiconductor companies, ZigBee will emerge as the dominant wireless mesh networking technology.

Wireless mesh networks are a mosaic of proprietary and non-proprietary implementations. The IEEE 802.15.4 Working Group was designed to create unified standards for short range, self-configuring mesh networks. ZigBee is a networking layer that is built on top of the IEEE 802.15.4 standard. The ZigBee Alliance is an organization that has been the keeper of the ZigBee standard and is an open community of 200 companies that is charged with the promotion of the technology and testing of equipment.

"ZigBee is designed to create interoperability among silicon vendors and facilitate common software and profile platforms for end users in specific applications," says Chris Kissel, In-Stat analyst. "The addition of ZigBee to 802.15.4 gives an OEM or other end-user the assurance of multiple sources of silicon."

Recent research by In-Stat found the following:

- In 2006, In-Stat estimates between 4.5 million and 10.5 million ZigBee RF components will be sold.

• Commercial building control is, and will continue to be, the largest 802.15.4/ZigBee application.
• In 2005, North America represented 53 percent of all 802.15.4/ZigBee nodes in use.

The research, "Building up ZigBee and 802.15.4 Chipsets and Applications," covers the market for 802.15.4/ZigBee components. It includes analysis of how companies differentiate their products on the component level, a status update on how countries plan to regulate ZigBee, estimated bill of materials of ZigBee chipsets and ZigBee modules. It also includes detailed scenarios about the challenges 802.15.4/ZigBee faces in market verticals—residential automation, commercial applications, medical, industrial and smart cards. Forecast breakouts through 2010 of 802.15.4/ZigBee shipments by region, frequency and application, and in-depth vendor profiles of ZigBee silicon, systems and software providers are provided.

This research is part of In-Stat's Multimedia and Interface Technologies Service, which identifies and forecasts key interface technologies and multimedia semiconductors. It examines competitors, industry agendas, market shares, technology platforms, semiconductor technology and shipments. Technology penetration within a myriad of end equipment market is explored. Supply and demand-side insights are combined to examine these dynamic, evolving technologies.

Over 500 Million Mobile Broadband Users by 2010

According to Strategy Analytics' recent report, "Beyond 3G: Looking for True Mobile Broadband," new alternative technologies will contribute just six percent of the forecast 500 million mobile broadband users globally by 2010. Despite all the hype surrounding alternative technologies, like WiMAX, it is iterations of existing technologies which will dominate the mobile broadband arena in the short term. Technologies such as mobile WiMAX and UMTS TDD will lead the alternative technology camp, but enhancements to existing technologies, including HSPA and EV-DO revision A+ will comprise the bulk of the market and are where the money lies in the short term. "We are not likely to see technologies like mobile WiMAX or indeed, anything else, really take-off until the next decade," comments Sara Harris, senior industry analyst at Strategy Analytics and author of this report. "However, HSPA and EV-DO will be more than acceptable for most users, giving them the speed and flexibility they want to use their fixed Internet applications on the move." ■

INDUSTRY NEWS

■ **Kulicke & Soffa Industries Inc.** closed the previously announced purchase of **Alphasem**, a supplier of die bonder equipment, from Dover Technologies International Inc., a subsidiary of Dover Corp. The purchase price was $27.1 M in cash, after a working capital adjustment and subject to further post closing adjustments.

■ **Fox Electronics**, a supplier of frequency control products, announced the opening of a new Asia Pacific sales office in Taiwan. The new office has been established to support the rapid growth of the company's sales in the Asia Pacific region, including Taiwan and China. The new Fox Asia Pacific sales office is located at 12F-6, 378 Ming An West Road, Hsin-Chuang, Taipei Hsien 242 Taiwan, ROC.

■ **Tehuti Networks**, a semiconductor company providing 10 Gigabit Ethernet single-chip, low power TCP/IP acceleration controllers, announced it has opened a new office and expanded its personnel in Taiwan. The office is headed by Jerry Lee, who serves as the company's Asia-Pacific regional sales manager. Lee will manage the sales and technical support of Tehuti Networks' controller and board-level products throughout the Asia-Pacific.

■ **Micro-Ant Inc.** is relocating its operations to a larger facility in Easton, MA. The additional space is required to accommodate the company's growing staff and manufacturing department, and will include a 40-foot, fully-instrumented anechoic test chamber for antenna measurements. Micro-Ant is an established leader in the design and manufacture of antennas for the satellite communications industry, including satellite radio, GPS and two-way voice/data.

■ **Applied Wave Research Inc.** (AWR®), El Segundo, CA, and Shanghai Research Institute of Microelectronics (SHRIME), **Peking University**, China, announced that AWR is donating its entire suite of radio frequency (RF) design software in a collaborative effort to advance Peking University's high frequency design curriculum. The donation is the first step in a long-term program that will establish a joint RF design and research laboratory at the university's research institute. The laboratory will spearhead high frequency research projects in Shanghai and develop unified process design kits (PDK) and value-added RF intellectual property (IP) for key foundry processes in China.

■ **Keithley Instruments Inc.**, a leader in solutions for emerging measurement needs, announced it has partnered with **Mesatronic Group**, Voiron, France, to develop advanced probe cards for semiconductor parametric testers used in RF and low current DC applications.

■ **QUALCOMM Inc.** and **Motorola Inc.** announced an expansion in their relationship. In addition to collaborating on CDMA2000®, the two companies will now be working together to bring UMTS handsets to global markets. Motorola Mobile Devices has approved QUALCOMM's Mobile Station Modem™ chipsets for incorporation into future UMTS handset designs.

■ **Melexis Microelectronic Integrated Systems N.V.** and **Atmel® Corp.** announced their collaboration to propose innovative solutions for 13.56 MHz RFID readers and Near Field Communication (NFC) devices. They will target applications such as passport and ID verification, contactless payment, transaction and peer-to-peer information exchange.

■ **SiGe Semiconductor Inc.** and **Nordnav Technologies AB** announced they have collaborated on a GPS/Galileo receiver for consumer electronic products. The companies have combined SiGe's SE4120L radio front-end with Nordnav's E5000 software to offer a receiver system with the high performance, small size and power efficiency that is essential for mobile devices.

■ Customer premises equipment (CPE) manufacturers can now deliver WiMAX-enabled products to market even faster with a production-ready reference design from **Freescale Semiconductor**, **Wavesat** and **Celestica**. Celestica, a world leader in electronics manufacturing services, has joined a pre-existing collaboration between Freescale and Wavesat to enhance a comprehensive platform for the rapid creation of WiMAX-enabled products.

■ **StratEdge**, a leader in the design and production of semiconductor packages for microwave, millimeter-wave and high speed digital devices, announced that one of its SE20 power amplifier packages is playing a key role in transmitting signals with information gathered from Mars Exploration Rovers *Spirit* and *Opportunity* back to earth. The power amplifier package is used to protect the gallium arsenide monolithic microwave integrated circuits (MMIC) and ensure signal integrity.

■ **Gilland Electronics**, Morgan Hill, CA, announced that its business partner, **ELVA-1 Ltd.**, St. Petersburg, Russia, received FCC equipment authorization for PPC-1000-E point-to-point wireless radios. This authorization enables these 1.25 Gbps, full-duplex wireless Ethernet links, operating in the 71 to 76 GHz and 81 to 86 GHz bands, to be made available to the United States market.

■ **Amphenol RF** announced that it is now authorized to market the QN interface as a member of the Quick Lock Formula® Alliance. Amphenol RF signed a QMA and QN license agreement with **Huber+Suhner AG** and **Radiall SA** earlier this year and is now QLF® certified on both the QMA and QN interface.

■ **Compel Electronics SpA**, a designer and manufacturer of interconnection systems and cable assemblies, announced that the company has received ISO 14001 certification.

■ **White Mountain Labs**, a leader in test and characterization of advanced technologies, announced that its new testing facility has passed the ISO 17025 reaccreditation audit. The company acquired full accreditation for the second consecutive year and received a rare, perfect audit for the new testing facility, The Center for ESD. This achievement designates White Mountain Labs as the only ESD laboratory with ISO 17025 accreditation globally.

■ Hiromichi Toda, president of **Anritsu Corp.**, announced that the company has been awarded the prestigious 2006 Test & Measurement Global Excellence of the Year Award by Frost & Sullivan. The Frost & Sullivan Global Excellence of the Year Award is bestowed upon the company that has demonstrated global excellence in given business functions, such as sales, marketing, customer service, technology innovation, product quality, supply chain management and growth strategy.

■ At the Association for Manufacturing Excellence (AME) International Lean Enterprise Conference, **M2 Global Technology Ltd.** was named winner of the Southwest Region AME Manufacturing Excellence Award. The company was recognized for its commitment to attainment of excellence in manufacturing and productivity.

CONTRACTS

■ **ITT Corp.** announced it will provide comprehensive spectrum engineering support to the Defense Information Systems Agency (DISA), Joint Spectrum Center (JSC) on the Electromagnetic Spectrum Engineering Services Contract. Under the contract, ITT will provide engineering systems support, technical analysis, test support and long-term strategic planning as JSC meets national security and military objectives related to the use of the electromagnetic spectrum. The contract has a three-year base value of $147 M and if all options on the contract are exercised, a potential total value of $545 M.

■ Naval Surface Warfare Center Crane Division has awarded a five-year contract valued in excess of $6.3 M to **Triton Electron Technology Division**, Easton, PA, for the repair, remanufacture or replacement of traveling wave tubes in support of the AN/ALQ-126B ECM system.

■ **Skyworks Solutions Inc.**, an innovator of high performance analog and mixed-signal semiconductors enabling mobile connectivity, announced that **MediaTek Inc.**, a supplier of worldwide consumer IC chipsets, will be incorporating Skyworks' Helios™ radio across several next-generation EDGE wireless communication platforms. This agreement demonstrates Skyworks' ability to effectively partner with a leading system solution provider following the company's exit of the baseband business.

FINANCIAL NEWS

■ **ANADIGICS Inc.** reports sales of $44.8 M for the third quarter ended September 30, 2006, compared to $29.3 M for the same period in 2005. Net loss for the quarter was

$1.3 M ($0.03/per share), compared to a net loss of $6.8 M ($0.20/per share) for the third quarter of last year.

■ **Electro Rent Corp.** reports sales of $30 M for the first quarter of 2007 ended August 31, 2006, compared to $26.6 M for the same period in 2006. Net income for the quarter was $4.8 M ($0.18/per diluted share), compared to a net income of $5 M ($0.19/per diluted share) for the first quarter of last year.

■ **Ansoft Corp.** reports sales of $20.5 M for the second quarter of fiscal 2007 ended October 31, 2006, compared to $18 M for the same period in 2006. Net income for the quarter was $3.7 M ($0.14/per diluted share), compared to a net income $4.1 M ($0.16/per diluted share) for the second quarter of last year.

■ **Endwave Corp.** reports sales of $18.8 M for the third quarter of 2006 ended September 30, 2006, compared to $14.3 M for the same period in 2005. Net income for the quarter was $911,000 ($0.06/per diluted share), compared to a net loss of $193,000 ($0.02/per share) for the third quarter of last year.

■ **Tower Semiconductor Ltd.**, a pure-play independent specialty foundry, announced that it has expanded its equity private placement, originally announced on November 1, 2006, and raised additionally approximately $11 M in immediate gross proceeds from Israeli investors.

■ **Technical Communities Inc.**, a service provider for technical organizations that sell to US government agencies and prime federal contractors, has completed a Series D Convertible Preferred financing. While specific terms were not disclosed, the privately held company announced the financing included participation by all previous leading venture investors including Crosspoint Venture Partners, Netmarket Partners, New Enterprise Associates (NEA) and Technology Crossover Ventures (TCV). Technical Communities plans to use the funds to expand its offer to additional markets and for potential acquisitions.

NEW MARKET ENTRIES

■ **PulseWave RF™** is a fabless semiconductor company that has developed a digital high efficiency RF power amplifier module for wireless infrastructure. The company's proprietary Class M Power technology is a digital MCPA module that simultaneously sets new industry benchmarks for cost, size and efficiency. Based in Austin, TX, PulseWave RF is a privately held company with funding from Oak Investment Partners, Austin Ventures, Bay Partners, Genesis Campus and Freescale.

■ **The Phoenix Co.** introduces a new design and manufacturing capability to provide unique solutions for ruggedizing COTS antenna elements. This capability consists of taking a customer selected antenna element, designing an electrical and mechanical transition from the antenna element to the connector and packaging it together to meet demanding environmental and mechanical requirements such as IP67 or 68. An engineered mechanical transition is utilized to overcome the effects of different coefficients of linear thermal expansion between the antenna element and the connector. The antennas can be supplied with FCC Rule 15 compliant connectors. For more information, visit www.phoenixofchicago.com.

PERSONNEL

■ RF Micro Devices Inc. (RFMD) announced that **John (Jack) Harding**, the co-founder, chairman, president and CEO of eSilicon Corp., has been elected to the RFMD board of directors. Harding was elected to fill an existing vacancy at the November 1 board meeting and his appointment to the board was effective immediately. Harding co-founded eSilicon Corp., a privately held company, which designs and manufactures complex, custom chips for a broad and growing portfolio of large and small firms. eSilicon is venture-capital backed and has attained an annual revenue run rate approaching $100 M.

■ UltraSource Inc., a supplier of custom thin film circuits and ceramic interconnect devices, announced the addition of **Jeff Bergart** as chief financial officer (CFO). Prior to his employment at UltraSource, Bergart held financial management roles at several New England-based organizations, including as CFO at Digital Equipment Corp. and KROHNE Inc. In his role as CFO, Bergart will be responsible for managing UltraSource's Finance, IT and Talent Management Groups.

■ Antenova Ltd. announced the appointment of **Mike Edwards** as vice president of worldwide sales and marketing. Antenova further announced the promotion of **CL Lim** to vice president and general manager of Asia. Edwards has over 25 years experience of direct and indirect sales, marketing and senior management in the semiconductor and components industry. Lim has more than 26 years in international sales, business development and technical operations in the wireless and telecommunication industry.


▲ *Jim Greene*

■ LPKF Laser & Electronics has recently announced the promotion of **Jim Greene** to the position of vice president, sales and marketing. With this new position Greene will be responsible for the control and management of sales and marketing throughout North America. Greene began his career with LPKF North America in 2001, with his latest position being national sales manager.

■ Auriga Measurement Systems LLC announced the addition of **Ted Lewis** as director of global sales. Lewis has over 20 years of experience of growing sales and focusing on building strong customer relations. Previous to Auriga, Lewis was self-employed as a consultant providing specialized services in the development of sales and customer-centered organizations. In addition, Lewis was head of worldwide sales and marketing at Unitek Benchmark in Goffstown, NH, a capital equipment manufacturer serving the microelectronics industry. At Auriga, Lewis will refine and establish Auriga's Global Sales Strategy and Global Sales Channels to grow sales in the three core business lines of Modeling and Design Services, Characterization Instruments, and Test and Measurement Systems.

▲ Peter Barnwell

■ **Peter Barnwell** has been appointed as European business manager for Barry Industries, an Attleboro, MA-based manufacturer of microwave and microelectronic components and packaging solutions. Barnwell will be based in the UK with responsibility for the sales and marketing activity throughout Europe.

■ RFMW Ltd. hired **Jane Cavin** as the company's new inside sales person for southern California and Arizona. Cavin has more than 20 years of experience in sales, product management, human resources and office management. Cavin comes to RFMW Ltd. from CK Associates, a M/A-COM rep and has experience with distribution from her days at Time, Avnet and Newark.

▲ John Larson III

■ Avago Technologies, a privately held semiconductor company, announced that **John Larson III** was named an IEEE Fellow at the 2006 International Ultrasonics Symposium in Vancouver, British Columbia, Canada. IEEE Fellows are nominated by their peers in numerous engineering fields for extraordinary accomplishment. In his 34-year career with Avago, beginning with Hewlett-Packard Laboratories and Agilent Laboratories, Larson has been part of and has led diverse research and development teams that achieved significant results in acoustics. Today, Avago Technologies' acoustics-based products are embedded in millions of mobile phones, data cards and other wireless devices worldwide. Among his notable contributions to engineering, the IEEE Fellow award recognizes the breakthrough in Film Bulk Acoustic Resonator (FBAR) devices he and his teammates developed as a commercial product for cell phones.

REP APPOINTMENTS

■ **Giga-tronics Inc.**, a manufacturer of instruments, subsystems and microwave components that have broad applications in both commercial and military wireless telecommunications systems, announced a new partnership agreement with **TestMart**, a leading marketplace operator and service provider for the IT, network maintenance, and test and measurement industries. The agreement authorizes TestMart to present a catalog of Giga-tronics' RF and microwave test equipment in bench top and VXI bus configurations.

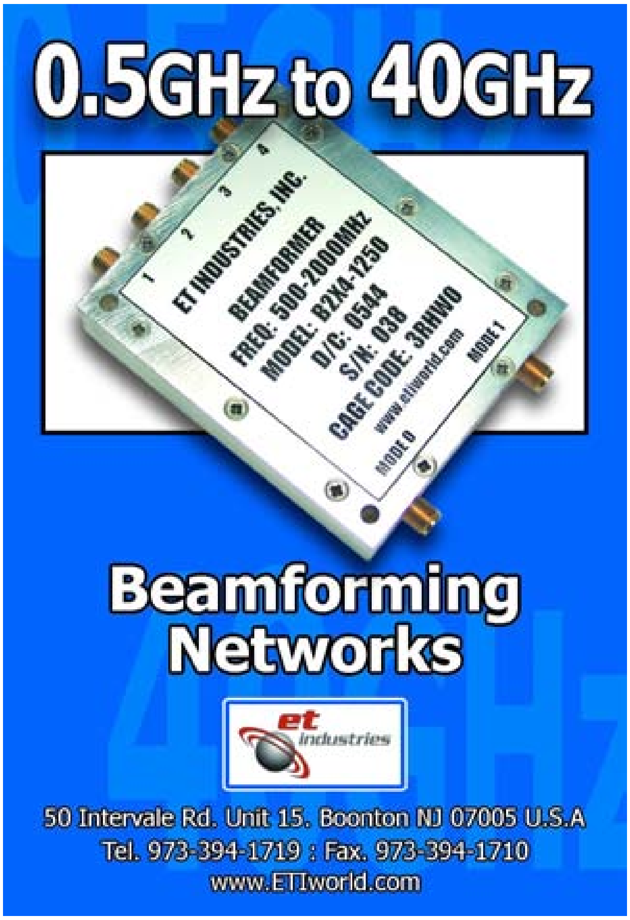

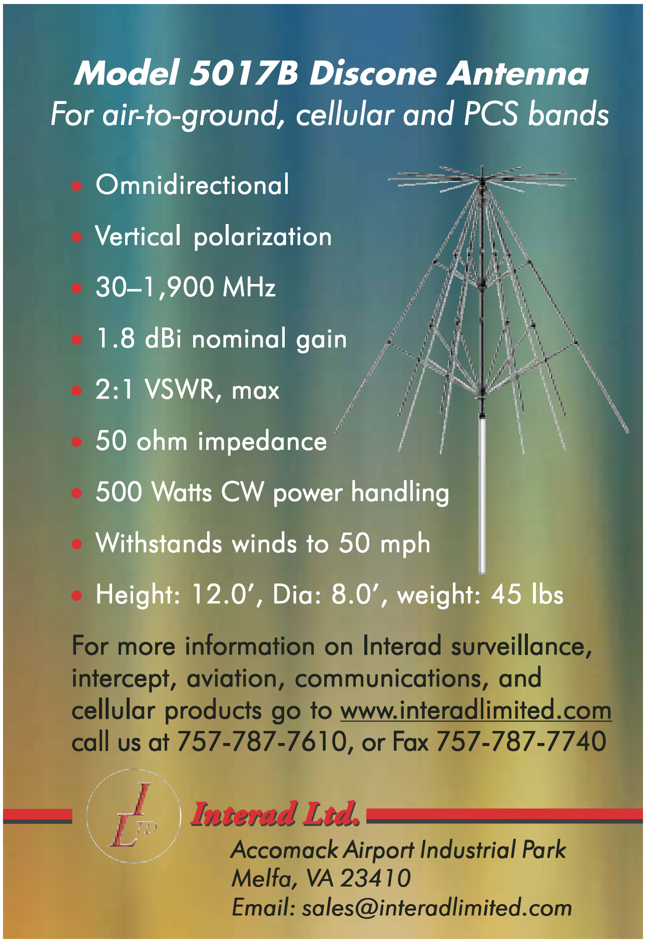

■ **Digi-Key Corp.**, an electronic component distributor, and **SMC Corp. of America** announced the signing of a global distribution agreement. SMC products stocked by Digi-Key include pressure switches, vacuum switches, digital pressure regulators, digital flow switches and accessories. These products are available directly from Digi-Key and are featured in its print and on-line catalogs.

■ **Zilker Labs Inc.** announced that it has signed an agreement with technology distributor **Avnet Electronics Marketing Asia**, an operating group of Avnet Inc. Avnet Electronics Marketing will support Zilker Labs' business throughout the Asia-Pacific region, including major markets such as Korea, Taiwan, China and Hong Kong. Zilker Labs also has an Asian subsidiary, Zilker Labs Asia Ltd., based in Hong Kong, that supports customers throughout Asia.

■ **Centerline Technologies** announced the appointment of **JDM Associates** as the company's exclusive sales representative in Florida and Georgia. In related news, Centerline Technologies also announced the appointment of **Chalman Technologies** as the company's exclusive sales representative in southern California and Arizona.

■ **Reactel Inc.**, a manufacturer of RF and microwave filters, multiplexers, switched filter banks and subassemblies to the commercial, military, industrial and medical industries, announced the appointment of **McBride Scientific Sales** as the company's representative in Texas, Louisiana, Oklahoma and Arkansas. For more information about McBride Scientific Sales, visit www.mcbridescientific-sales.com or call Todd McBride at (972) 494-5000.

■ **RLC Electronics Inc.**, a manufacturer of RF and microwave components to both the commercial and military industries, has announced the appointment of **Marktron Inc.** as the company's sales representative in the states of Maryland, Virginia, Delaware and the District of Columbia. Marktron Inc. can be contacted at 1688 East Guide Drive, #304, Rockville, MD 20850 (301) 251-8990, fax: (301) 424-0766 or e-mail John Haynos: johnh@marktron.com.

■ **Aethercomm Inc.** appointed **Youngewirth & Olenick** as the company's exclusive sales representative in southern California, Arizona and New Mexico. Youngewirth & Olenick will represent and support Aethercomm's entire product offering. Youngewirth & Olenick can be reached at 17621 Irvine Blvd., Suite 101, Tustin, CA 92780 (800) 515-1554 or visit: www.yando.com.

WEB SITE

■ **Cornell Dubilier** announces its newly executed capacitor web site, www.cde.com. It features one-click access to 10 technical papers, three capacitor life-temperature calculators, a new thermal modeling applet and one-click access to capacitor types by dielectric, application or type letters. Advanced parametric search pulls up individual ratings and links to data sheets. Application guides and product selector guides make it easy to steer a user through the company's more than 220 capacitor types.

MEMORY EFFECT MINIMIZATION AND WIDE INSTANTANEOUS BANDWIDTH OPERATION OF A BASE STATION POWER AMPLIFIER

Linear amplification and reduction of the memory effect of a wide bandwidth signal have been realized for a next generation base station power amplifier. Using a simple nonlinear LDMOS model, the third-order intermodulation distortion current is analyzed using a third-order power series. The limitations in shorting the envelope and second harmonics are studied. From the analysis, it is proven that the envelope is a more critical component than the second harmonic for the memory effect and linearity. In order to minimize the envelope voltages, a new matching topology is proposed, which consists of a series LC circuit for shorting the device at a low frequency while maintaining a matchable impedance at the operating frequency. The proposed power amplifier was constructed using a 90 W PEP LDMOSFET at a 2.14 GHz center frequency and tested for two-tone and multi-carrier WCDMA signals. The test results show that the memory effect and nonlinearity are drastically reduced for the proposed amplifier. For the two-tone signals, an asymmetry of less than 2 dB up to 60 MHz tone spacing is achieved for the IMD3 and up to 40 MHz for the IMD5. For the WCDMA 20FA signal with a bandwidth of 100 MHz, a linearity improvement of approximately 15 dB is achieved by minimizing the envelope impedances.

The next generation of mobile communication systems will provide a wide variety of new services, from high quality voice to high definition video and high data-rate wireless channels. Moreover, the systems will provide combined services, including the established wire and wireless communications and broadcasting networks. In order to support these services, a wide frequency spectrum will be assigned. The base station power amplifiers for the next generation systems will therefore have to cover a wide instantaneous signal bandwidth, together with a highly linear amplification. However, the wideband signals may cause severe memory effects and nonlinearities in the power amplifiers.[1]

JEONGHYEON CHA, ILDU KIM, SUNGCHUL HONG AND BUMMAN KIM
Pohang University of Science and Technology (POSTECH)
Gyeongbuk, South Korea
JONG SUNG LEE AND HAN SEOK KIM
Samsung Electronics Co. Ltd.
Gyeonggi, South Korea

TABLE I

DEFINITION OF THE NONLINEAR COEFFICIENTS FOR THE AC DRAIN CURRENT

gm	$\partial i_D/\partial v_{GS}$
$k2_{gm}$	$1/2 \bullet (\partial^2 i_D/\partial^2 v^2{}_{GS})$
$k3_{gm}$	$1/6 \bullet (\partial^3 i_D/\partial v^3{}_{GS})$
go	$\partial i_D/\partial v_{DS}$
$k2_{go}$	$1/2 \bullet (\partial^2 i_D/\partial v^2{}_{DS})$
$k3_{go}$	$1/6 \bullet (\partial^3 i_D/\partial v^3{}_{DS})$
$k2_{gm\ \&\ go}$	$(\partial^2 i_D/\partial v_{GS}\partial v_{DS})$
$k3_{2gm\ \&\ go}$	$1/2 \bullet (\partial^3 i_D/\partial v^2{}_{GS}\partial v_{DS})$
$k3_{gm\ \&\ 2go}$	$1/2 \bullet (\partial^3 i_D/\partial v_{GS}\partial v^2{}_{DS})$

The memory effects are defined as changes in the amplitude and phase of the distortion components, due to the previous signals. The simplest method for characterizing them is to use a two-tone signal.[1–4] The two-tone signals, with varying tone spacing, are applied to an amplifier to measure the distortion components. If the distortion characteristics are identical, regardless of the tone spacings, the amplifier can be expected to be memory-less and to operate properly for wideband signals. Therefore, the memory effect becomes a very important design consideration for wideband base station power amplifiers. It is also the limiting factor for the cancellation of distortion when linearizing a power amplifier (PA) by predistortion techniques.[2,5,6] Many previous authors have tried to analyze the memory effect or reduce it.[1,4,7,8] The effect is still a big problem for the current base station power amplifiers and is significant even for amplifiers for the universal mobile telecommunications system (UMTS), which has only a 20 MHz signal bandwidth. The objective of this work is to minimize the memory effect of a base station PA and to realize a linear power amplification of a 100 MHz bandwidth signal, which is very important for the next generation PAs. First, the memory effect is analyzed using a simple LDMOS model[1,9] and then a detailed simulation is carried out using Freescale's MRF5S21090 LDMOS model. The analysis and simulation show that the drain envelope impedance is the most important factor for reducing the memory effect and nonlinearity. A new matching topology is proposed for minimizing the drain and gate envelope impedances. The matching topology consists of a series LC circuit for shorting the device at a low frequency while maintaining a matchable impedance at the operating frequency. The circuits are connected to the gate and drain terminals, rather than to the bias lines, since the circuit can produce a very low impedance, not limited by the quarter-wavelength bias line. For the experimental demonstration, based on the analysis and simulation, a power amplifier was implemented at a 2.14 GHz center frequency and tested using two-tone and multi-carrier down-link wideband code division multiple access (WCDMA) signals. The amplifier, with the reduced envelope impedances, provides drastically reduced memory effects and very linear amplification performance for wideband signals.

ANALYSIS FOR IM3

A general metal-oxide semiconductor (MOS) transistor is a four-terminal device, the terminals being gate, drain, source and bulk, and the voltages in the transistor are either referred to the source or to the bulk. In the case of a laterally diffused MOS field-effect transistor (LDMOSFET) used in this work, the voltage between the source and the bulk, v_{bs}, can be neglected because they are tied together. The drain current is described as a function of the gate-to-source voltage, v_{gs}, and the drain-to-source voltage, v_{ds}, and the AC drain current, up to the third-order nonlinear term, can be expressed by the following third-order power series[1,9]

$$
\begin{aligned}
i_d = g_m v_{gs} &+ K2_{gm} v_{gm}^2 + K3_{gm} v_{gs}^3 \\
&+ g_0 v_{ds} + K2_{g0} v_{ds}^2 + K3_{g0} v_{ds}^3 \\
&+ K2_{gm\&g0} V_{gs} v_{ds} \\
&+ K3_{2gm\&g0} v_{gs}^2 v_{ds} + K3_{gm\&2go} v_{gs} v_{ds}^2 \qquad (1)
\end{aligned}
$$

where the nonlinear coefficients are defined in ***Table 1***.

In order to extract the third-order intermodulation distortion (IM3) level from Equation 1, a FET model is adopted, containing nonlinear C_{gs}, g_m, g_0 and C_{ds}. The gate-to-drain nonlinear capacitance, C_{gd}, has been excluded to simplify the analysis. The nonlinear components can be replaced by linear components and corresponding distortion current sources.[1,9] The linearized model is shown in ***Figure 1***, which contains Norton's equivalent circuit for the input terminal and three nonlinear current sources, i_{NL}, C_{gs}, $i_{NL,gm}$ and $i_{NL,g0\&Cds}$. Notice that the nonlinear current sources from g_0 and C_{ds} are combined in one source. v_{gs} and v_{ds} are written as functions of frequency as

$$v_{gs}(\omega) = -Z_S(\omega) i_{gs}(\omega) \qquad (2)$$

$$v_{ds}(\omega) = -Z_L(\omega) I_{ds}(\omega) \qquad (3)$$

where

$$Z_S(\omega) = Z_{S,ext}(\omega) \,||\, 1/j\omega C_{gs} \qquad (4)$$

$$Z_L(\omega) = Z_{L,ext}(\omega) \,||\, 1/J\omega C_{ds} \,||\, 1/g_0 \qquad (5)$$

$$i_{gs}(\omega) = i_{NL,Cgs}(\omega) - i_{IN}(\omega) \qquad (6)$$

$$i_{ds}(\omega) = g_m v_{gs}(\omega) + i_{NL,gm}(\omega) + i_{NL,g0\&Cds}(\omega) \qquad (7)$$

In Equations 6 and 7, the input current, i_{IN}, has only a fundamental signal component but the nonlinear currents, i_{NL}, have no fundamental component. If an equal power two-tone input signal is applied to the amplifier, from Equation 1, the upper IM3 (IM3U) drain current is found to be

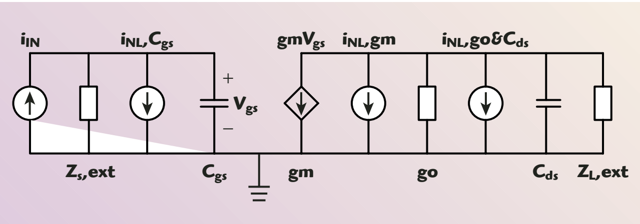

▲ *Fig. 1 FET model containing distortion current sources generated by nonlinear C_{gs}, gm, go and C_{ds}.*

$$\begin{aligned} i_d\left(2\omega_2-\omega_1\right) &= g_m v_{gs}\left(2\omega_2-\omega_1\right) \\ &+K2_{gm} v_{gs}\left(\omega_1\right) v_{gs}\left(2\omega_2\right) \\ &+K2_{gm} v_{gs}\left(\omega_2\right) v_{gs}\left(\omega_2-\omega_1\right) \\ &+\frac{3}{4}K3_{gm}+v_{gs}\left(\omega_1\right) v_{gs}^2\left(\omega_2\right) \\ &+g_0 v_{ds}\left(2\omega_2-\omega_1\right) \\ &+K2_{g0} v_{ds}\left(\omega_1\right) v_{ds}\left(2\omega_2\right) \\ &+K2_{g0} v_{ds}\left(\omega_2\right) v_{ds}\left(\omega_2-\omega_1\right) \\ &+\frac{3}{4}K3_{g0} v_{ds}\left(\omega_1\right) v_{ds}^2\left(\omega_2\right) \\ &+K2_{gm\&g_0} v_{gs}\left(\omega_1\right) v_{ds}\left(2\omega_2\right) \\ &+K2_{gm\&g0} v_{ds}\left(\omega_1\right) v_{gs}\left(2\omega_2\right) \\ &+K2_{gm\&g0} v_{gs}\left(\omega_1\right) v_{ds}\left(\omega_2-\omega_1\right) \\ &+K2_{gm\&g0} v_{ds}\left(\omega_1\right) v_{gs}\left(\omega_2-\omega_1\right) \\ &+\frac{3}{4}K3_{2gm\&g0} v_{ds}\left(\omega_1\right) v_{gs}^2\left(\omega_2\right) \\ &+\frac{3}{4}K3_{gm\&2g0} v_{gs}\left(\omega_1\right) v_{ds}^2\left(\omega_2\right) \end{aligned} \quad (8)$$

The lower IM3 (IM3L) current is identical, but ω_1 and ω_2 are exchanged and the (ω_1–ω_2) term is the complex conjugate of (ω_2–ω_1). Among the fourteen rows of Equation 8, the values of the first, fourth, fifth, eighth, thirteenth and fourteenth rows are not controllable by a matching circuit because the in-band impedance is fixed by the optimum matching point. The values of the remaining eight rows are controllable since they are functions of the gate envelope (third and twelfth rows), gate second harmonic (second and tenth rows), drain envelope (seventh and eleventh rows) or drain second harmonic (sixth and ninth rows) voltages, which are dependant on the harmonic impedances. For convenience, hereafter, the term 'harmonic' is applied to the 'second harmonic' ($2\omega_1$ and $2\omega_2$) components and separated from the term 'envelope' for the (ω_2–ω_1) frequency component. The memory effect is generated by the controllable terms and to reduce them, the envelope and second harmonic voltages should be reduced to zero by proper terminations. Conventionally, the short is provided at the bias line after a quarter-wave transmission line. In this case, a wideband short is difficult to achieve, since the dispersion of the line limits the achievable minimum impedance level. Thus, the short should be provided at the gate and drain directly without passing through a quarter-wave line. The termination was achieved by using a simple series LC circuit as will be shown in the following sections.

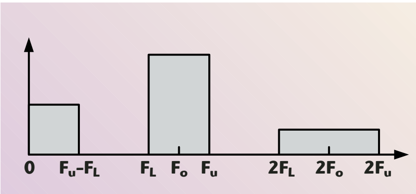

▲ *Fig. 2 Spectra distribution of the envelope and second harmonic signals.*

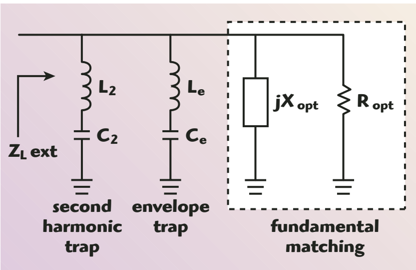

▲ *Fig. 3 Ideal output matching circuit with envelope and second harmonic trap circuits.*

OUT-OF-BAND IMPEDANCE LIMITATIONS

In this section, the realizable lower limits of the impedances at the second harmonic and envelope frequencies are investigated. This study provides the design guideline for the power amplifier with reduced memory effect.

Ideal Situations

Consider a signal with a center frequency f_o and bandwidth (f_U–f_L). The signal distribution is shown in ***Figure 2***, together with the envelope and second harmonic signals. It is assumed that

$$f_0=\frac{\left(f_U+f_L\right)}{2}\approx\sqrt{f_U f_L} \quad (9)$$

An ideal matching topology for the output terminal of the FET model is shown in ***Figure 3***. The input matching circuit will be identical to the output one. The figure includes the envelope and second harmonic trap circuits as well as an optimum matching circuit for the fundamental signal. This circuit topology is beneficial for the termination of the harmonic voltages compared to the conventional termination at the bias line, since the impedance dispersion caused by the quarter-wave bias line is eliminated. However, the circuit effectively adds up a reactive impedance at the fundamental frequency and should be designed properly. In order to have impedances of the same magnitude at both frequency edges, $2f_L$ and $2f_U$, the second harmonic trap circuit, L_2 and C_2, must resonate at $2\sqrt{\omega_U\omega_L}$. That is

$$L_2C_2=1/4\omega_U\omega_L\approx 1/\left(2\omega_0\right)^2 \quad (10)$$

If the envelope trap and fundamental matching circuits have fairly high impedances at the second harmonic frequency, the output load impedances for the second harmonics, $Z_{L,ext}(2f_U)$ and $Z_{L,ext}(2f_L)$, are complex conjugate and their magnitudes are

$$\left|Z_{L,ext}\left(2f_U\right)\right|=\left|Z_{L,ext}\left(2f_L\right)\right|=4\pi L_2\left(f_U-f_L\right) \quad (11)$$

As expected, the impedances are related to the inductance and signal bandwidth.

Next, a very large capacitor C_e is needed to short the envelope signal. Again, the second harmonic trap and fundamental matching circuits are assumed to have fairly high impedances at the envelope frequency. Then the magnitude of $Z_{L,ext}(f_U–f_L)$ is given by

$$\left|Z_{L,ext}\left(f_U-f_L\right)\right|=2\pi L_e\left(f_U-f_L\right) \quad (12)$$

From Equations 11 and 12, it can be expected that the envelope impedance, $Z_{L,ext}(f_U–f_L)$, is one half of the second harmonic impedance, $Z_{L,ext}(2f_U)$, for the same magnitude of L_e and L_2. Finally, the optimal fundamental signal matching is achieved by

$$-jX_{opt}(\omega) = \left\{ j\omega L_2 + 1/\left(j\omega C_2\right)\right\} \,||\, j\omega L_e \,||\, 1/j\omega C_{ds} \quad (13)$$

where $\omega_L \le \omega \le \omega_U$. If the impedances of the envelope and second harmonic trap circuits at the fundamental frequency are extremely small, it may be impossible to match it in practice. Such a matching problem will restrict the values of L_e, L_2 and C_2. Thus, the lower limits of the realizable second harmonic and envelope impedances are determined.

Practical Situations

Since a base station PA designer generally uses a packaged transistor, one cannot avoid the inductive effect of the bond-wires between the transistor die and the package lead-frame. The bond-wire inductance may give a certain advantage, such as stabilization of the device and increase of the usable bandwidth, when it is used together with an internal matching circuit. However, it obviously acts as an obstacle in controlling the envelope and harmonic impedances. For this work, the packaged MRF5S21090 LDMOSFET manufactured by Freescale was chosen. The transistor is composed of two 45 W cells and is able to deliver 90 W peak envelope power (PEP). The equivalent circuit with the internal matching of a 45 W cell is shown in ***Figure 4***. At the envelope frequency, the capacitors for the internal matching can be ignored and thus the external envelope impedance is changed according to frequency by just the series bond-wire inductors, L_{g1} and L_{g2} for the gate and L_{d2} for the drain. The impedances at the envelope frequency for the input and output, $Z_{S,ext}$ $(f_U–f_L)$ and $Z_{L,ext}$ $(f_U–f_L)$, are then given by

$$\left|Z_{S,ext}\left(f_U - f_L\right)\right| = 2\pi\left(L_{g1} + L_{g2} + L_e\right)\left(f_U - f_L\right) \quad (14)$$

and

$$\left|Z_{L,ext}\left(f_U - f_L\right)\right| = 2\pi\left(L_{d2} + L_e\right)\left(f_U - f_L\right) \quad (15)$$

On the other hand, for the second harmonic terminations, the gate and drain external matching impedances outside the package, $Z'_{S,ext}$ and $Z'_{L,ext}$, are given by

$$Z'_{S,ext}\left(\omega = 2\omega_1 \approx 2\omega_2\right) = -1/\left(j\omega C_{pad}/2\right) \,||\, \left[j\omega L_{g2} + \left(j\omega L_{g1} \,||\, 1/j\omega C_{g,mos}\right)\right] \quad (16)$$

$$Z'_{L,ext}\left(\omega = 2\omega_1 \approx 2\omega_2\right) - 1/\left(j\omega C_{pad}/2\right) \,||\, j\omega L_{d2} \quad (17)$$

Equations 16 and 17 can be realized easily by a harmonic matching circuit including the series L_2C_2 resonant circuit, because it has a narrow fractional bandwidth contrary to the wide bandwidth of the envelope signal. For the implementation of the envelope termination, a very large capacitor, such as a large tantalum capacitor, with a rather small inductor should be used. The impedance level is limited by the inductors as shown in Equations 14 and 15. Therefore, the envelope is harder to terminate than the second harmonic and the envelope components can be more important than the second harmonics in linearity as well as memory effect. In a practical sense, however, one cannot guarantee that the envelope trap and fundamental matching circuits have fairly high impedances compared to the second harmonic impedance. As a result, in the envelope trap circuit, a simultaneous matching for the fundamental signal and second harmonic is needed. If the values of the internal matching components are not exactly known, it is very difficult to design the termination circuits. Thus, the circuit has been optimized experimentally for a low memory effect and high linearity, focused on the envelope signal.

SIMULATIONS

To show the contributions to the memory effect from the gate and drain envelope components, the MRF5S21090 LDMOS model has been simulated using the Advanced Design System version 2004A (ADS2004A) for two-tone signals with a 2.14 GHz center frequency and tone spacings of up to 100 MHz. ***Figure 5*** shows the circuit diagram for the simulation. In the simulation, a high voltage tantalum capacitor for the envelope trap has been selected and its scattering parameters were extracted with a network analyzer and used to support the practical implementation. The tantalum capacitor has a capacitance of 10 μF, which is large enough to short the envelope signal up to 100 MHz and also has parasitic frequency-dependant resistive and inductive components. The measured impedances of the tantalum capacitor are 0.15 +j0.75 Ω and 0.84 + j15.7 Ω at 100 MHz and 2.14 GHz, respectively. The parasitic inductive impedance, which is approximately 1.2 nH, was used for blocking the fundamental signal instead of L_e. Of course, the inductance should be resonated out by the fundamental matching circuit. It should be noted that the tantalum capacitor, used for the memory effect control, is on the matching circuit, not on the bias line. The gate and drain bias voltages are supplied through the quarter-wave transmission lines which are used to design the conventional narrowband PA. The characteristic impedances of the lines are 50 Ω and the bias voltages are V_{GG} = 4.063 and V_{DD} = 27 V, respectively. The amplifier operates in class-AB mode with a quiescent drain current of 850 mA.

In order to investigate the effect of the tantalum capacitors, the simulations have been performed for four cases: (1) without the tantalum capacitors; (2) with the tantalum capacitor on the gate only; (3) with

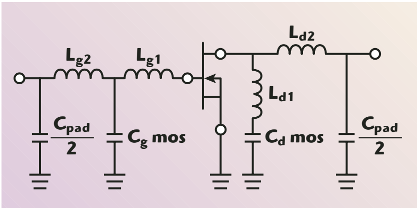

▲ *Fig. 4 Equivalent circuit of half of the packaged MRF5S21090 LDMOS.*

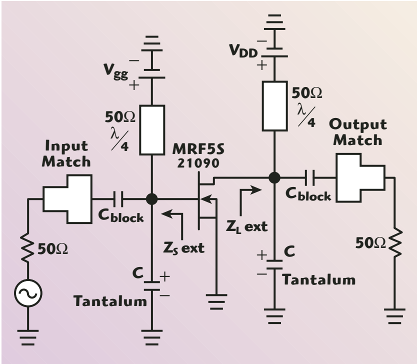

▲ *Fig. 5 Circuit diagram for the MRF5S21090 LDMOS.*

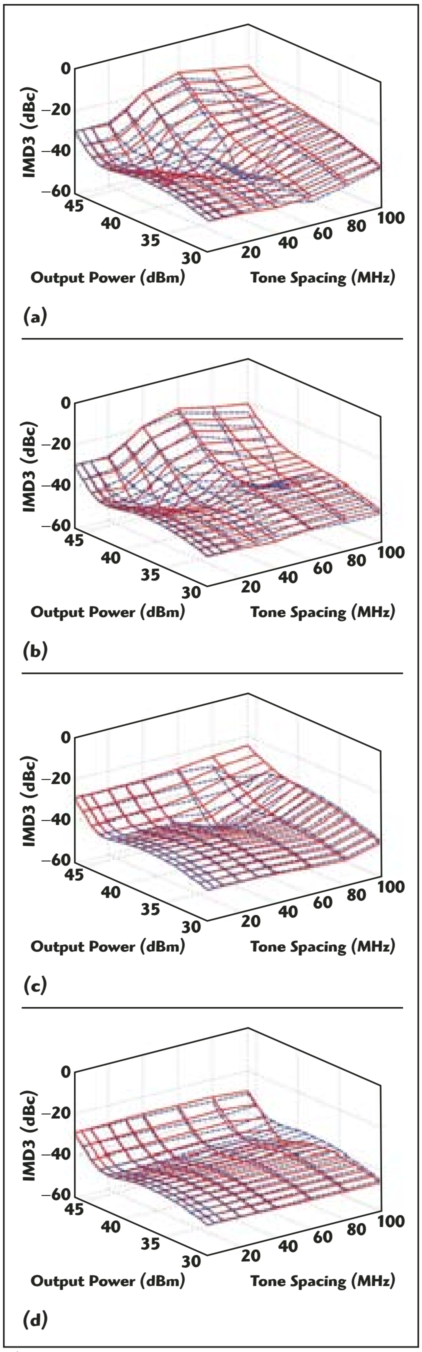

▲ *Fig. 6 Simulation results for the two-tone signals; (a) without capacitors, (b) with a capacitor on the gate only, (c) with a capacitor on the drain only and (d) with capacitors on both gate and drain.*

the tantalum capacitor on the drain only; and (4) with the tantalum capacitors on both the gate and drain. In all cases, the input and output matching circuits have been optimized to have the same fundamental impedances, $Z_{S,ext}$ (2.14 GHz) = 2.08 –j3.54 Ω and $Z_{L,ext}$ (2.14 GHz) = 2.15 –j2.0 Ω, and for a gain flatness within 0.2 dB over the 100 MHz bandwidth and high linearity for a two-tone signal with 1 MHz tone spacing. The simulation results for the two-tone signals are shown in ***Figure 6***. The IMD3 (power ratio of IM3 to the fundamental signal) has been plotted as a function of the average output power and the two-tone spacing. The output power has been swept from 30 to 46 dBm in 1 dB steps for tone spacings of 1, 5, 10, 20, 30, 40, 60, 80 and 100 MHz. The red and blue lines represent the upper and lower limits of IMD3 (IMD3U and IMD3L), respectively. The simulation results show that the proposed PA of case 4 has a drastically reduced memory effect and an improved IMD performance for all tone spacings compared to the conventional one. Thus, it is clear that the envelope component is more important than the second harmonic for the device, since only the envelope has been controlled. The following additional information can be obtained:

- For a narrow-band signal, the quarter-wave transmission line can provide sufficient short for the envelope signal and the memory effect is not important.
- For a medium-band signal, the drain envelope voltage is the dominant component for the memory effect and linearity.
- For a low power and wideband signal, the gate envelope voltage is more important than the drain one. It may be due to the larger multiplication factor than for the drain envelope.
- For a high power and wideband signal, the drain envelope voltage is more important than the gate voltage but both the gate and drain envelope voltages should be controlled to reduce the memory effect and nonlinearity.

As a result, the best way is to minimize both the gate and drain envelope impedances.

EXPERIMENTAL RESULTS

Wideband Performance Test Using Multi-carrier WCDMA Signals

For experimental demonstration, two PAs have been implemented, with and without the tantalum capacitors (cases 1 and 4), at 2.14 GHz using the MRF5S21090 LDMOS transistors and RF35 printed circuit boards. The PAs have been optimized to have similar performance in gain flatness and linearity to a down-link WCDMA 1FA signal at the same bias point, V_{DD} = 27 V and I_{DSQ} = 850 mA. ***Figure 7*** shows the measured small-signal gains and power spectral densities (PSD) at an average output power of 40 dBm. The drain efficiencies of the two amplifiers are nearly the same, approximately 18.5 percent at 40 dBm. The PAs deliver flat gains within 0.2 dB over a 100 MHz bandwidth and adjacent channel leakage ratios (ACLR) of approximately –38 dBc.

Like for the simulation, the two PAs have been tested for the two-tone signal. ***Figure 8*** shows the measured IMD3. The IMD5 has also been measured and the results are shown in ***Figure 9***. For convenience, their cross sectional view at 40 dBm is shown in ***Figure 10***. The proposed PA, with the tantalum capacitors, displays a state-of-the-art IMD perfor-

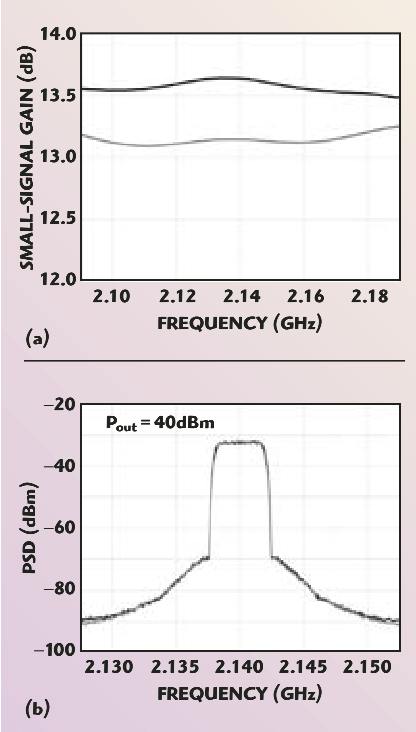

Fig. 7 The measured small-signal gain (a) and WCDMA 1FA spectra (b) at 40 dBm for the conventional (w/o tantalum capacitors) and the proposed (with tantalum capacitors) PAs.

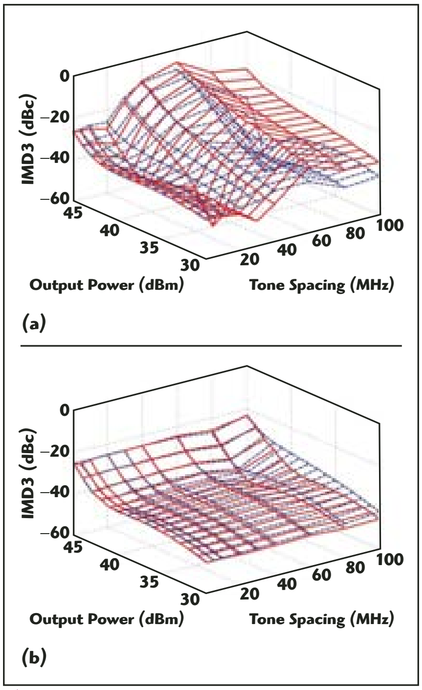

Fig. 8 Measured IMD3 for the two-tone signals (a) without tantalum capacitors and (b) with tantalum capacitors.

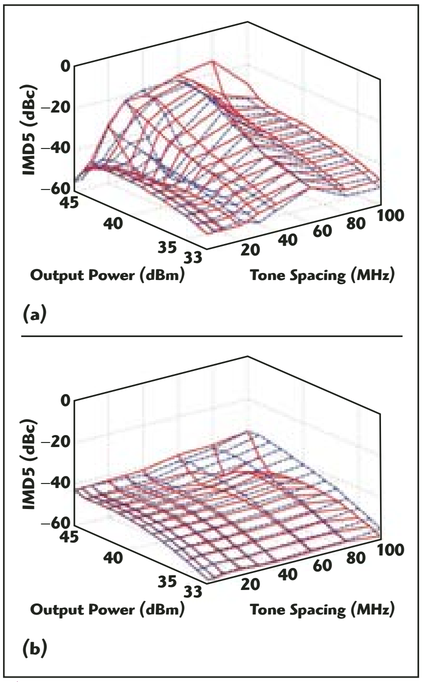

Fig. 9 Measured IMD5 for the two-tone signals (a) without tantalum capacitors and (b) with tantalum capacitors.

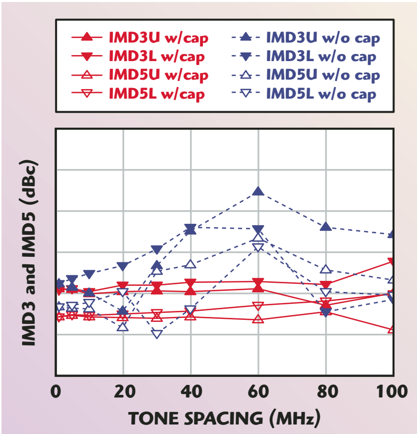

Fig. 10 IMD3 and IMD5 measured at 40 dBm.

TABLE II

AVERAGE OUTPUT POWER MEASURED AT –35 dBc ACLR ACCORDING TO THE NUMBER OF WCDMA SIGNAL CARRIERS

Number of Carriers (FA)	Signal Bandwidth (MHz)	Output Power (dBm)	PAR @ 0.01% CCDF (dB) (Number of Signal Source (EA))
4	20	40.3	9.82 (1)
6	30	40.0	10.23 (1)
8	40	40.3	9.82 (2)
12	60	40.0	10.23 (2)
16	80	39.6	11.30 (2)
20	100	38.9	12.43 (2)

mance in terms of memory effect and linearity. It has an asymmetry of less than 2 dB up to 60 MHz tone spacing for the IMD3 and up to 40 MHz for the IMD5, over all power levels. In order to show the instantaneous wideband performance of the proposed PA, it has been tested for the WCDMA 4, 6, 8, 12, 16 and 20 FA signals, which have 20, 30, 40, 60, 80 and 100 MHz bandwidths, respectively. The 4 and 6 FA signals are generated using Agilent's E4438C signal generator and the remainders using two generators. The test method is to measure the average output power at –35 dBc ACLR for the respective signals and the results are shown in ***Table 2***, together with the signal information. The test result shows that the performance of the proposed PA is mainly dependent on the peak-to-average power ratio (PAR), but not on the signal bandwidth. This is due to the extended instantaneous bandwidth of the PA. ***Figure 11*** shows the measured power spectral densities (PSD) for the WCDMA 12 and 20 FA signals. For the comparison, the spectra of the conventional PA have been also displayed. The proposed PA delivers a linear power amplification performance for a wideband signal compared to the conventional one.

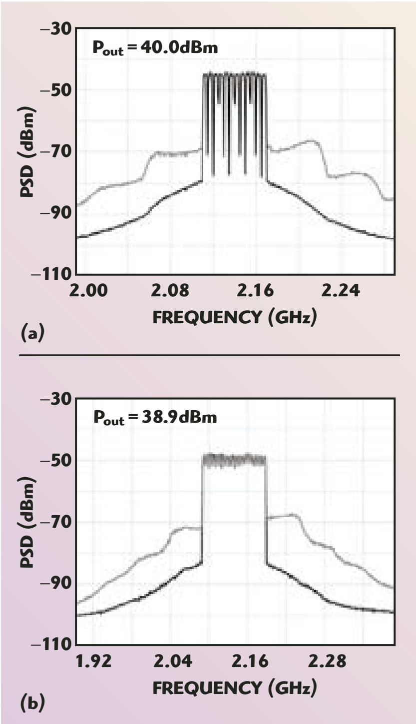

▲ *Fig. 11 Measured WCDMA 12 (a) and 20FA (b) spectra for amplifiers with and without tantalum capacitors.*

Predistortion Linearization Test for Confirming the Reduced Memory Effect

In order to confirm the reduced memory effect, the output spectra of the two PAs have been compared for a WCDMA 4FA signal with 20 MHz bandwidth and linearized the pro-

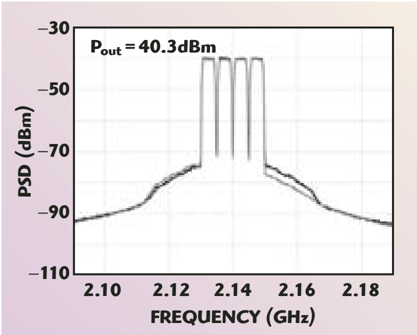

▲ *Fig. 12 Measured WCDMA 4FA spectra for PAs with and without tantalum capacitors.*

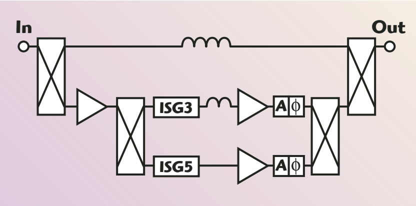

▲ *Fig. 13 Block diagram of the implemented third- and fifth-order analog predistorter.*

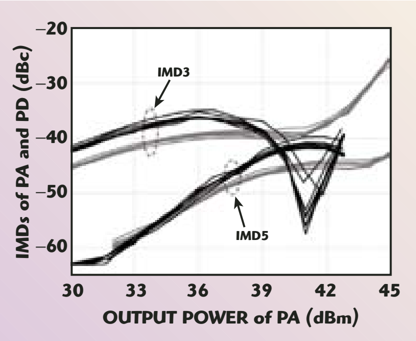

▲ *Fig. 14 Measured two-tone (up to 2 MHz spacing) characteristics of the PA and PD.*

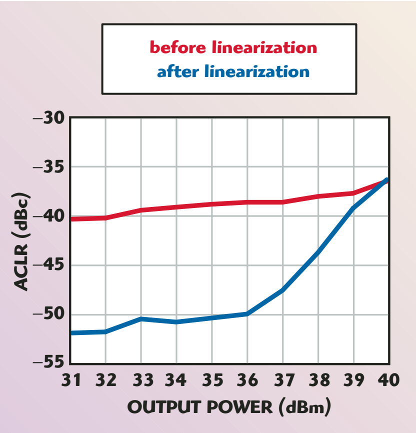

▲ *Fig. 15 Measured ACLR for the WCDMA 4FA signal before and after linearization.*

posed PA using an analog predistorter (PD). It is a good approach, since the memory effect restricts mainly the linearization level of PDs. ***Figure 12*** shows the measured WCDMA 4FA spectra, which deliver an average output power of 40.3 dBm with an ACLR of approximately –35 dBc. As predicted, the proposed PA delivers a well-balanced spectrum but the conventional one does not.

A third- and fifth-order analog PD was constructed to linearize the proposed PA. The block diagram for the implemented PD is given in ***Figure 13***.[6] The two-tone characteristics for the proposed amplifier and PD up to 20 MHz tone spacing are represented in ***Figure 14***. As shown, the IMD characteristics between the PA and PD are similar up to the output power of about 39 dBm, implying that the PA can be linearized below that power if it is memory-less.[2] ***Figure 15*** shows the linearization result for the WCDMA 4FA signal. The PA has been linearized by more than 11 dB at average output powers below 36 dBm. If the IMD characteristic of the PD at high power levels is similar to that of the PA, a better linearization performance could be achieved at the high power levels. Nevertheless, the test results are sufficient to show that the memory effect of the proposed PA is drastically reduced. Contrary to the low memory PA, the conventional PA does not produce any significant error cancellation, less than 2 dB linearization.

CONCLUSION

The IM3 components of a power amplifier have been analyzed using third-order power series. The envelope and second harmonic voltages create additional nonlinear components over the internal IM3 generation. The voltages are major sources of memory effect. They can be eliminated by providing a short at the envelope and second harmonic frequencies on the gate and drain terminals of the device. But there are some practical limits for reduced impedances. Through analysis and simulation, it was proved that the envelope voltage is a more important source than the second harmonic for the memory effect and linearity. In order to minimize the memory effect and extend the instantaneous bandwidth, the envelope signals have been shorted using a large capacitor and small inductor. The inductor is practically a short at the envelope frequency, but has a high impedance at the fundamental frequency. The circuit can be realized using a large tantalum capacitor, with its parasitic inductive impedance of about 1.2 nH used to block the fundamental signal, instead of using additional inductors. For two-tone signals with up to 100 MHz tone spacing, the contributions to the memory effect and nonlinearity of the gate and drain envelope voltages have been simulated according to tone spacings and power levels. The simulation results have displayed the drastically reduced memory effect and the improved IMD performance for the proposed amplifier.

For the experiment, the proposed amplifier has been implemented using Freescale's MRF5S21090 LDMOSFET with a 90 W PEP at 2.14 GHz and tested using two-tone and downlink multi-carrier WCDMA signals. For the two-tone signals, the experimental results are similar to the simulation. For the multi-carrier down-link WCDMA signals up to 20 FA, with a 100 MHz signal bandwidth, a nearly bandwidth-independent linearity characteristic has been found for the amplifier. The proposed amplifier has delivered well-balanced and considerably linearized spectra for the multi-carrier WCDMA signals, up to 20 FA, compared to the conventional one. The reduced memory effect could be confirmed by a predistortion linearization test for a WCDMA 4FA signal. These experimental results demonstrate clearly that the proposed power amplifier is the best performing wideband amplifier for next generation base station applications. ■

ACKNOWLEDGMENTS

This work was supported in part by the Telecommunication R&D Center of Samsung Electronics Co. Ltd. and the Korean Ministry of Education under the BK21 project.

References

1. J. Vuolevi and T. Rahkonen, *Distortion in RF Power Amplifiers*, Artech House Inc., Norwood, MA, 1999.
2. J. Cha, J. Yi, J. Kim and B. Kim, "Optimum Design of a Predistortion RF Power Amplifier for Multi-carrier WCDMA Applications," *IEEE Transaction on Microwave Theory and Techniques*, Vol. 52, No. 2, February 2004, pp. 655–663.
3. S.C. Cripps, "*Advanced Techniques in RF Power Amplifier Design*," Artech House Inc., Norwood, MA, 2002.
4. A. Rabany, L. Nguyen and D. Rice, "Memory Effect Reduction for LDMOS Bias Circuits," *Microwave Journal*, Vol. 46, No. 2, February 2003, pp. 124–130.
5. J.S. Kenney and A. Leke, "Design Considerations for Multi-carrier CDMA Base Station Power Amplifiers," *Microwave Journal*, Vol. 42, No. 2, February 1999, pp. 76–84.
6. J. Yi, Y. Yang, M. Park, W. Kang and B. Kim, "Analog Predistortion Linearizer for High Power RF Amplifier," *2000 IEEE MTT-S International Microwave Symposium Digest*, Vol. 3, pp. 1511–1514.
7. N.B. de Carvalho and J.C. Pedro, "Two-tone IMD Asymmetry in Microwave Power Amplifiers," *2000 IEEE MTT-S International Microwave Symposium Digest*, Vol. 1, pp. 445–448.
8. J.C. Pedro and N.B. de Carvalho, "A Comprehensive Explanation of Distortion Sideband Asymmetries," *IEEE Transactions on Microwave Theory and Techniques*, Vol. 50, No. 9, September 2002, pp. 2090–2101.
9. W. Piet and S. Willy, *Distortion Analysis of Analog Integrated Circuits*, Kluwer Academic Publishers, 2001.

Jeonghyeon Cha *received his BS degree in electronics and information from Chon-buk National University, Jeonju, Korea, in 2001, and is currently working toward his PhD degree at the Pohang University of Science and Technology (POSTEC), Pohang, Korea. His research interests include RF power amplifier design, linearization techniques and efficiency improving techniques.*

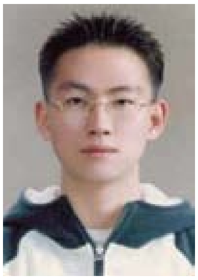

Ildu Kim *received his BS degree in electronics and information engineering from Chon-nam National University, Kwangju, Korea, in 2004. He is currently working toward his PhD degree at the Pohang University of Science and Technology, Pohang, Gyungbuk, Korea. His research interests include RF power amplifier design and linearity and efficiency improvement techniques.*

Sungchul Hong *received his BS degree in electrical and electronic engineering from Yonsei University, Seoul, Korea, in 2003, and is currently working toward his MS degree at the Pohang University of Science and Technology, Pohang, Gyungbuk, Korea. His research interests include RF power amplifier design and digital predistortion techniques.*

Bumman Kim *received his PhD degree in electrical engineering from Carnegie-Mellon University, Pittsburgh, PA, in 1979. From 1978 to 1981, he was engaged in fiber-optic network component research with GTE Laboratories Inc. In 1981, he joined the central research laboratories, Texas Instruments Inc., where he was involved in the development of GaAs power field-effect transistors and monolithic integrated circuits. He has developed a large-signal model of a power FET, dual-gate FETs for gain control, high power distributed amplifiers and various millimeter-wave MMICs. In 1989, he joined the Pohang University of Science and Technology, Pohang, Korea, where he is a professor in the electronic and electrical engineering department, and director of the microwave application research center, where he is involved in device and circuit technology for RFICs.*

Jong Sung Lee *received his BS degree in radio sciences and communication engineering from Honjik University, Seoul, Korea, in 1996. He has been working in the area of high power amplifiers for base stations at Samsung Electronics in South Korea since 1996. He is currently a senior engineer at Samsung Electronics Telecommunication R&D Center.*

Han Seok Kim *received his BS degree from Yonsei University, Seoul, Korea, in 1990, his MS degree in electrical engineering from the University of Illinois at Urbana-Champaign in 1993, and his PhD degree from the University of Illinois in 2004. Between 1994 and 2000, he worked at LG Electronics Inc., South Korea, where his primary research included microwave systems and power applications. He is currently a principal engineer at Samsung Electronics Telecommunication R&D Center, working on high power amplifiers and RF systems. His research interests include RF and microwave amplifiers, wireless communication systems architectures and circuits, electromagnetic and radio wave propagation, RF instrumentation and microwave power applications.*

DUAL-BAND ASSEMBLY OF INTEGRATED SHORT BACKFIRE ANTENNAS

A dual-frequency assembly of two short backfire (SBF) antennas, one large for low frequencies (LF) and one small for high frequencies (HF), is described in this article. The two antennas are located on the same axis and, since they have a common reflector, are regarded as integrated. Such integration is cost-effective, compact, robust and simple to build. Simple design equations for the octagonal reflectors are proposed in this article and a method of moment (MoM)-based electromagnetic solver was utilized for a numerical study of two SBF antenna constructions: a 3 GHz single (not integrated) antenna and a 1.2/4.8 GHz dual-frequency antenna assembly. The accuracy of the design and numerical analysis procedure was confirmed by comparing the results obtained for the 3 GHz octagonal SBF, with reliable experimental data of an antenna prototype with circular reflectors. The single 1.2 and 4.8 GHz octagonal SBF antennas were found to have gain values of 14.4 and 15 dB, respectively, while the corresponding values for the integrated version are 14.2 and 15.4 dB.

The short backfire (SBF) is a highly effective aperture antenna of simple and compact construction. Basically, it consists of three elements: two parallel reflectors, large and small, spaced a half-wavelength apart, which form a leaky resonant cavity, and a cavity feed (half-wave dipole,[1–3] waveguide or horn,[4,5] or microstrip antenna[6,7]). The large and small antenna reflectors are usually circular in shape and have diameters that may vary within the ranges $(1.5–2.3)\lambda_0$ and $(0.3–0.65)\lambda_0$, respectively. However, from classical gain, bandwidth, match and size considerations, the large reflector is typically set to $2\lambda_0$ and the small reflector to $0.5\lambda_0$. The dipole feed is positioned at the mid-point between reflectors, that is at a distance $0.25\lambda_0$ from each of them. Here, λ_0 is the antenna resonant (design) wavelength. As a rule, the large reflector is fit with a quarter- or half-wavelength wide rim, which results in side lobe and back lobe pattern reduction and a gain increase. The SBF antenna dimensions given above are based on the extensive experience of many researchers[8] and provide the reference for this work.

H.D. HRISTOV AND R. FEICK
Universidad Técnica Federico Santa María
Valparaíso, Chile
R.J. URUMOV AND G.S. KIROV
Technical University of Varna
Bulgaria

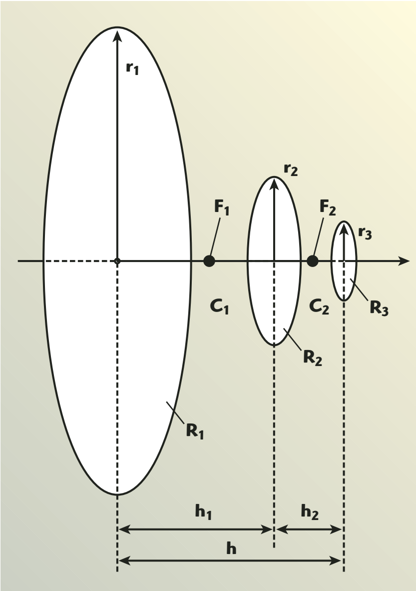

▲ *Fig. 1 Geometry of a dual-band SBF antenna assembly with circular reflectors.*

Henceforth, they are referred to as standard dimensions. Although often circular, the backfire reflectors can have various shapes: polygonal (square, hexagonal, octagonal), elliptical, etc. The short backfire antenna has been used extensively as a directive building element in various single-band broadside arrays.[9,10] A dual-frequency assembly (array) of two short backfire antennas (large or LF and small or HF) is described in this article. The antennas are arranged on the same axis and, since they have a common reflector, are regarded as integrated. In this way, the following advantageous effects are achieved. First, the common reflector plays two roles at once: as a small reflector for the LF antenna and as a large reflector for the HF antenna. Second, the blocked aperture region, resulting from the small reflector of the LF antenna, is exploited for the HF antenna. Such integration makes the SBF assembly simple to build, compact and robust. For standard radii of the disk reflectors, the low and high design frequencies of the two dipole-fed antennas should be in the standard proportion 1:4.[1,2] Circular (disk) reflectors are frequently replaced by polygonal, and, in particular, by octagonal reflectors, which are close in shape to the circular ones and are very practical for construction.[11,12] This article's first author originally introduced the dual-band assembly of two integrated octagonal short back-

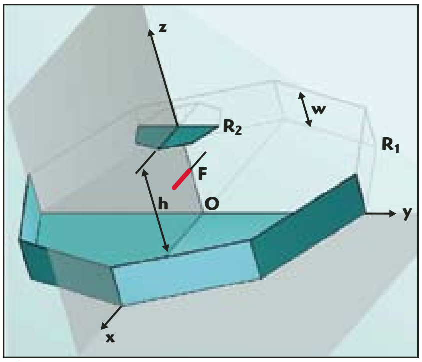

▲ *Fig. 2 Half portion of a single SBF antenna computer-simulated model.*

fire antennas.[8] This SBF antenna system was employed 25 years ago in an UHF earth station for satellite tracking and space telemetry that operated at the frequencies 137 and 470 MHz, that is for a reflector design frequency ratio of 1:3.43, which differs from the standard frequency proportion. At that time, the dual-frequency SBF antenna assembly was designed based on approximated analytical equations and was optimized experimentally by means of the conventional "cut and try" routine. The work reported here started with the design of a single 3 GHz SBF antenna with octagonal reflectors. The resultant numerically obtained radiation parameters were checked against experimental ones for a SBF antenna with circular reflectors,[3] and found equivalent in gain. This allowed a validation of the design procedure. Next, the SBF antenna design and numerical procedures were extended to the axial arrangement of two integrated octagonal SBF antennas, large and small, and tuned respectively at 1.2 and 4.8 GHz, according to the optimum frequency proportion of 1:4. In contrast with the previous dual-band SBF antenna development, the availability of specialized electromagnetic tools, such as the method of moments (MoM)-based WIPL-D software,[13] now allows a more rapid, thorough and precise design process.

BASIC GEOMETRY OF TWO INTEGRATED SHORT BACKFIRE ANTENNAS

Figure 1 shows the basic configuration of a dual-frequency assembly of two integrated SBF antennas, stacked along the Z axis. The disk reflectors are specified as R_1, R_2 and R_3. They have radii r_1, r_2 and r_3, correspondingly, which are chosen here equal to the standard values

$$r_1 = \lambda_{1,0}$$
$$r_2 = 0.25\lambda_{1,0} = \lambda_{2,0}$$
$$r_3 = 0.25\lambda_{2,0} \qquad (1)$$

where $\lambda_{1,0}$ and $\lambda_{2,0}$ are the two design wavelengths.

The reflector doublets R_1R_2 and R_1R_3 form the two open SBF resonant cavities (antennas) C_1 and C_2 of axial lengths $h_1 \approx 0.5\ \lambda_{1,0}$ and $h_2 \approx 0.5\ \lambda_{2,0}$, respectively. Thus, the total antenna length is $h = h_1 + h_2 \approx 0.625\ \lambda_{1,0} \approx 2.5\ \lambda_{2,0}$. The second disk reflector R_2 is common to the two antenna cavities and acts as a small reflector for the cavity C_1 and a large reflector for the cavity C_2, that is the two SBF cavities (antennas) are integrated in one double-frequency structure. The cavities are fed by single-wire half-wave dipoles, F_1 and F_2, respectively, and are matched to their feed cables at the design frequencies $f_{1,0} = c/\lambda_{1,0}$ and $f_{2,0} = \lambda c/\lambda_{2,0}$. Here, c = 3 10^8 m/s is the free-space wave velocity. From Equation 1, it follows that the frequency ratio $k_f = f_{2,0}/f_{1,0}$ is equal to four as is the ratio between the disk radii, $r_I/r_{I+I} = k_f = 4$, i = 1,2.

COMPUTER-AIDED DESIGN: VALIDATION OF THE METHODOLOGY FOR SINGLE SHORT BACKFIRE ANTENNA WITH OCTAGONAL REFLECTORS

Figure 2 shows the half portion of the 3D computer simulation model of a single SBF antenna. The antenna comprises two octagonal reflectors, the rimmed large reflector R_1 and the planar small reflector R_2, made of a metal sheet of thickness t = 2 mm. The leaky cavity formed by the reflectors is fed through a half-wave dipole F positioned in the middle of them. The reflector rim has a half-wavelength width. The general n-sided polygonal reflector is regarded as a good approximation to the disk reflector when both have equal surfaces.[13] This condition is satisfied if the j-th (j = 1 or 2) polygonal reflector is inscribed into the corresponding circle of equivalent radius r'_j given by

$$r'_j = r_j \sqrt{\frac{2\pi}{n \sin\left(\frac{2\pi}{n}\right)}} \qquad (2)$$

where r_j is equal to $r_1 = \lambda_0$ or $r_2 = 0.25\lambda_0$, the radius of the respective large and small circular reflectors, where λ_0 is the design wavelength.

In the case of octagonal reflectors $n = 8$ and $r'_j = 1.054r_j$, and thus, for the single octagonal reflector SBF antenna, Equation 1 yields

$$r'_1 = 1.054r_1$$
$$r'_2 = 1.054r_2 = 0.264\lambda_0 \qquad (3)$$

The circular reflectors of radii r_1 and r_2, and the equal-in-surface octagonal reflectors of radii r'_1 and r'_2, respectively, are projected together in the transverse plane x0y, as shown in ***Figure 3***. A design frequency of 3 GHz was chosen to compare the computational results with the reliable experimental data for a SBF antenna that, as part of separate research, was built and measured at AFCRL.[3] The present numerical

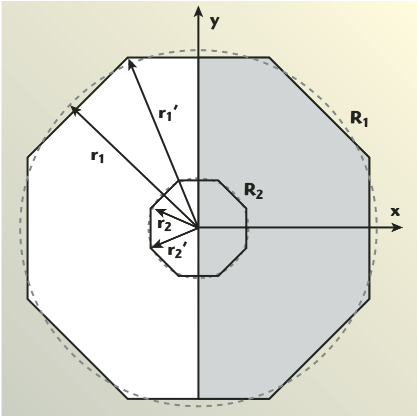

▲ *Fig. 3 xOy-plane projection of the computer-simulated model of the half portion of a single octagonal SBF antenna.*

TABLE I

DIMENSIONS AND RADIATION PARAMETERS OF 3 GHz ANTENNAS WITH CIRCULAR AND EQUIVALENT OCTAGONAL REFLECTORS

Basic Dimensions and Parameters
Big reflector diameter (mm) $2\gamma_1 = 200\ (2\lambda_0)$* $2\gamma'_1 = 210.8\ (2.11\lambda_0)$**
Small reflector diameter (mm) $2\gamma_2 = 50\ (0.5\lambda_0)$* $2\gamma'_2 = 52.7\ (0.527\lambda_0)$**
Distance between big reflector and dipole feed (mm) 25 $(0.25\lambda_0)$*
Distance between big and small reflector (antenna length) (mm) 50 $(0.5\lambda_0)$*
Rim depth (mm) 50 $(0.5\lambda_0)$*
Metal sheet thickness (mm) 2**
Directive gain (dB) 15.1* 14.7**
Aperture efficiency (%) 83* 76**
Half-power beamwidth 34°* 34° average**
First side lobe level (dB) ≤–22* ≤–23**
Back lobe level (dB) < –30* < –27**
Max. cross-polar level (dB) –21 (at 45° plane)**
*Standard Prototype with Disk Reflectors[3,8] **Computer-simulated Model with Octagonal Reflectors

treatment considers octagonal reflectors designed according to Equations 2 and 3, and the analysis was made by means of the WIPL-D electromagnetic software. The measured and numerical dimensions and radiation parameters of the circular SBF prototype and its equivalent octagonal model are summarized and compared in ***Table 1***.

The WIPL-D simulated numerical patterns of the 3 GHz octagonal model and the experimental patterns of the corresponding AFCRL circular prototype are shown in ***Figure 4*** for the E-plane and the H-plane cuts. As seen, the octagonal-reflector antenna has numerical radiation parameters very close to those measured for the corresponding circular-reflector prototype. This provides evidence that Equations 1 and 3, introduced by the authors, and the numerical simulation procedure, are well suited for the design of equivalent octagonal reflector SBF antennas and assemblies. The resonant input resistance of the free-space located single-wire feed dipole, with a 0.005 to 0.01 radius to lambda ratio, ranges from approximately 60 to 70 Ω and is therefore roughly matched to a 50 Ω cable. But, placed between the two reflectors, its input resistance decreases to approximately 17 to 20 Ω, which corresponds to a VSWR of 3.0 to 2.5. A better input match can be achieved by using an appropriate matching device, which may cause additional antenna loss and bandwidth reduction. The present work has shown that, in the case of a short backfire antenna, a very good input match to a 50 Ω cable is possible by using one of the following two techniques: a feed antenna with much greater free-space input resistance, 300 Ω folded dipole, for instance,[14] or a small deviation from the standard half-wavelength SBF antenna length. In both cases, the feed dipole is positioned in the middle between the reflectors.

The input match for three versions of the SBF antenna is illustrated in

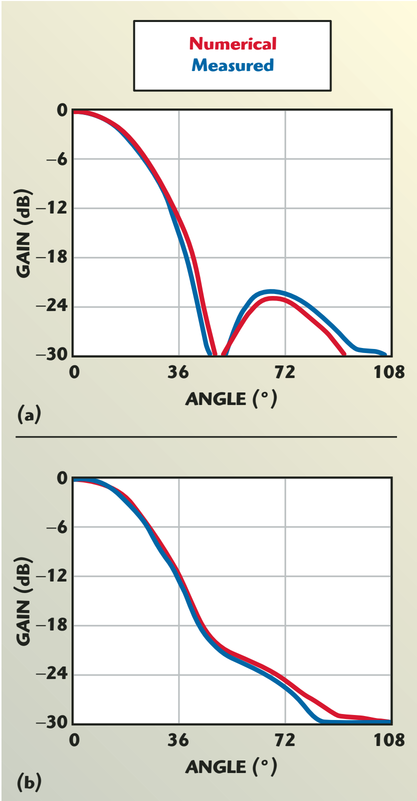

▲ *Fig. 4 Computer-simulated and measured gain radiation pattern of a 3 GHz single BF antenna; (a) E-plane and (b) H-plane.*

Figure 5, where the reflection coefficient S_{11} is drawn versus the frequency. Case 1 is for a standard-size SBF antenna fed by a single-wire half-wave dipole with a diameter of 1.5 mm and a length of 20.7 mm, or equal to 0.207λ. For the design frequency f_0 = 3 GHz, S_{11} is –7.25 dB. This corresponds to a VSWR (at f_0) of 2.45, or to a mismatch power loss of 0.9 dB. Case 2 is for the same standard-size SBF antenna but fed by a folded two-wire dipole, 5 mm in width and 17.5 mm in length. The first dipole wire, in the center of which the feed terminals are located, is 2 mm in diameter, while the second dipole wire has a diameter of 1.5 mm. In Case 3, the SBF antenna is similar to that of Case 1 with the only difference that the antenna length is slightly increased for better impedance match: from $0.5\lambda_0$ (50 mm) to $0.56\lambda_0$ (56 mm). The minimum or design frequency values of S_{11} in Case 2 and Case 3 are smaller than –40 dB, which is far below the –10 dB level. It is known that the free-space single-wire half-wave dipole has a smaller input bandwidth than the corresponding folded (two-wire) dipole. Placed in the cavity of the increased-length SBF antenna, the single-wire dipole has a bandwidth of 6.2 percent, which is much greater than the bandwidth of 2.8 percent for the SBF antenna fed by the folded dipole. The SBF antenna rim width is not very important for the input match quality, but it plays a key role for the antenna gain, radiation pattern shape and polarization. If w =0, the SBF antenna with octagonal reflectors has a gain of 13.2 dBi, which is 1.8 dB below the gain of the SBF antenna with a half-wave rim (see Table 1).

DESIGN OF TWO INTEGRATED SHORT BACKFIRE ANTENNAS WITH OCTAGONAL REFLECTORS

Based on the previous results, a system of two integrated SBF antennas (see ***Figure 6***) is considered, compris-

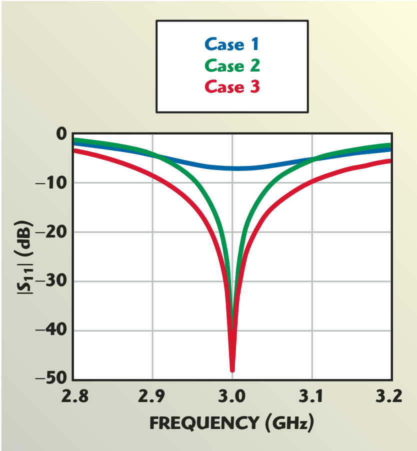

▲ *Fig. 5 Magnitude of S_{11} for three different cases.*

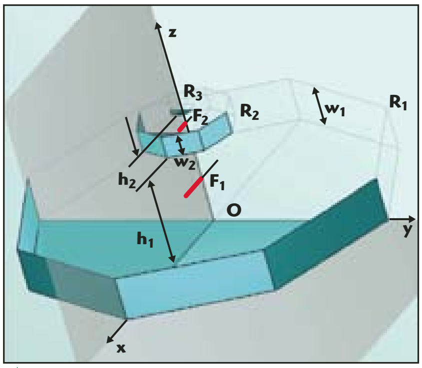

▲ *Fig. 6 Half portion of an integrated octagonal short SBF antenna computer-simulated model.*

ing three octagonal rather than circular reflectors, R_1 and R_2 (rimmed) and R_3 (not rimmed), and two half-wave dipoles as feeds, F_1 and F_2. As was found from Equation 2, in the case of octagonal reflectors $r'_j = 1.054 r_j$, and thus Equations 1 are modified here to

$$r'_1 = 1.054\lambda_{1,0}$$
$$r'_2 = 0.264\lambda_{1,0} = 1.054\lambda_{2,0}$$
$$r'_3 = 0.264\lambda_{2,0} \qquad (4)$$

In ***Table 2***, the basic dimensions of a dual-band assembly consisting of two SBF integrated octagonal antennas are summarized for the respective design frequencies (wavelengths): $f_{1,0}$ = 1.2 GHz ($\lambda_{1,0}$ = 250 mm) and $f_{2,0}$ = 4.8 GHz ($\lambda_{2,0}$ = 62.5 mm). The reflector radii r'_1, r'_2 and r'_3 have been calculated from Equations 2 and 4, and the half-wave rim widths w_1 and w_2 of reflectors R_1 and R_2 were set to $0.25\lambda_{1,0}$ and $0.5\lambda_{2,0}$, respectively. For the given dipole-wire radii, $a_1 = 0.008\lambda_{1,0}$ and $a_2 = 0.008\lambda_{2,0}$, the rest of the dimensions, that is the individual antenna lengths h_1 and h_2 and the feed-dipole resonant lengths l_1 and l_2, were found by computer optimization for best possible gain and input match to a 50 Ω cable. In both antennas, a good input match was produced by a small increase of the standard half-wavelength antenna length, 5.2 percent for the LF antenna and 16.2 percent for the HF antenna. As seen from Table 2, the optimum antenna lengths h_1 and h_2 expressed in the corresponding design wavelengths are different, which is due to the dissimilarity in their rim widths w_1 and w_2, joint antenna positioning and electromagnetic influence. The total antenna length includes also the second reflector thickness t_2, or $h = h_1 + h_2 + t_2$. In order to increase the compactness of the overall design, the rim of the large reflector R_1 was chosen as $\lambda_{1,0}/4$, whereas for the HF antenna, gain improvement results from choosing the rim of the common reflector R_2 as $\lambda_{2,0}/2$. The radiation patterns of the optimized single and integrated octagonal short backfire antennas are subsequently presented. ***Figure 7*** illustrates the co-polar (a) and cross-polar (b) 45°-plane gain radiation patterns of the 1.2 GHz single and integrated SBF anten-

TABLE II

DIMENSIONS OF DUAL-BAND ASSEMBLY OF OCTAGONAL SBF ANTENNAS FOR DESIGN FREQUENCIES (WAVELENGTHS) 1.2 GHz (250 mm) AND 4.8 GHz (62.5 mm)

r'_1 = 263.5mm or $1.054\lambda_{1,0}$
r'_2 = 65.9 mm or $0.264\lambda_{1,0}$
r'_3 = 16.5 mm or $0.264\lambda_{2,0}$
w_1 = 62.5 mm or $0.250\lambda_{1,0}$
w_2 = 31.2 mm or $0.500\lambda_{2,0}$
h_1 = 131.5 mm or $0.526\lambda_{1,0}$
h_2 = 36.3 mm or $0.581\lambda_{2,0}$
h = 169.3 mm or $0.667\lambda_{1,0}$
α_1 = 2.0 mm or $0.008\lambda_{1,0}$
α_2 = 0.5 mm or $0.008\lambda_{2,0}$
l_1 = 48.9 mm or $0.196\lambda_{1,0}$
l_2 = 10.5 mm or $0.168\lambda_{2,0}$
t_1 = 2.5 mm or $0.010\lambda_{1,0}$
t_2 = 1.5 mm or $0.024\lambda_{2,0}$

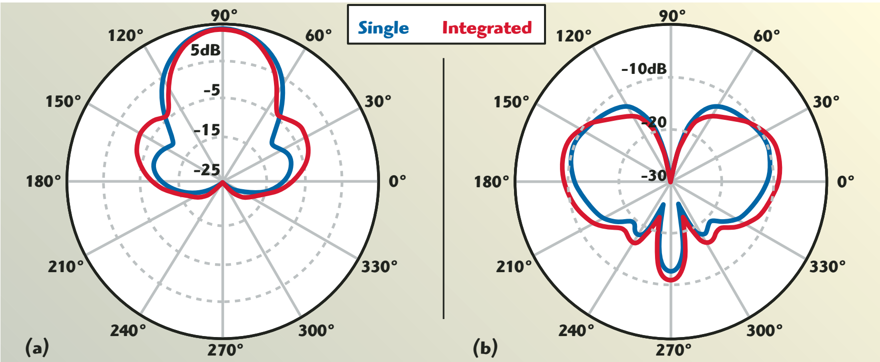

Fig. 7 Co-polar (a) and cross-polar (b) 45°-plane radiation patterns of 1.2 GHz single and integrated SBF antennas.

nas. As seen from these figures, the integrated short backfire antennas have radiation patterns that do not differ much from those of the single backfire antennas. The co-polar 45°-plane patterns of the single and integrated antennas are close except in the side lobe regions, where the electromagnetic shadowing by the small antenna causes approximately a 5 dB increase in the side lobe levels. It is found that the antenna integration produces a gain reduction of only 0.2 dB and a maximum cross-polarization increase of 1.4 dB. Similar co-polar and cross-polar radiation patterns of the single and integrated 4.8 GHz antennas are shown in ***Figure 8***. Here the integration does not produce a gain reduction but a gain enhancement of 0.4 dB. This apparent inconsistency in the gain behavior may be attributed to the difference in the rim widths and to the dissimilarity in the electromagnetic shadowing and mutual input coupling. Because the feed dipoles of the two SBF antennas are well isolated by their leaky wave cavities, the mutual coupling between the

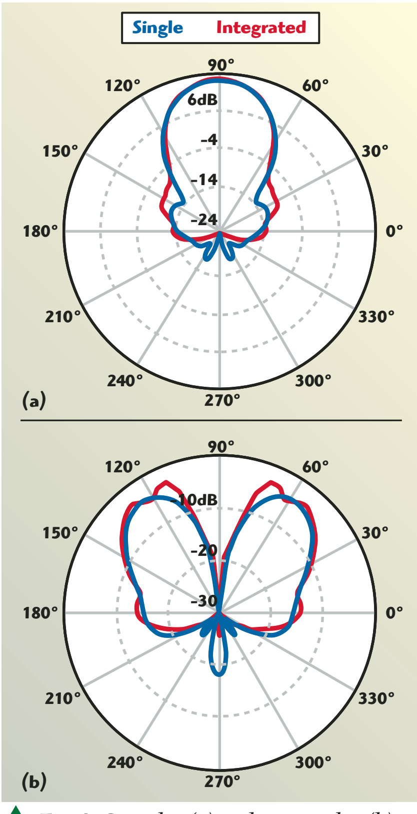

Fig. 8 Co-polar (a) and cross-polar (b) 45°-plane radiation patterns of 4.8 GHz single and integrated SBF antennas.

two feed ports is very small, less than –50 dB at the LF port and less than –35 dB at the HF port.

In both LF and HF SBF antennas, the size adjustment resulting from the optimization process does not significantly deteriorate the original or standard-size antenna radiation patterns. ***Figures 9*** and ***10*** show the co-polar radiation patterns of the 1.2 GHz and 4.8 GHz integrated SBF antennas in three cut planes: E-plane, 45°-plane and H-plane. It is seen that the main lobe of the 1.2 GHz antenna has an almost rotational symmetry, which does not hold for the 4.8 GHz antenna main lobe and for the side lobes of both antennas. In the HF antenna, a significant side lobe reduction compared to the LF antenna is produced, ranging from 3 to 15 dB in an angular region of 150°. ***Figure 11*** compares the corresponding co-polar and cross-polar 45°-plane radiation patterns of the 1.2 and 4.8 GHz integrated antennas. From the co-polar patterns, it is obvious that the HF antenna has a

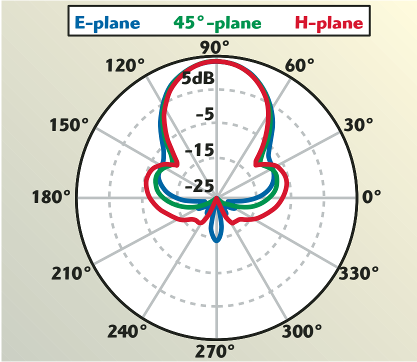

▲ *Fig. 9 Co-polar gain patterns of an integrated 1.2 GHz SBF antenna.*

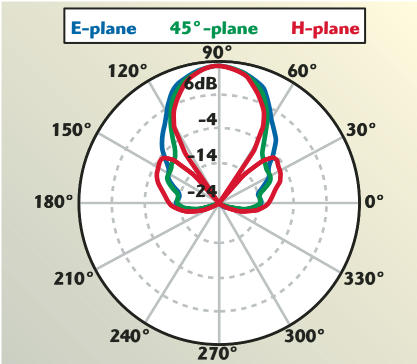

▲ *Fig. 10 Co-polar gain patterns of a 4.8 GHz antenna.*

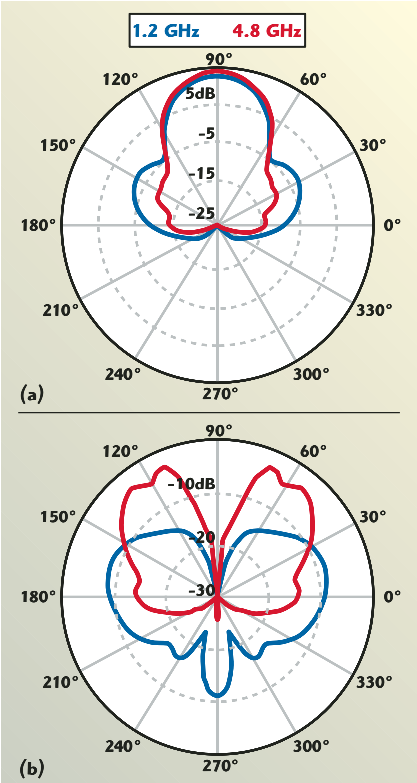

▲ *Fig. 11 Co-polar (a) and cross-polar (b) 45°-plane radiation patterns of two integrated antennas.*

1.2 dB larger gain and much lower secondary lobes and back-to-front ratio. In contrast, the LF antenna has a broader and lower level cross-polar pattern in the main lobe area.

Finally, the 3D co-polar and cross-polar gain patterns are plotted in ***Figure 12*** for the 1.2 GHz integrated antenna and in ***Figure 13*** for the 4.8 GHz integrated antenna. The basic antenna parameters of the single (non-integrated) and integrated SBF antennas are summarized in ***Table 3***, which also specifies the match and bandwidth antenna properties. The integrated SBF antennas have a very good resonance input match and frequency bandwidth, which are better than those of the non-integrated SBF antennas matched also by means of antenna length optimization.

CONCLUSION

An assembly of two axially integrated short backfire antennas, tuned at frequencies in a ratio of 1:4, was described and studied numerically. An approximate design equation for dimensioning the SBF antenna octagonal reflectors is proposed and combined with a MoM-based electromag-

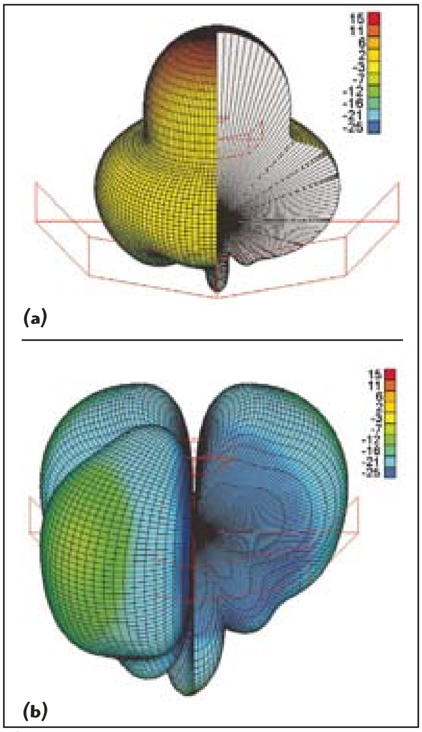

▲ *Fig. 12 Three-dimensional co-polar (a) and cross-polar (b) gain patterns of a 1.2 GHz integrated antenna.*

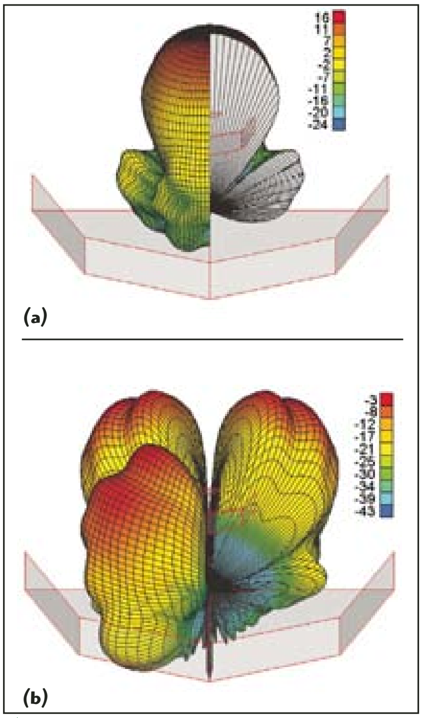

▲ *Fig. 13 Three-dimensional co-polar (a) and cross-polar (b) gain patterns of a 4.8 GHz integrated antenna.*

TABLE III

RADIATION AND INPUT MATCH PARAMETERS OF SINGLE AND INTEGRATED SBF ANTENNAS

Integrated SBF Antennas	*1.2 GHz Antenna: Integrated/Single*	*4.8 GHz Antenna: Integrated/Single*
Directive gain (dB)	14.2/14.4	15.4/15
Aperture efficiency (%)	67/70	88/81
45° plane max side lobe (dB)	–15.2/–20.8	–23/–25
45° plane beamwidth (°)	31.3/34.5	30/33
45° plane max. cross-polar (dB)	–23.3/–24.6	–20/–20.5
45° plane back-to-front ratio (dB)	–20.8/–21.5	–28.2/–26.5
S_{11} at design frequency (dB)	–21/–22	–23/–25
Input bandwidth, (%) at S_{11} = –10 dB	6.3/5.5	7/4.5

netic analysis tool for a numerical design, size optimization and antenna parameter analysis. The thorough numerical examination of the antenna assembly has demonstrated that it is not only compact and simple to build, but also possesses attractive properties for many applications, such as a double-band operation, a reasonable gain of approximately 14 to15 dB, good linear polarization and match characteristics. For both antennas, mismatch losses less than 0.05 dB at the design frequency, and less than 0.45 dB over the frequency band of approximately 6 to 7 percent, have been attained by means of the proposed antenna length-variation technique. The approach may also lend itself to the design of circular polarization antennas by using two orthogonal feed dipoles. ■

ACKNOWLEDGMENT

H.D. Hristov and R. Feick gratefully acknowledge the financial support received under the Chilean Conicyt/Bicentenario Project ACT-11/2004.

References

1. H.W. Ehrenspeck, "The Short Backfire Antenna," *Proceedings of the IEEE*, Vol. 53, No. 4, August 1965, pp. 1138–1140.
2. H.W. Ehrenspeck, "A New Class of Medium-size High Efficiency Reflector Antennas," *IEEE Transactions on Antennas and Propagation*, Vol. 22, No. 2, March 1974, pp. 329–332.
3. H.W. Ehrenspeck and J.A. Strom, "The Short Backfire Antennas as Element for High Gain Arrays," *Report AFCRL-71-0234 Air Force Cambridge Research Laboratories*, Bedford, MA, April 1971.
4. A.C. Large, "Short Backfire Antenna with Waveguide and Linear Fields," *Microwave Journal*, Vol. 19, No. 8, August 1976, pp. 49–52.
5. M.S. Leong and P.S. Kooi, "Rectangular-waveguide-excited Short Backfire Antenna with Corrugated Rim," *Electronics Letters*, Vol. 15, No. 17, August 1979, pp. 533–535.
6. A.A. Kishk and L. Shafai, "Gain Optimization of Short Backfire Antenna with Different Excitation Types," *1986 IEEE Antennas and Propagation Society Symposium Digest*, pp. 923–926.
7. C.D. Kaloi, D. Hatfield and P. Simon, "Microstrip Backfire Antenna," *1981 IEEE Antennas and Propagation Society Symposium Digest*, pp. 343–346.
8. A. Kumar and H.D. Hristov, *Microwave Cavity Antennas*, Artech House Inc., Norwood, MA, 1989.
9. H.W. Ehrenspeck and J.A. Strom, "Short-backfire Antenna-A Highly Efficient Assembly Element," *Microwave Journal*, Vol. 20, No. 5, May 1977, pp. 47–49.
10. A. Andersson, P. Bengtsson and A. Molker, "Short Backfire Antenna Arrays for Space

Communications," *1977 IEEE Antennas and Propagation Society Symposium Digest*, pp. 194–197.
11. L.R. Dod, "Backfire Antennas for Telemetry and Tracking Applications," *Proceedings of the 1969 NTC*, Washington, DC, 1969, pp. 77–84.
12. O.M. Woodward, "Short Backfire Antenna with Sum and Error Patterns," *US Patent 4240080*, December 1980.
13. WIPL-D Pro v5.1, *3D Electromagnetic Solver*, WIPL-D d o. o., 2004.
14. H.D. Hristov, J.R. Urumov, R. Feick and G.S. Kirov, "Dual-band Array of Integrated Short Backfire Antennas," accepted for presentation, *2006 ANTEM/URSI International Symposium*, Montreal, Canada.

Hristo D. Hristov *received his PhD and DSc degrees in radio engineering from Technical University, Sofia, Bulgaria. Since 1965, he has been with the Technical University of Varna, Bulgaria. He is currently a research professor with Universidad Técnica Federico Santa María, Valparaíso, Chile. He was a researcher at the Strathclyde University of Technology, Queen Mary College and the Eindhoven University of Technology. His research interests include high frequency electromagnetism, antennas, propagation, microwave devices and wireless communications.*

Rodolfo Feick *received his degree in ingeniero civil electronico from Universidad Técnica Federico Santa María, Chile, in 1970, and his MSc and PhD degrees in electrical engineering from the University of Pittsburgh in 1972 and 1975, respectively. He has been with the department of electronics engineering at Universidad Técnica Federico Santa María since 1975, where he is now the head of the telecommunication group. His research interests include wireless systems and data communications.*

Jordan R. Urumov *graduated from the St. Petersburg Electrotechnical University, Russia, in 1972. He received his PhD degree from the Technical University of Sofia. In 1990, he became associate professor in the department of radio engineering, Technical University of Varna, Bulgaria. His research interests include high frequency electromagnetism, antennas, propagation, microwave circuits and devices, optoelectronics and optical communications.*

Georgi S. Kirov *received his MSc and PhD degrees in radio engineering from the University of Varna, Bulgaria. In 1969, he joined the department of radio engineering and, in 1999, became the head of the department. From 1981 to 1986, he was with the University of Setif, Algeria, as a lecturer in the field of telecommunications. He specialized in microwave antennas at Moscow Technical University and the Moscow Technical University of Communications and Informatics. He also was a researcher at the University of Magdeburg, Germany. His research interests include high frequency electromagnetism, antennas and wave propagation, microwave/optical devices and wireless communications.*

Visit page 184 of this month's issue for a complete listing of new radar and antenna products.

BROADBAND DESIGN OF A SMALL NON-SYMMETRIC GROUND λ/4 OPEN SLOT ANTENNA

The broadband design of a small size, λ/4 open slot antenna is investigated. By properly choosing the dimensions of the open slot and of the rectangular conducting plate, which is connected to the end of the 50 Ω microstrip-line feed, a broadband antenna with a bandwidth of 94 percent is achieved with an overall size of 35 × 30 × 0.8 mm. This design can be applied to small-size devices for wireless applications.

The wireless communication industry is developing rapidly and wireless communication products, PDAs, laptops and cell-phones are becoming a necessity of life. Communication systems need a wide frequency bandwidth to transmit and receive multimedia information at high data rates. Mobile wireless communication products must be easily portable and cheap to make them attractive to people. Because microstrip-line-fed slot antennas have a wide impedance bandwidth and a simple structure that is easily manufactured at low cost, they can be suitable for communication products such as wireless local area network (WLAN) or Bluetooth applications.

Many studies of wideband slot antennas fed by microstrip lines have been published.[1-4] These studies demonstrate that the design of a small size, wideband slot antenna is not an easy task. They show that while broadband designs are achievable, getting a small size as well is not easy. Therefore, how to reduce the antenna size and decrease its manufacturing cost are important. Some broadband and small size slot antennas have recently been proposed.[5–8] A monopole slot, at the center of the ground plane, was studied parametrically for its impedance bandwidth.[5] The bandwidth obtained is approximately 50 percent. Two new designs of microstrip open slot antennas (L-slot and inverted T-slot) have been described[6] to attain wider bandwidths with shorter vertical lengths. A quarter-wavelength slot antenna[7] with an L-shaped horizontal and vertical tuning stub has also been published. The bandwidth of the quarter-wavelength slot antenna is 3 to 5 GHz, but it is not enough to cover most wireless communications. A WLAN notch antenna for dual-band and wideband operation has been implemented.[8] The published open-slot antennas are

WEN-SHAN CHEN AND KUANG-YUAN KU
Southern Taiwan University of Technology Tainan Hsien, Taiwan, ROC

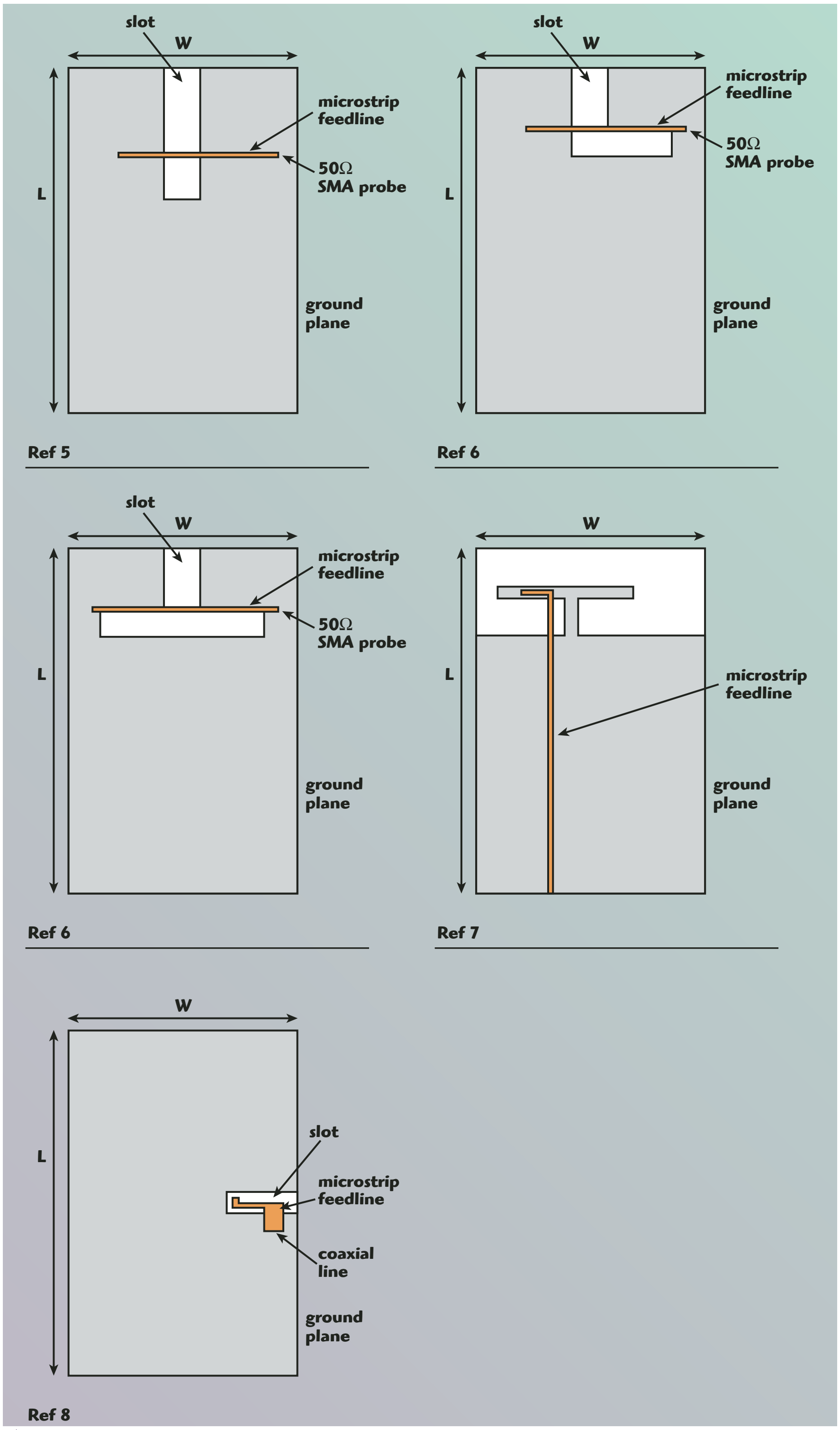

▲ *Fig. 1 Geometrics of the antennas described in Ref. 5 to 8.*

compared in ***Figure 1*** and their results are shown in ***Table 1***.

In this article, a novel design for a non-symmetric ground λ/4 open slot antenna with a microstrip-line feed is proposed. By choosing the proper dimensions of the rectangular conducting plate, which terminates the 50 Ω microstrip-line feed, and that of the open slot, a wide impedance bandwidth and a miniaturized antenna area can be obtained. The proposed antenna, printed on an FR4 substrate and fed by a 50 Ω microstrip-line, is implemented and investigated. The frequency range of the proposed antenna is approximately 2.2 to 6.1 GHz (94 percent), which can be used in mobile wireless communication products, WLAN, Bluetooth and UWB.

ANTENNA DESIGN

The geometry of the proposed antenna is shown in ***Figure 2***. The antenna is printed on an FR4 substrate with a thickness h = 0.8 mm, a relative permittivity $\varepsilon_r = 4.4$ and dimensions L_1 and W_1. The open slot consists of one open-ended, x-directed slot of length W_2 and one open-ended, z-directed slot of length L_5, connected together on the right side of the ground plane. The open slot is etched in the ground plane and its location results in the non-symmetric ground. The coupling, between the rectangular conducting plate terminating the open end of the 50 Ω microstrip-line feed and the open slot on the non-symmetric ground, generates the wideband impedance of the small area antenna.

The length of the open-ended, x-directed slot W_2 and the length of the open slot, y-directed slot length L_5 are the major parameters, which determined the lower resonant mode. The higher resonant mode is excited by adjusting the dimensions of the feed structure. By properly choosing the dimensions of the open-ended, x-directed slot W_2 and the open-ended, y-directed slot L_5, these two resonant modes can be coupled to provide a wide impedance bandwidth. The location of the rectangular conducting plate is close to the end edge of the open-ended, x-directed slot of length W_2, which generates a good impedance matching of the proposed antenna. The center length of the open slot (approximately 32.5 mm) is approximately a quarter-wavelength in free space at 2.2 GHz.

PARAMETRIC STUDY AND DISCUSSION

The parametric study supplied helpful information to the antenna designers. It included the dimensions of the slot, the rectangular plate and the ground plane. Through these investigations, an optimal design is obtained, suitable for mobile wireless communication products in WLAN, Bluetooth and UWB.

Different Values of Rectangular Plate Width W_3

Figure 3 shows the return loss for different widths of the rectangular

TABLE I

COMPARISON OF SIZE AND BANDWIDTH FOR THE ANTENNAS DESCRIBED IN REFERENCES 5 TO 8

Reference	Antenna Size ($W \times L$) (mm)	Frequency Range (GHz)	Bandwidth (%)
5	50×80	2.42~4.31	56.17
6	50×80	2.24~5.36	82.11
6	50×80	2.56~5.80	77.51
7	50×80	2.37~4.38	59.56
8	40×80	3~5	50.00

patch W_3. The other antenna dimensions are $L_1 = 35$ mm, $L_2 = 7$ mm, $L_3 = 14$ mm, $L_4 = 6$ mm, $L_5 = 14$ mm, $W_1 = 30$ mm, $W_2 = 18.5$ mm, $W_4 = 1.53$ mm and $W_5 = 5$ mm. As W_3 increases, the impedance bandwidth moves to a high frequency. It shows that the bandwidth is not very sensitive to W_3.

Different Values of Slot Width L_4

Figure 4 shows the return loss with different widths for slot L_4 from 2 to 8 mm, with the other dimensions $L_1 = 35$ mm, $L_2 = 7$ mm, $L_3 = 14$ mm, $L_5 = 14$ mm, $W_1 = 30$.mm, $W_2 = 18.5$ mm, $W_3 = 6$ mm, $W_4 = 1.53$ mm and

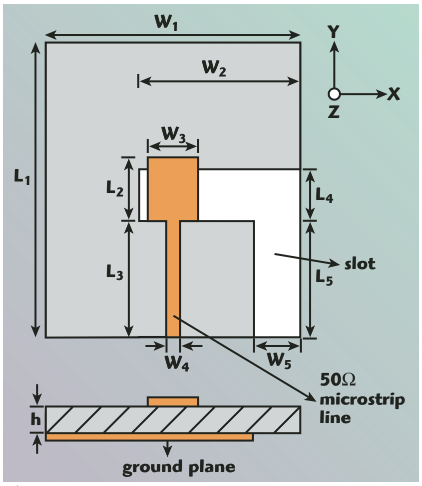

▲ *Fig. 2 Geometry of the proposed antenna.*

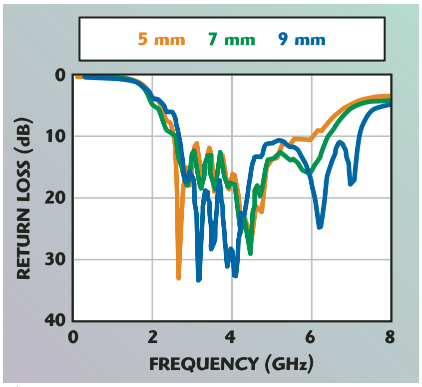

▲ *Fig. 3 Measured return loss for different values of W_3.*

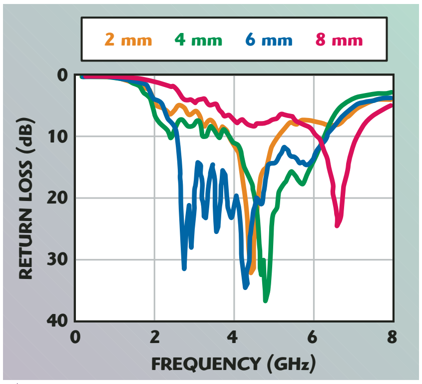

▲ *Fig. 4 Measured return loss for different values of L_4.*

W_5 = 5 mm. The results indicate that the bandwidth is very sensitive to L_4. When L_4 = 6 mm, a broader impedance bandwidth occurs. From these results, the dimension L_4 of the slot is set at 6 mm.

Different Values of Slot Width W_5

Figure 5 shows the return loss with different widths for slot W_5. The other dimensions are L_1 = 35 mm, L_2 = 7 mm, L_3 = 14 mm, L_4 = 6 mm, L_5 = 14 mm, W_1 = 30 mm, W_2 = 18.5 mm, W_3 = 6 mm and W_4 = 1.53 mm. It shows that the bandwidth is more sensitive to W_5 than to W_3. The symmetric structure (slot W_5 = 0 mm) exhibits a dual-frequency characteristic. However, the impedance matching at the higher frequency is not sufficient. With the slot W_5 added, a higher resonant mode is excited, which couples to the lower resonant mode to create a wide impedance bandwidth.

Different Dimensions of the Ground Plane, L_1 and W_1

The measured return loss for different sizes of the ground plane is shown in ***Figure 6***, with L_2 = 7.5 mm, L_3 = 14 mm, L_4 = 6 mm, L_5 = 14 mm, W_2 = 19 mm, W_3 = 6 mm, W_4 = 1.53 mm and W_5 = 5.5 mm. For the case with the ground plane dimensions L_1 = 80 mm and W_1 = 50 mm, the bandwidth obtained is more than 90 percent, which is larger than those shown in Table 1. Since the purpose of this work is to broaden the impedance bandwidth of an open slot antenna with a small size, it is observed that the broadband impedance bandwidth operation of the proposed design can be sustained with a small size ground plane of dimensions 35 × 30 mm.

OPTIMIZED DESIGN

From these investigations, an optimized wideband slot antenna with small dimensions, 35 × 30 mm, can be obtained. The optimized parameters are ε_r = 4.4, h = 0.8 mm, L_1 = 35

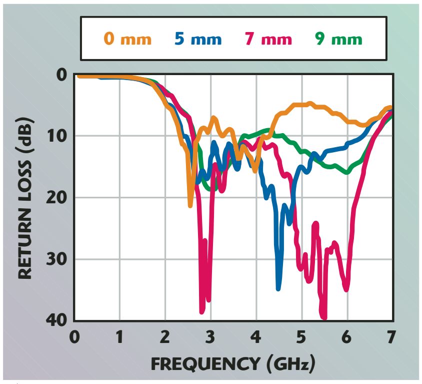

▲ *Fig. 5 Measured return loss for different values of W_5.*

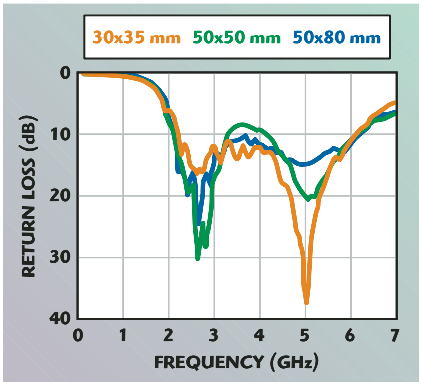

▲ *Fig. 6 Measured return loss for different sizes of the ground plane.*

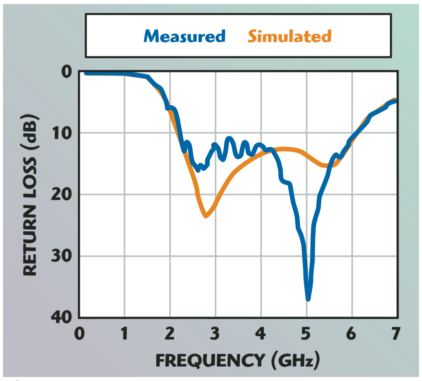

▲ *Fig. 7 Measured and simulated return loss of the proposed antenna.*

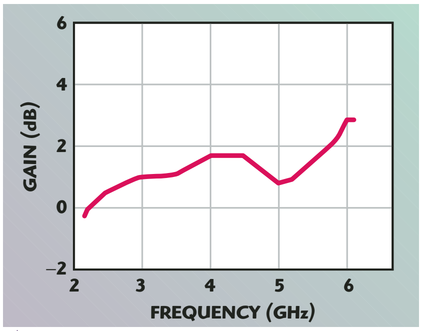

▲ *Fig. 8 Measured gain of the proposed antenna.*

mm, L_2 = 7.5 mm, L_3 = 14 mm, L_4 = 6 mm, L_5 = 14 mm, W_1 = 30 mm, W_2 = 19 mm, W_3 = 6 mm, W_4 = 1.53 mm and W_5 = 5 mm. ***Figure 7*** shows the measured and simulated return loss of the proposed antenna. The measured data agree with the simulated data. The wide impedance bandwidth of the proposed antenna is approximately 94 percent (2.2 to 6.1 GHz), as determined from a 10 dB return loss, which is suitable for Bluetooth (2.4 to 2.4835 GHz) and WLAN (2.4 to 2.4835 GHz, 5.15 to 5.35 GHz and 5.725 to 5.850 GHz), and for the low band UWB (3.1 to 5.15 GHz) applications. In addition, the bandwidth obtained with a small size is larger than that of the ones shown in Table 1. ***Figure 8*** shows the measured gain of the proposed antenna. The gain variation over the operating bandwidth of the proposed design is less than 3.08 dB. The measured radiation patterns of the proposed antenna at two typical operation frequencies are also investigated. ***Figure 9*** shows the measured and simulated radiation patterns at 2.45 and 5.2 GHz. At higher frequencies, the radiation patterns of the proposed antenna degenerate because high order modes are excited. These radiation patterns are

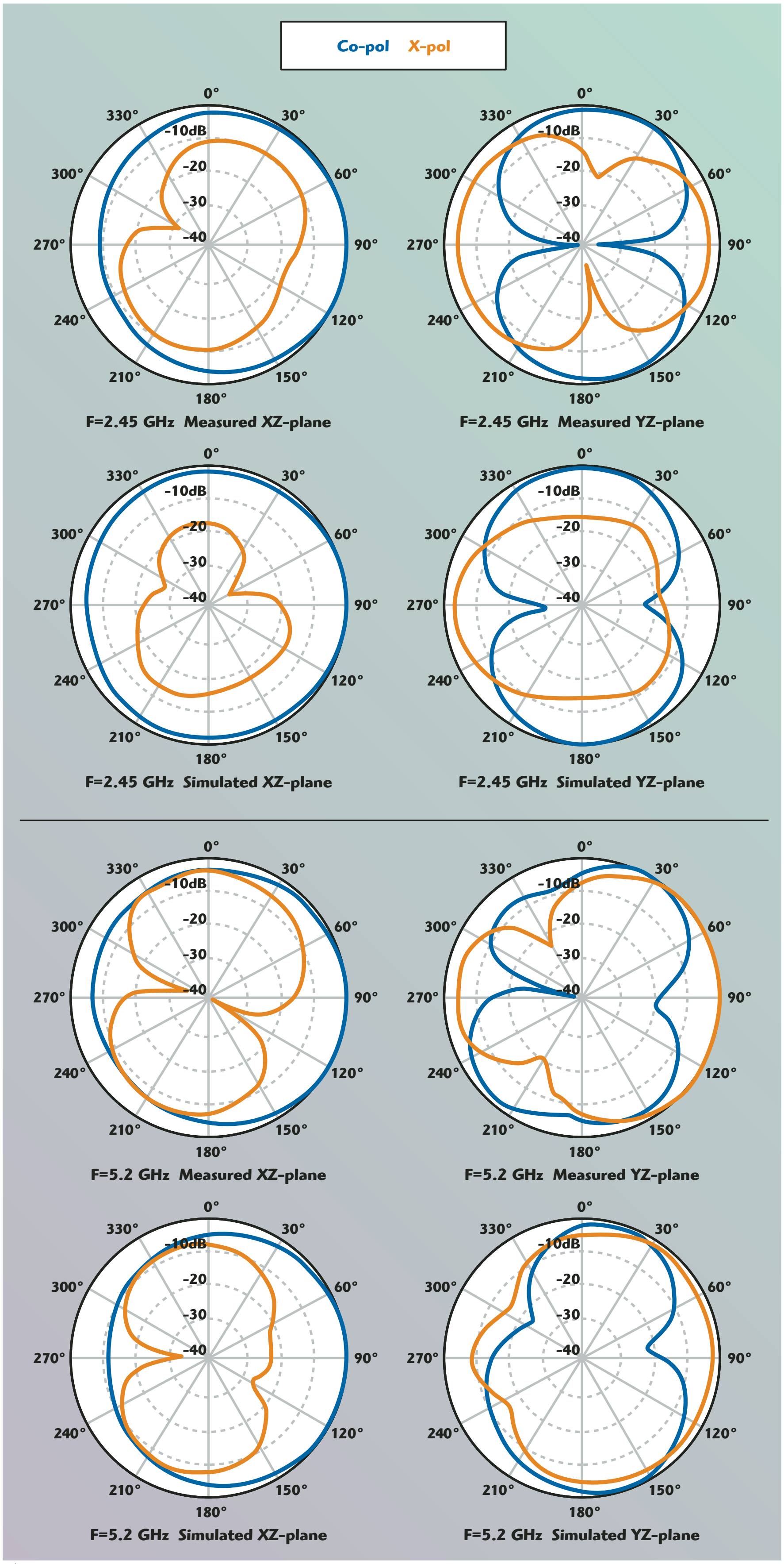

▲ *Fig. 9 Measured and simulated H-plane (XZ) and E-plane (YZ) radiation patterns of the proposed antenna.*

acceptable for most wireless applications.

CONCLUSION

This article focuses on the wideband design of a small slot antenna. The coupling between the rectangular conducting plate, which is attached to the open end of the 50 Ω microstrip-line feed, and the λ/4 open slot with the non-symmetric ground, generates a wideband impedance for a small area antenna. The 94 percent impedance bandwidth of the proposed antenna is achieved by using proper dimensions for the open slot and rectangular conducting plate. The overall size of the proposed antenna is 35 × 30 × 0.8 mm. The proposed broad bandwidth, small size antenna is suitable for portable devices in wireless applications. ■

ACKNOWLEDGMENT

The financial support of this study by the National Science Council, Taiwan Republic of China, under contact number NSC94-2213-E-218-006, is gratefully acknowledged.

References

1. Y.W. Jang, "Broadband Cross-shaped Microstrip-fed Slot Antenna," *Electronics Letters*, Vol. 36, No. 25, December 2000, pp. 2056–2057.
2. Y.H. Suh and I. Park, "A Broadband Eccentric Annular Slot Antenna," *2001 IEEE Antennas and Propagation Society International Symposium Digest*, Vol. 1, pp. 94–97.
3. X. Qing, M.Y.W. Chia and X. Wu, "Wide-slot Antenna for UWB Applications," *2003 IEEE Antennas and Propagation Society International Symposium Digest*, Vol. 1, pp. 834–837.
4. Y.F. Liu, K.L. Lau, Q. Xue and C.H. Chan, "Experimental Studies of Printed Wide-slot Antenna for Wideband Applications," *IEEE Antennas and Wireless Propagation Letters*, Vol. 3, 2004, pp. 273–275.
5. S.I. Latif, S.K. Sharma and L. Shafai, "Wideband Microstrip Monopole Slot Antenna," *2003 IEEE International Symposium on Antennas, Propagation and EM Theory*, pp. 54–57.
6. S.I. Latif, L. Shafai and S.K. Sharma, "Bandwidth Enhancement and Size Reduction of Microstrip Slot Antennas," *IEEE Transactions on Antennas and Propagation*, Vol. 53, 2005, pp. 994–1003.
7. A.P. Zhao and J. Rahola, "Quarter-wavelength Wideband Slot Antenna for 3 to 5 GHz Mobile Applications," *IEEE Antennas and Wireless Propagation Letters*, Vol. 4, 2005, pp. 421–424.
8. N. Behdad and K. Sarabandi, " A Compact Dual-/Multi-band Wireless LAN Antenna," *2005 IEEE Antennas and Propagation Society International Symposium Digest*, Vol. 2B, pp. 527–530.

Wen-Shan Chen *received his BS degree in electronic engineering technology from the National Taiwan Institute of Technology (now the National Taiwan University of Technology) and his PhD degree from National Sun Yat-Sen University, Kaohsiung, Taiwan, ROC, in 2001. From 2001 to 2002, he was an assistant professor at the Chien-Kuo Institute of Technology, Changhua, Taiwan, ROC. He is currently an assistant professor of electronic engineering at the Southern Taiwan University of Technology, Tainan, Taiwan, ROC. His research interests include antenna design, RF and microwave circuits.*

Kuang-Yuan Ku *received his BS degree from the Chung-Chou Institute of Technology, Changhua, Taiwan, ROC, in 2004. He is currently a master student in the department of electronic engineering at the Southern Taiwan University of Technology. His main research interests include printed antennas for wireless communications, especially the wideband slot antenna for WLAN applications.*

THE REQUIREMENTS AND PROCEDURES FOR TESTING WIMAX EQUIPMENT

The potential for WiMAX technology is driving its development at a pace aimed at effective mass deployment. This article outlines the requirements necessary for the development of specific test procedures and equipment.

WiMAX is a technology for fixed, nomadic and mobile applications that promises the delivery of broadband wireless access to the masses. For fixed and portable access applications, a delivery capacity of 40 Mbps per channel can be expected for typical cells with a radius of 3 to 10 km. Mobile network deployments are expected to provide up to 15 Mbps of capacity within a typical cell diameter of up to 3 km. There are conceptually three ways to achieve this high data throughput in mobile radio communication systems: large bandwidth, higher order modulation schemes and multiple antenna systems, referred to as multiple-input, multiple-output (MIMO). WiMAX deploys all three, each requiring dedicated testing. Also, to optimize the efficiency in terms of time and frequency resources and to enable flexibility for the network operator, WiMAX uses orthogonal frequency division multiple access (OFDMA) as the modulation scheme. This article explains the three techniques for achieving high data throughput and focuses on their impact on test and measurement requirements.

LARGE BANDWIDTH SYSTEMS

Larger bandwidths increase the data throughput because higher modulation frequencies enable more symbols (a symbol being the smallest unit of data transmitted at one time) to be transmitted per unit time. In other words, a large bandwidth results in a short symbol duration. This can be critical in multipath fading environments where a signal travels from the transmitter to the receiver along different scattered paths and possibly a direct line of sight path. Therefore, a receiver experiences a superposition of the same signal with different attenuations, phases and delays. The delay spread of the paths depends very much on the physical environment. Indoors, for example, the signals travel similar distances resulting in a smaller delay spread than in the countryside where the difference between the distances a signal travels can be large. Due to the delay spread, different symbols arrive at

JAN E. PROCHNOW
Rohde & Schwarz
Munich, Germany

the same time making it hard for the receiver to distinguish between them, especially if the delay spread is large compared to the symbol duration. This effect is referred to as inter-symbol interference.

The orthogonal frequency division multiplexing (OFDM) transmission technique used by WiMAX has advantages in such fading environments because OFDM signals fill the bandwidth with a series of sub-carriers that individually have smaller bandwidths. This results in a longer symbol duration making the signal less susceptible to fading effects. WiMAX supports different bandwidths from 1.25 to 28 MHz and different numbers of sub-carriers, according to the system requirement and spectrum availability. The number of used sub-carriers can vary between 256, 512, 1024 and 2048. Furthermore, OFDM allows the symbol duration to be increased with redundant information by employing cyclic prefixes—the last part of a symbol is repeated at its beginning. To adapt to different fading environments, WiMAX permits this cyclic prefix to be 1/4, 1/8, 1/16 or 1/32 of the symbol length. The drawback of a long cyclic prefix is a reduction in data throughput. Also, the large bandwidth of WiMAX makes the system susceptible to multi-path fading effects. How efficiently a receiver demodulates a signal under fading conditions can most easily be tested with signal generators that generate standard conforming signals and have an internal fading simulator. The large bandwidth of WiMAX also requires special testing of the transceiver components. For example, in a transmitter, a low frequency or I/Q signal from the baseband chip modulates an RF carrier, which is then amplified. For optimizing the transmitter, it is necessary to distinguish the performances of the baseband chip, I/Q modulator and amplifier. Therefore, modern signal generators and analyzers have to be utilized, not only to generate, demodulate and analyze broadband RF signals, but also the corresponding baseband signals. The large bandwidth of WiMAX signals is a challenge for power amplifier and I/Q modulators. These components are typically tested by feeding a high purity signal to the component and analyzing the output signal to measure the deterioration of the signal caused by the component under test. The in-band deterioration is typically measured in terms of spectral flatness and flatness difference, which is the difference in level between adjacent sub-carriers. The modulated OFDM sub-carriers add up to an RF signal with a high dynamic range. This is typically quantified as the difference between peak and average power and referred to as the crest factor. WiMAX signals have high crest factors of the order of 12 dB. To avoid modulation errors, the power amplifier must be linear throughout such dynamic ranges. To test how an amplifier behaves for signals with different signal characteristics, tools are available to set the crest factor of a WiMAX signal generated by a signal generator. The out-of-band deterioration is measured in terms of the adjacent channel leakage ratio (ACLR). The ACLR gives the power that leaks into the adjacent channel with respect to the in-band power. Such tests of components require signal generators and analyzers with an ACLR and frequency response that is much better than the deterioration due to the component under test.

HIGH ORDER MODULATION

In a digitally modulated OFDM system like WiMAX, an in-phase (I) and a quadrature phase (Q) signal are modulated to each of the radio frequency sub-carriers. The I and Q signals are conveniently visualized in a constellation diagram where I is plotted versus Q. ***Figure 1*** shows such a diagram measured with a signal analyzer. In this figure, there are constellation points, which are discrete I and Q values. During a symbol time one of these I/Q pairs is transmitted per sub-carrier. To each constellation point a bit or a bit sequence is mapped. The different WiMAX modulation schemes, BPSK, QPSK, 16QAM and 64QAM, have 2, 4, 16 and 64 constellation points each corresponding to 1, 2, 3 and 4 bits, respectively. Therefore, the more constellation points, the higher the order

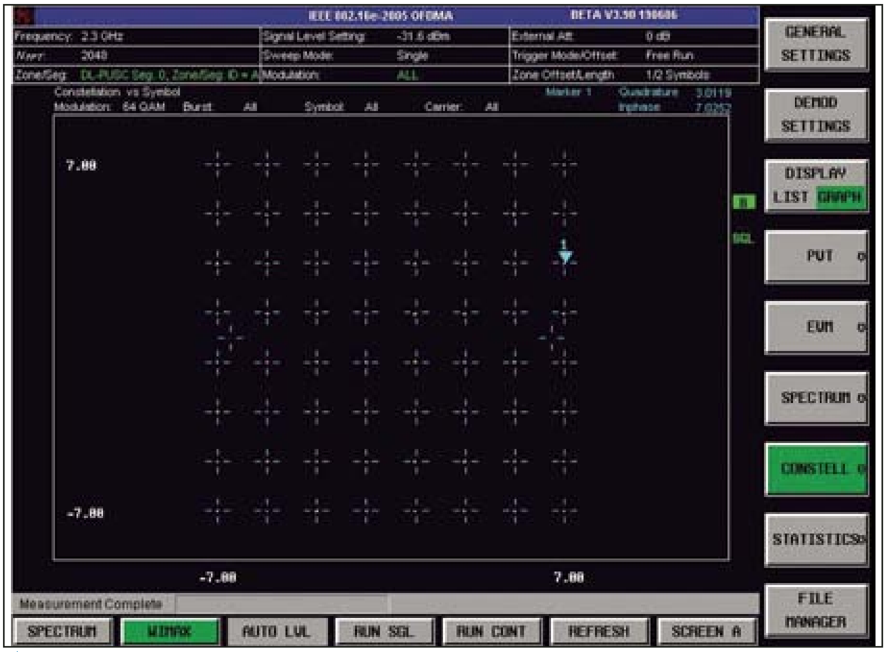

▲ *Fig. 1 Constellation diagram of a 64QAM WiMAX signal demodulated by a signal analyzer.*

of the modulation, the more bits are transmitted per symbol. This means that the data rate is increased without increasing the bandwidth. The price of such higher order modulations is that the constellation points move closer together, making it harder for the receiver to distinguish the points and thus demodulate the signal correctly. This is especially true for low signal-to-noise ratios, in the presence of interference and multi-path fading. WiMAX then adapts the order of the modulation and the coding according to the overall transmission conditions. To test how a WiMAX receiver can demodulate signals in the real world, the operator needs to generate a standard conforming signal and simulate noise, fading conditions and interference. This is conveniently done by signal generators with an internal noise generator, fading simulator and a second baseband source to simulate interference. To cope with the complication of high order modulation, the transmitter and receiver need to have good modulation accuracy, which is typically measured in terms of error vector magnitude (EVM). The EVM equals the distance between the actual measured and the ideal constellation point in the I/Q diagram, normalized to the magnitude of the ideal constellation point. Signal analyzers with WiMAX functionalities facilitate the measurement of the transmitter's EVM. The EVM can be measured for the individual subscriber, time slots or sub-carrier. To estimate the accuracy, with which a transmitter can generate a signal and a receiver demodulate it, requires a signal analyzer and a signal generator with an EVM much lower than the device under test. When designing transmitters and receivers with a low EVM, care must be taken with regards to some critical performance parameters, which require dedicated testing. In particular, the local oscillator that does the up- or down-conversion must be pure in terms of phase noise and broadband noise. Phase noise and broadband noise have a detrimental effect on the EVM because they lead to azimuthal and radial smearing of the constellation points, respectively. Also, the I/Q-modulator has to map the I and Q signals precisely at 90° with respect to each other and with a linear amplification in order to avoid distortions of the constellation diagram, resulting in an increased EVM.

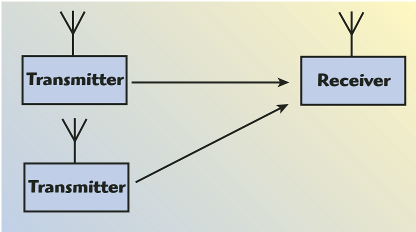

▲ *Fig. 2 Schematic illustration of a simple transmit diversity system.*

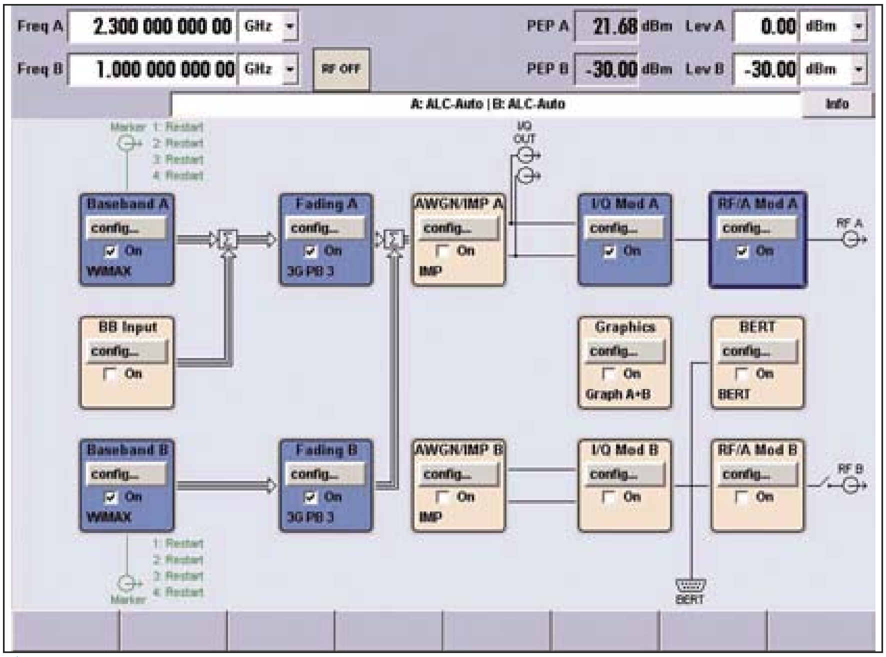

▲ *Fig. 3 Block diagram of a signal generator illustrating the signal flow for testing a transmit diversity system.*

MIMO

WiMAX, like other modern radio communication standards such as 802.11n and E-UTRA, employs multiple antenna systems referred to as MIMO or spatial diversity. The technique either increases the signal-to-noise ratio or increases the data throughput for a given resource or both. Transmit diversity refers to a system where different signals are transmitted from different antennas at the same time and frequency. ***Figure 2*** shows a schematic of such a system where the signals experience different multi-path fading. The characteristics of these fading channels are estimated by transmitting a known pattern and, with this channel estimation, the receiver can then distinguish between the signals from the transmit antennas. This requires the fading channels to be sufficiently different or uncorrelated. However, the antennas of a transceiver are bound to a limited physical area and residual cross talk between these antennas cannot be avoided. Due to this, the fading channels are actually correlated in amplitude and phase, deteriorating the performance of such a transmit diversity system. In the absence of multi-path fading or for 100 percent correlated fading channels, transmit diversity does not work. This means that the performance of a receiver for transmit diversity systems can only be evaluated with fading simulators that can simulate more than one fading channel and allow complex correlation factors between the paths of the fading channels. Such receivers are tested most effectively with a signal generator containing two baseband generators, which can generate standard conforming signals as they are transmitted from the two antennas, plus two internal fading simulators to simulate the different correlated fading channels. Such equipment means that a receiver in a transmit diversity system can be tested using only one box and with minimum cabling effort. ***Figure 3*** shows the block diagram of a signal generator configured for transmit diversity where the signals from the antennas are generated in the top and bottom blocks on the left; the two sig-

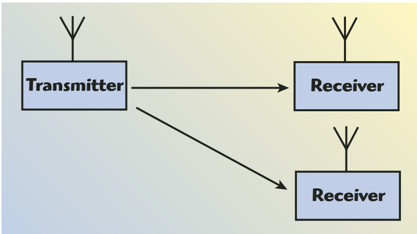

▲ *Fig. 4 Schematic illustration of a simple receive diversity system.*

nals are then faded in the next two blocks and then routed together and modulated to the RF carrier in the two blocks on the top right. This concept also applies to receive diversity systems, where a signal is transmitted from one antenna and received by two. ***Figure 4*** illustrates such a receive diversity system schematically. Performance measurements on receivers in receive diversity systems require one baseband signal, simulation of two correlated fading channels and radio frequency signals. ***Figure 5*** shows the block diagram of a signal generator set up for testing receive diversity systems.

OFDMA SYSTEMS

An OFDMA system is a combination of frequency division duplex (FDD) and time division duplex (TDD). This means that a part of the spectrum and time is allocated to each subscriber. In such a system, operators can offer different band-

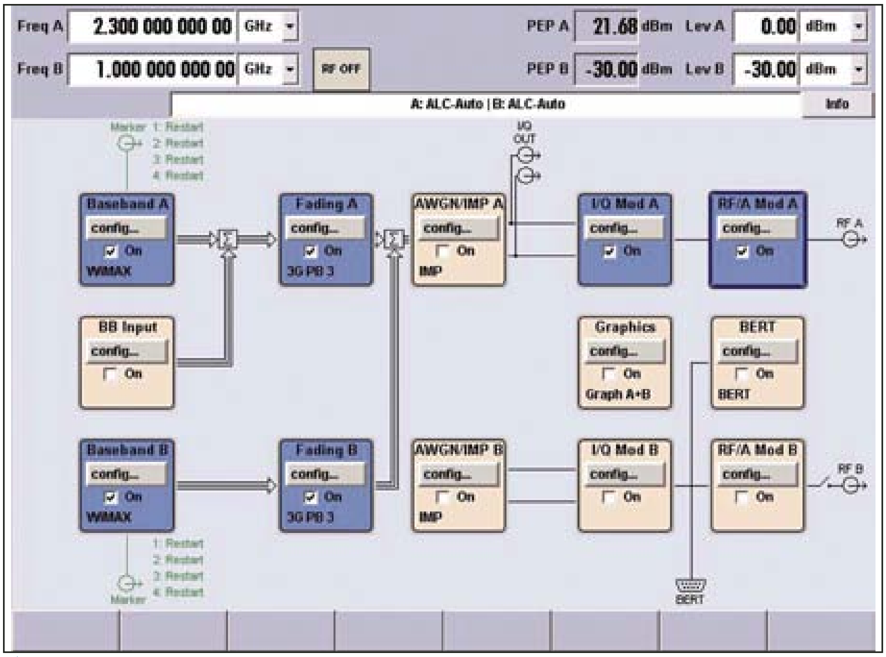

▲ *Fig. 5 Block diagram of a signal generator showing the signal flow for testing a receive diversity system.*

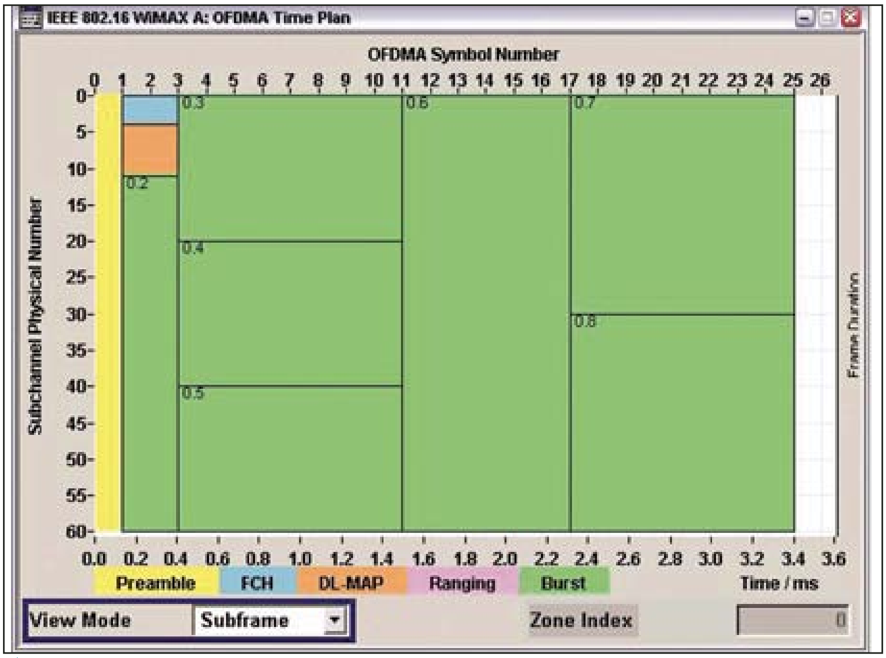

▲ *Fig. 6 Downlink map of an OFDMA WiMAX signal.*

widths and transmission time resources to the users according to their needs and level of service. In ***Figure 6***, a time plan for a downlink signal is shown, where, on the x- and y-axes, the time and sub-channel numbers are plotted, respectively. The logical sub-channels are allocated to the physical sub-carrier according to defined permutation algorithms. The orange square in the figure represents the downlink-map or DL-Map. In this field, the time and sub-channel allocation of the users is described. To enable different base stations to operate in the same physical area, different times and sub-channels can be allocated to them. As can be seen, OFDMA systems offer a great deal of flexibility in optimizing resources efficiently. However, this flexibility comes at the price of a complex physical layer with many free parameters. This complexity is a challenge for the user interface of test and measurement equipment as many parameters need to be set and the impact of the parameter must be illustrated to the user (in the form of graphical displays and concise tables, for example). Also, the high complexity of the physical layer presents the risk that manufacturers of transceivers will run into configuration problems. Emulating transmitters and receivers with signal generators and signal analyzers with flexible parameters helps to solve such configuration problems. These tests require the measurement equipment to make fast and easy changes to the WiMAX parameters. Such equipment has proved to be very useful during interoperability testing between subscribers and base stations—by using a signal analyzer, the contents of the DL-Map and UL-Map can automatically be demodulated down to the bit level. This allows the bits demodulated by the signal analyzer to be compared with the ones demodulated by the mobile station. During troubleshooting of an interoperability test, this is one of the first steps that needs to be taken, as the subscriber station needs to demodulate the DL-Map in order to know what sub-carriers to demodulate and when. Once the DL-Map is demodulated correctly, the next logical step is to verify the contents of the UL-Map, which tells each subscriber station how to configure its transmitter in terms of what sub-carriers to use and when to do so. Only if the mobile station transmits its information at the requested sub-carriers with the correct timing, will the base station be able to demodulate the signal correctly. This highlights that timing is a parameter that may cause interoperability problems. Here, a signal analyzer can speed up the troubleshooting process, as it is able to record and display the signal in both link directions.

CONCLUSION

Large bandwidth signals are susceptible to fading effects. To cope with this, WiMAX deploys the robust OFDM modulation technique. The downside being that the signals have a high crest factor, requiring very linear power amplifiers. Furthermore, the large bandwidth requires power amplifiers and I/Q modulators with a flat frequency response. Transmitting signals with a high order of modulation requires very good modulation accuracy and a receiver that is able to distinguish between the constellation points even in the presence of noise, fading conditions and interference. Besides the generation of multiple signals, the receiver tests for multiple antenna systems require the simulation of multiple fading channels. The flexibility of an OFDMA system also comes at the price of a complex physical layer, which makes interoperability tests a challenge. Therefore, the testing of WiMAX equipment requires high end, easy to use test and measurement equipment to generate and analyze standard conform signals and to simulate interference effects. ■

Jan E. Prochnow *studied physics at the University of Technology, Aachen, Germany, and received his PhD degree in the field of accelerator physics at CERN, Geneva, Switzerland. He has been a product manager for signal generator and power meters at Rohde & Schwarz headquarters in Munich, Germany, since 2004. His tasks include the marketing of test and measurement equipment for WiMAX.*

A TRIPLE-BAND POLYGONAL SLOT ANTENNA FOR WIMAX APPLICATIONS

A printed polygonal slot antenna, fed by a 50 Ω microstrip-line and with two narrow strips for three-band operation, is proposed and experimentally studied. The polygonal slot antenna was found to be broadband (1.85 to 5.83 GHz). When two narrow strips were inserted into the polygonal slot antenna, two bands were rejected. By properly choosing the length and location of the two narrow strips, a triple-band antenna can be achieved. The good impedance matching, good radiation patterns and antenna gain of the proposed antenna are investigated in this article. The design of the proposed antenna is suitable for WiMAX applications.

In recent years, wireless communications have progressed very rapidly. The IEEE 802.16 Working Group has created a new standard, commonly known as WiMAX (Worldwide Interoperability for Microwave Access), for a low cost, broadband, wireless access at high speed, which is easy to deploy.[1] WiMAX technology can reach a theoretical 30-mile radius coverage and achieve data rates up to 75 Mbps, a throughput higher than the 1.5 Mbps performance of typical broadband services.[2] At present, the development of WiMAX technology is the focus of the receiving industry. How to design the antennas for WiMAX applications has become important.

Microstrip-line slot antennas are light and easy to manufacture, are broadband, and have low profile and low cost. Several designs of broadband slot antennas have been proposed.[3–5] WiMAX has been allocated three frequency bands, which will be called the low band (2.495 to 2.695 GHz), the median band (3.25 to 3.85 GHz) and the high band (5.25 to 5.85 GHz), respectively. A broadband antenna must add filters to separate the bands, leading to a higher cost. Therefore, a broadband antenna is not very suitable for WiMAX. A wideband stubby monopole was reported[6] that is broadband but with a more complex structure. To design a triple-band antenna that fit the exact bands of WiMAX is not an easy task. In this article, a new design for a microstrip-line-fed printed polygonal slot antenna, with two rectangular narrow strips to obtain the dual band-rejected frequencies at 3 and 4.5 GHz, is proposed. The proposed antenna can easily be excited by a 50 Ω microstrip-line, printed on an FR-4 dielectric substrate. With this

WEN-SHAN CHEN AND
BAO-HUNG KAO
Southern Taiwan University of Technology
Tainan Hsien, Taiwan, ROC

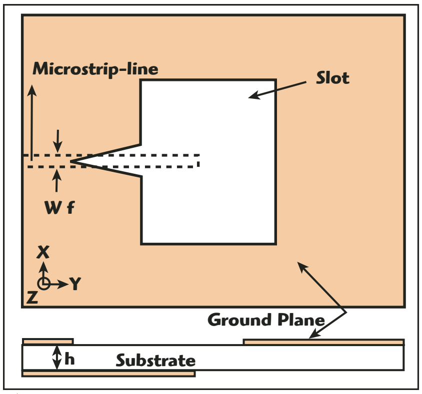

▲ *Fig. 1 Structure of the broadband polygonal slot antenna.*

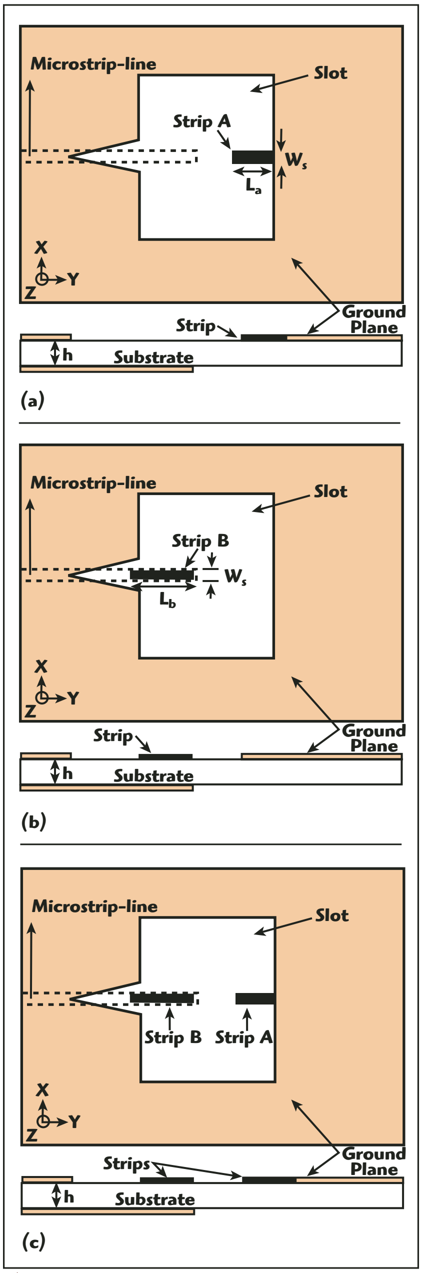

▲ *Fig. 2 Structure of the proposed antenna (a) with strip A inserted, (b) with strip B inserted and (C) with both strips inserted.*

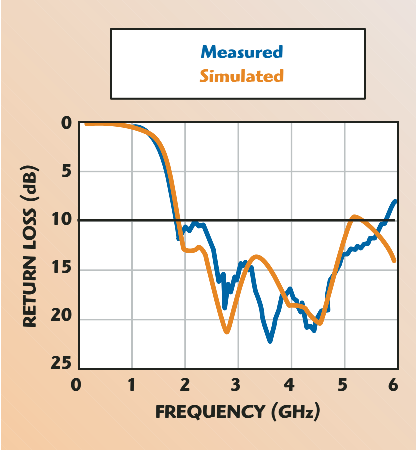

▲ *Fig. 3 Measured and simulated return loss of the broadband antenna.*

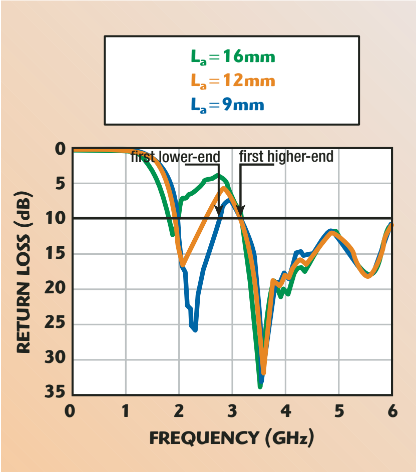

▲ *Fig. 4 Measured return loss with different lengths of strip A.*

antenna design, a good impedance match and good radiation characteristics can be obtained. Details of the design and the experimental results of the proposed antenna are discussed.

ANTENNA DESIGN

Figure 1 shows the geometry of the broadband design of the polygonal slot antenna on a dielectric substrate. In this study, the dielectric material is FR-4, with a thickness h and a relative permittivity ε_r. For design convenience, the proposed antenna is fed by a 50 Ω microstrip-line, printed on the dielectric substrate. The microstrip-line was placed symmetrically with respect to the centerline (y axis) of the polygonal slot. Then, by fine-tuning the polygonal slot and adjusting the length of the 50 Ω microstrip-line, a new resonant mode can be excited in the proximity of the fundamental resonant mode, and a good impedance matching over a broadband can be obtained. Then, two rejected bands are created, located at the proper frequencies to form the triple frequency bands used in WiMAX applications. ***Figure 2*** shows the geometry of the triple-band polygonal slot antenna on a dielectric substrate. Two narrow strips are inserted along the centerline of the polygonal slot. The width of the strips, w_s, is equal the width w_f of the microstrip-line. In order to reject two different frequency bands, the length of strip A is different from strip B. Strip A is connected to the ground plane of the polygonal slot antenna and its length is adjusted to reject the frequency band from 2.69 to 3.3 GHz. Strip B, which is coupled to the 50 Ω microstrip-line, is approximately a quarter-wavelength at the center frequency of the second rejected band (4.525 GHz). With two strips inserted, the polygonal slot antenna will have two rejected bands, leading to a triple-band WiMAX antenna.

EXPERIMENTAL RESULTS AND DISCUSSION

Polygonal Slot Antenna

Figure 3 shows the measured and simulated return loss of the polygonal slot antenna. The simulation was performed using the high frequency structure simulation (HFSS) software package from Ansoft, and the prototype characteristics of the proposed antenna were measured with a HP-

TABLE I

CHARACTERISTICS OF THE PROTOTYPES WITH DIFFERENT LENGTHS L_a

Antenna	L_a (mm)	1st Lower-end Frequency (GHz)	1st Higher-end Frequency (GHz)
A_1	16	1.98	3.18
A_2	14	2.28	3.18
A_3	12	2.52	3.21
A_4	10	2.67	3.21
A_5	9	2.76	3.21

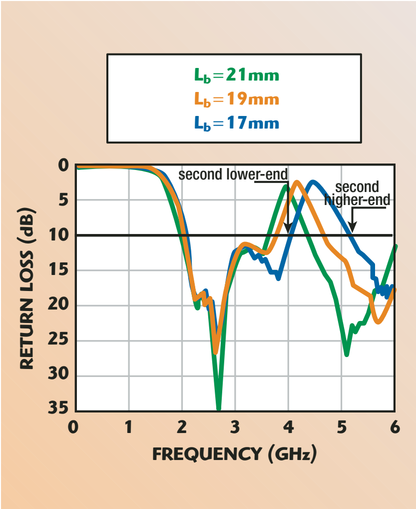

▲ *Fig. 5 Measured return loss with different lengths of strip B.*

8072E network analyzer. The impedance bandwidth was greater than 100 percent (1.85 to 5.83 GHz) for a VSWR = 2.0. The broadband property of the polygonal slot antenna is obvious.

TABLE II

CHARACTERISTICS OF THE PROTOTYPES WITH DIFFERENT LENGTHS L_b

Antenna	L_b (mm)	2nd Lower-end Frequency (GHz)	2nd Higher-end Frequency (GHz)
B_1	23	3.60	4.29
B_2	21	3.69	4.35
B_3	19	3.70	4.62
B_4	17	3.99	5.10
B_5	15	4.35	5.64

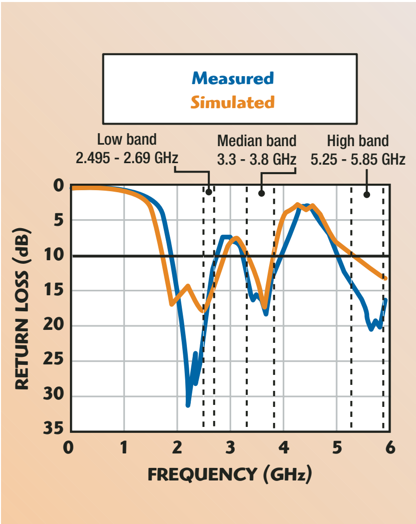

▲ *Fig. 6 Measured and simulated return loss of the proposed antenna.*

Inserted Different Values of the Strip A

Figure 4 shows the measured return loss of the antenna, with a strip A of different lengths L_a inserted. As the length L_a decreases, the center frequency of the rejected band shifts to a higher frequency. When L_a= 9 mm, the lower end frequency of the first rejected band is above 2.695 GHz. It is observed that when L_a decreases, the higher end frequency of the first rejected band is slightly affected. The related results are listed in ***Table 1*** with the parameters $w_f = w_s = 3.0$ mm, h = 1.6 mm, $\varepsilon_r = 4.4$.

Inserted Different Values of the Strip B

Figure 5 shows the measured return loss of the antenna with a strip B of different lengths L_b inserted. As L_b decreases, the center frequency of the second rejected band shifts to a higher frequency. When L_b = 17 mm, the frequency of the second rejected band ranges from 3.99 to 5.1 GHz. It is suitable for the present application, between the low and median bands. The length L_b is approximately a quarter-wavelength at the center frequency of the second rejected band (4.525 GHz). The higher end frequency of the second rejected band is greater than 5.25 GHz when L_b is less than 17 mm. Thus, setting L_b= 17 mm is a good choice for the present design. The related results are listed in ***Table 2***, with the same parameters as in Table 1.

Combined Strip A and Strip B Proposed Antenna Design

From what has been investigated, the relatively suitable strip lengths are L_a = 9 mm and L_b = 17 mm. After inserting the strips A and B simultaneously in the polygonal slot, the triple-band antenna for WiMAX applications can be obtained. ***Figure 6*** shows the measured and simulated return loss of the proposed antenna. The three bandwidths (1.95 to 2.73 GHz, 3.27 to 3.99 GHz and 5.1 to < 6 GHz) are suitable for the WiMAX

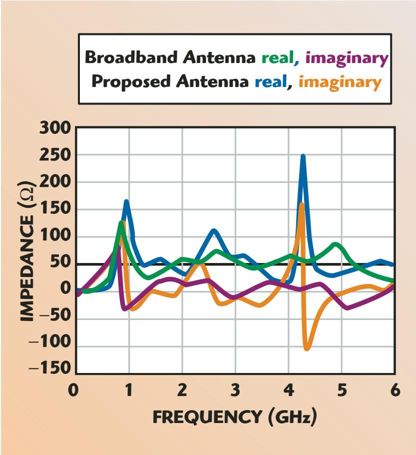

▲ *Fig. 7 Impedance of the proposed broadband antennas.*

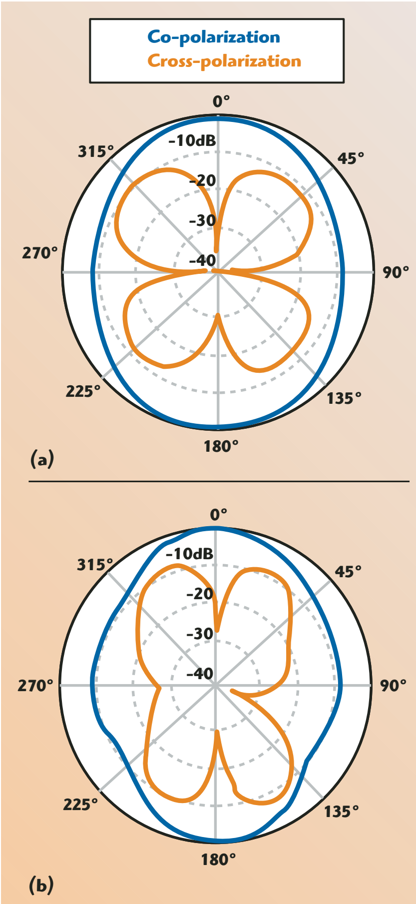

▲ *Fig. 8 Measured far-field radiation patterns of the proposed antenna in the x-z plane at (a) f=2.5 GHz and (b) f=5.75 GHz.*

frequency bands. ***Figure 7*** shows the impedance of both the proposed and broadband antennas. The real part of the impedance of the rejected band antenna is significantly increasing at the center frequency of the first and second rejected bands (2.995 and 4.525 GHz), and the maximum peak impedance of the second rejected

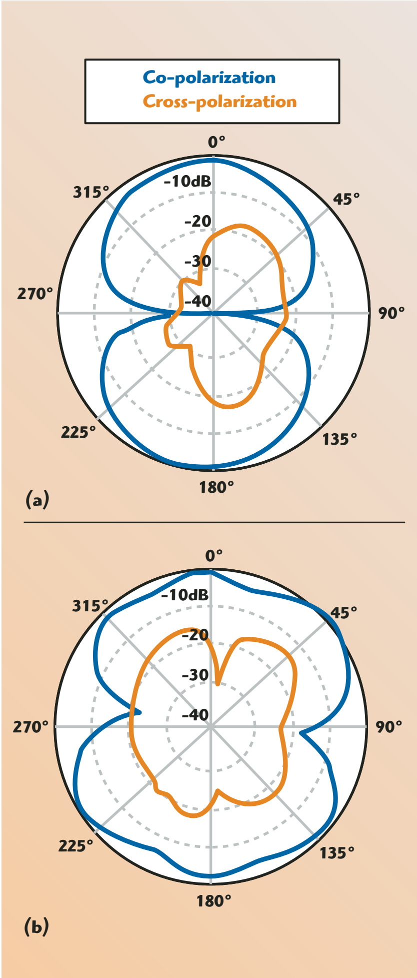

▲ *Fig. 9 Measured far-field radiation patterns of the proposed antenna in the y-z plane at (a) f=2.5 GHz and (b) f=5.75 GHz.*

band is 248 Ω. The variation of the imaginary part of the impedance of the proposed antenna, around the center frequency of the rejected bands, is larger than that of the broadband antenna. ***Figures 8*** and ***9*** show the measured radiation patterns in the x-z and y-z planes, at 2.5 and 5.75 GHz, for the proposed design. The radiation characteristics were also investigated. ***Figure 10*** shows the gain of the proposed antenna. The maximum peak antenna gains for the three operating bands are 5.7, 3.9 and 5.8 dBi, respectively, and the gain variations within the three bands are less than 2.9 dBi. The good gain characteristics of the antenna are very suitable for WiMAX applications.

CONCLUSION

A novel polygonal slot antenna for WiMAX applications has been implemented. Inserting two narrow strips along the centerline of the polygonal

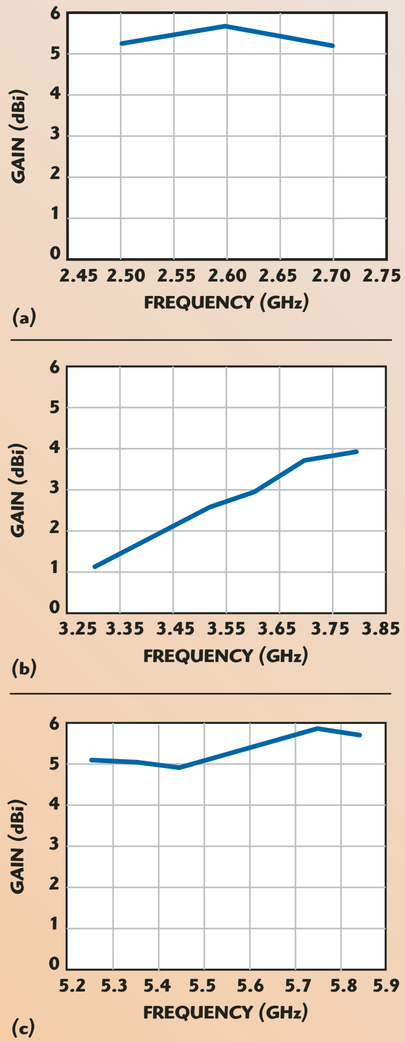

▲ *Fig. 10 Measured peak gain of the proposed antenna at the (a) low band, (b) median band and (c) high band.*

slot antenna leads to two rejected bands, from which the triple-bands for WiMAX applications can be obtained. The triple-bands of the proposed design satisfy the WiMAX standard. The proposed antenna can be easily excited by a 50 Ω microstripline printed on the FR-4 dielectric substrate, and good impedance matching can be obtained for the three operating frequency bands of WiMAX. The good gain of the proposed antenna is very suitable for WiMAX applications. ■

ACKNOWLEDGMENT

The financial support of this study by the National Science Council, Taiwan, Republic of China, under contact number NSC94-2213-E-218-006, is greatly acknowledged.

References

1. H.Y. Wei, S. Ganquly, R. Izmailov and Z.J. Haas, "Interference-aware IEEE 802.16 WiMAX Mesh Networks," *2005 IEEE Vehicular Technology Society International Symposium Digest*, Vol. 5, pp. 3102–3106.
2. Deploying License-exempt WiMAX Solutions, http://www.intel.com/netcomms/technologies/wimax/.
3. Y.F. Liu, K.L. Lau, Q. Xue and C.H. Chan, "Experimental Studies of Printed Wideslot Antenna for Wideband Applications," *IEEE Antennas and Wireless Propagation Letters*, Vol. 3, 2004, pp. 273–275.
4. H.L. Lee, H.J. Lee, J.G. Yook and H.K. Park, "Broadband Planar Antenna Having Round Corner Rectangular Wide Slot," *2002 IEEE Antennas and Propagation Society International Symposium Digest*, Vol. 2, pp. 460–463.
5. Y.W. Jang, "Broadband Cross-shaped Microstrip-fed Slot Antenna," *Electronics Letters*, Vol. 36, 2000, pp. 2056–2057.
6. T. Liu and K.L. Wong, "A Wideband Stub-by Monopole Antenna and a GPS for WiMAX Mobile Phones with E911 Function," *Microwave and Optical Technology Letters*, Vol. 46, 2005, pp. 485–487.

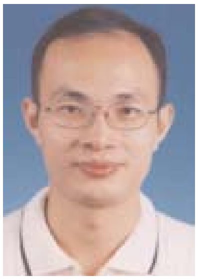

Wen-Shan Chen *received his BS degree in electronic engineering technology from the National Taiwan Institute of Technology (now the National Taiwan University of Technology) and his PhD degree from National Sun Yat-Sen University, Kaohsiung, Taiwan, ROC, in 2001. From 2001 to 2002, he was an assistant professor at the Chien-Kuo Institute of Technology, Changhua, Taiwan, ROC. He is currently an assistant professor of electronic engineering at the Southern Taiwan University of Technology, Tainan, Taiwan, ROC. His research interests include antenna design, RF and microwave circuits.*

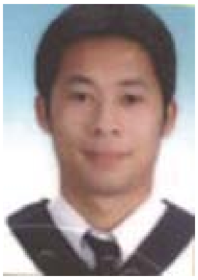

Bao-Hung Kao *received his BS degree from the Southern Taiwan University of Technology, Taiwan, ROC, in 2004. He is currently a student in the university's department of electronic engineering, where he is working toward a master's degree. His research interests include printed antenna for wireless communications and printed slot antenna for WiMAX applications.*

A 60 GHz Millimeter-wave CMOS RFIC-on-chip Dipole Antenna

This article presents a 60 GHz millimeter-wave RFIC-on-chip dipole antenna, fabricated with a 0.18 μm CMOS process. A planar dipole-antenna structure with an integrated microstrip via-hole balun was adopted to design this RFIC-on-chip antenna. The die size of the chip is 0.75 × 0.66 mm. A finite element method (FEM)-based 3-D full-wave EM solver, HFSS, is used for design simulation. The measured VSWR of the designed 60 GHz RFIC-on-chip antenna is less than 3 from 55 to 65 GHz. The simulated H-plane radiation pattern is close to an omni-directional pattern. The simulated antenna radiation efficiency is approximately 16 percent, due to the CMOS substrate loss. The measured maximum antenna power gain is approximately –10 dB.

There is an increasing demand for broadband multimedia components to satisfy the ever-increasing capacity of wireless networks. In particular, for dense local communications, the 60 GHz band for wireless personal area network (WPAN) applications is of special interest for short-range communications, due to the RF attenuation of the atmospheric oxygen by 10 to 15 dB/km, in a bandwidth of approximately 8 GHz, centered around 60 GHz. This makes the 60 GHz band of utmost interest for all kinds of short-range wireless communications.[1] In order to pursue the RF system-on-chip (SoC) approach for a 60 GHz radio, antennas integrated with a low cost monolithically integrated CMOS RF front-end circuitry have been studied.[2,3] In this article, a 60 GHz CMOS RFIC-on-chip dipole antenna is presented. A planar dipole-antenna structure with an integrated microstrip via-hole balun was adopted to design this RFIC-on-chip antenna. A FEM-based 3-D full-wave EM solver, Ansoft HFSS, is used for design simulation. The antenna chip is fabricated with a 0.18 μm CMOS process. On-wafer measurements of the input VSWR and the antenna gain of the designed RFIC-on-chip antenna were made with a microwave probe station.

ANTENNA DESIGN

The proposed planar printed dipole antenna is shown in ***Figure 1***. A microstrip via-hole balun acts as an unbalanced-to-balanced trans-

H.R. Chuang, S.W. Kuo, C.C. Lin and L.C. Kuo
National Cheng Kung University
Tainan, Taiwan, ROC

former between the feed coaxial line and the two printed dipole strips.[4] The length of the dipole strips is approximately a 1/4 wavelength. The ground plane of the microstrip line and the dipole strips are in the same plane. As indicated, a via-hole permits the feed (point 2) of a printed dipole strip to have the same phase as the feed (point 1) of the other printed dipole strip. Due to the 180° phase difference between the top conductor and the ground plane of the microstrip line, the feed at point 2 of the printed dipole strip will have a 180° phase difference with the other feed at point 1. The widths of the dipole arm strips are chosen to be approximately one-tenth of a wavelength. The width of the microstrip feed-line is designed to have a characteristic impedance of 50 Ω. The accurate dimensions of each part of the printed dipole and integrated via-hole balun must be numerically computed to achieve the de-

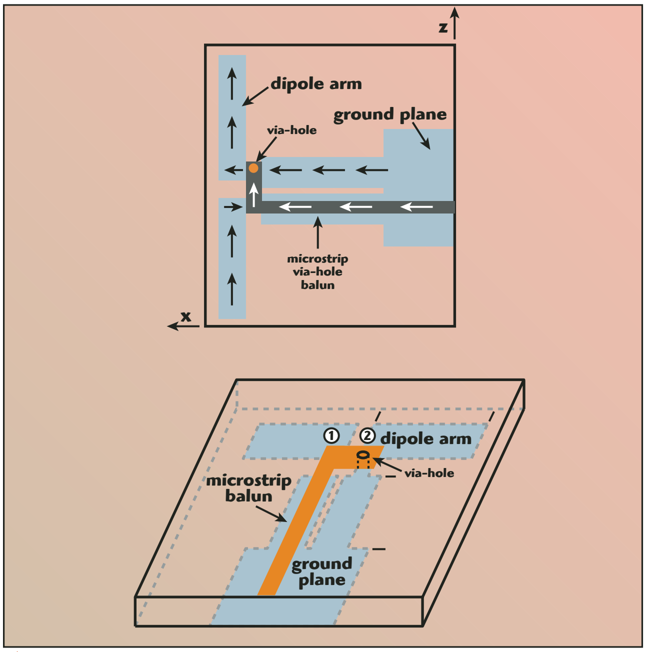

▲ *Fig. 1 Planar dipole antenna with an integrated via-hole balun.*

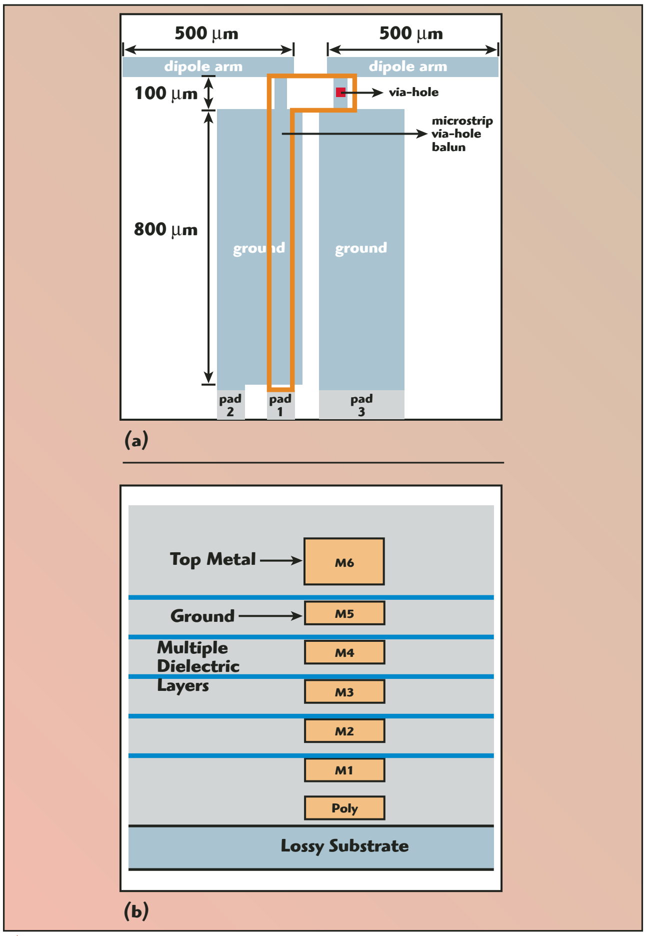

▲ *Fig. 2 Chip layout (a) and cross-section (b) of the 60 GHz CMOS RFIC-on-chip antenna.*

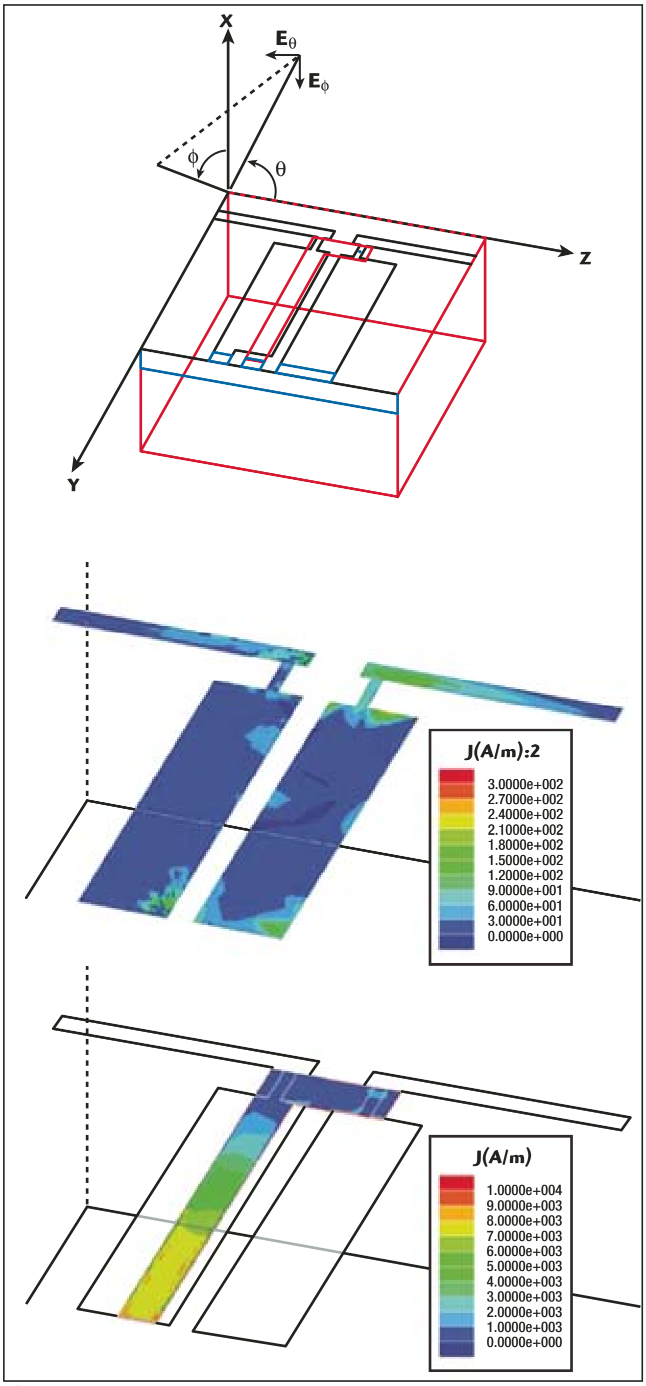

▲ *Fig. 3 HFSS simulation scheme and simulated antenna current distribution.*

sired performance of the printed dipole antenna. ***Figure 2*** shows the chip layout and the cross-section of the designed 60 GHz RFIC-on-chip dipole antenna fabricated with a 0.18 µm CMOS process.

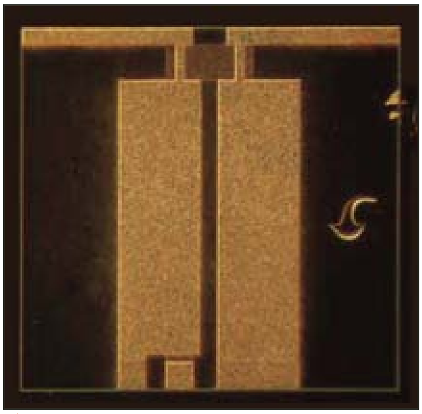

Fig. 4 Chip micrograph.

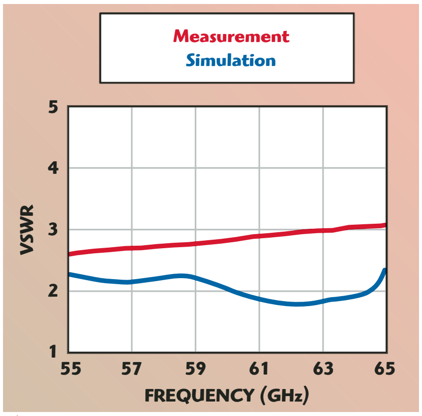

Fig. 5 Simulated and measured antenna input VSWR.

SIMULATION AND MEASUREMENT RESULTS

Figure 3 shows the HFSS simulated antenna current distribution. The simulated current density vectors on the top and bottom metals show the balanced current distribution and the 180° phase difference of the flowing current vectors at the two feed points of the printed dipole. This shows the working of the integrated microstrip balun. ***Figure 4*** shows a chip micrograph of a fabricated 60 GHz CMOS RFIC-on-chip antenna. The chip size is 0.75 × 0.66 mm with a substrate thickness of approximately 500 µm. ***Figure 5*** shows the input VSWR of the antenna, measured on-wafer, which is less than 3 from 55 to 65 GHz. ***Figure 6*** and ***Table 1*** show the simulated antenna radiation patterns and power gain values in the H- and E-planes at 60 GHz. Note that the antenna power gain (absolute gain), Gp, is defined as

$$Gp = \text{directive gain} \bullet \text{radiation efficiency} \qquad (1)$$

The simulated antenna radiation efficiency is approximately 16 percent, which may be due to the CMOS substrate loss. The H-plane pattern is close to an omni-directional pattern except for some attenuation in a certain direction. The simulated maximum, minimum and average power gains in the H-plane are approximately –9, –16 and –11 dBi, respectively. The absolute power gain of the antenna was measured on-wafer with the technique described by Simons and Lee.[5] As illustrated in ***Figure 7***, two identical RFIC-on-chip antennas are placed face-to-face within a distance R. One antenna is used as a transmitting antenna and the other as a receiving antenna. It is noted that the distance R separating the two identical antennas should satisfy the far-field condition, which is equal to or greater than[5]

$$R = \frac{2D^2}{\lambda_0} \qquad (2)$$

where D and λ_0 is the largest aperture dimension of the RFIC-on-chip antenna and the free-space wavelength at the operating frequency, respectively. From the Friis power transmission formula, the maximum antenna power gain (in the central forward direction of the dipole antenna) is given by

$$G_rG_t = G^2 = \left(\frac{P_r}{P_t}\right)\left(\frac{4\pi R}{\lambda_0}\right)^2 = \left|S_{21}\right|^2\left(\frac{4\pi R}{\lambda_0}\right)^2 \qquad (3)$$

where

G_t and G_r = gains of the transmitting and receiving antennas
P_t = power transmitted
P_r = power received

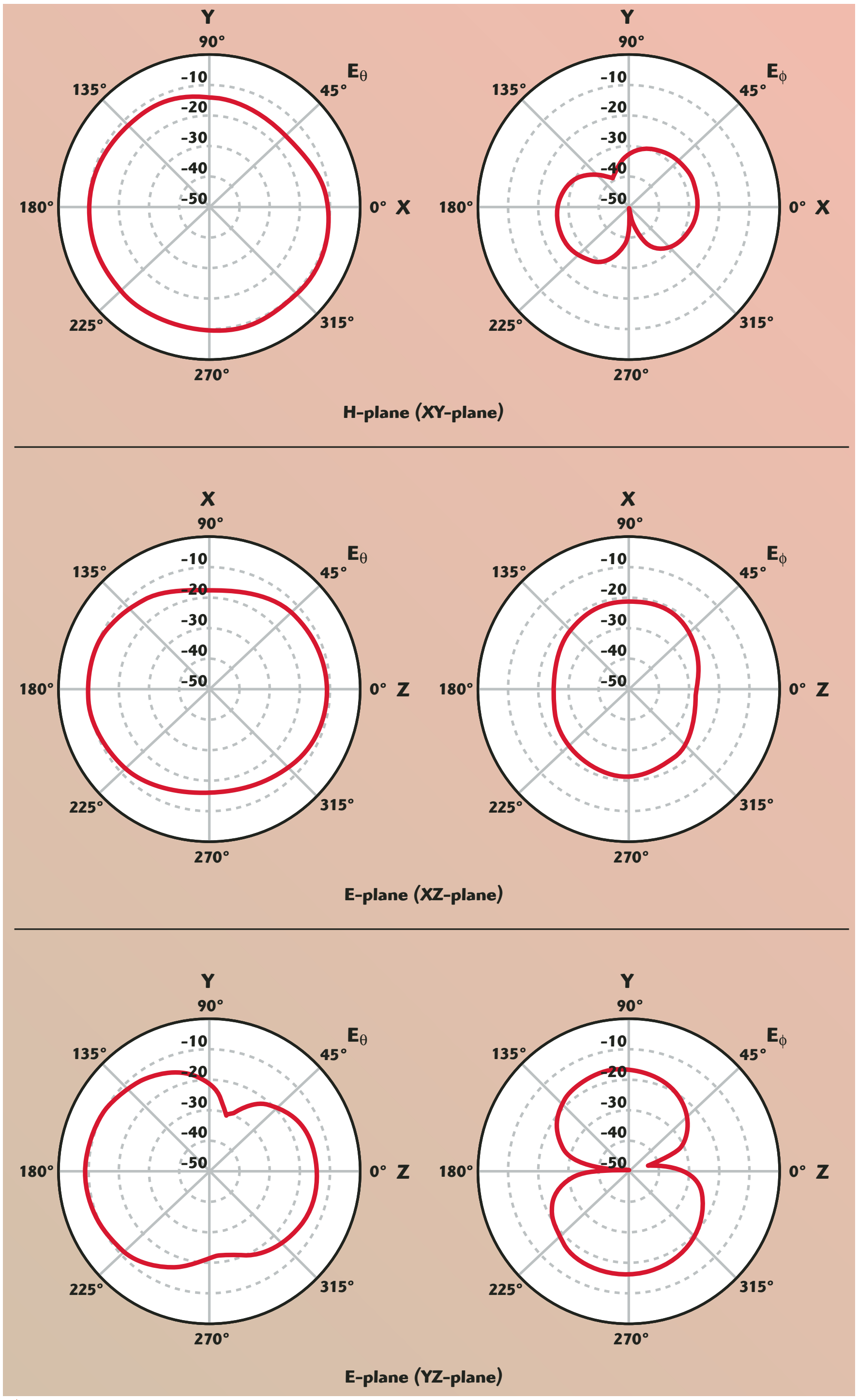

Fig. 6 Simulated antenna radiation patterns in the H- and E-planes at 60 GHz.

TABLE I

SIMULATED ANTENNA POWER GAIN AT 60 GHz

Simulated Power Gain	E_θ Field (dBi) Max	Min	Average	E_ϕ Field (dBi) Max	Min	Average
X-Y plane	–9.0	–15.9	–11.0	–25.4	–50.8	–31.0
X-Z plane	–9.9	–17.1	–13.0	–21.0	–27.2	–23.5
Y-Z plane	–9.2	–30.5	–15.8	–15.8	–53.9	–22.6

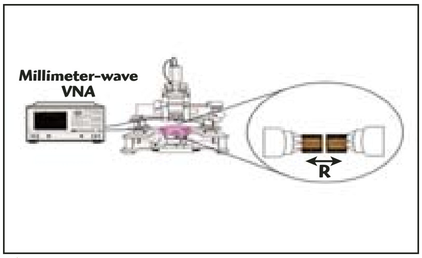

▲ *Fig. 7 Illustration of the on-wafer setup to measure the gain of the RFIC-on-chip antenna.*

▲ *Fig. 8 The probe station, on-wafer measurement setup.*

TABLE II

PERFORMANCE SUMMARY OF A 60 GHz CMOS RFIC-ON-CHIP DIPOLE ANTENNA WITH VIA-HOLE BALUN

	Simulation	*Measurement*
Frequency range (GHz)	57 to 64	55 to 65
VSWR	< 2.5	< 3.0
Radiation efficiency (%)	16	–
Max. antenna gain (dBi)	–9.0	–10.0
Chip size (mm)	0.75 × 0.66	

Similarly, since the two antennas are identical, $G_r = G_t = G$. The power ratio P_r/P_t is the measured direct transmission coefficient $|S_{21}|^2$ from the VNA. ***Figure 8*** shows a photograph of the probe-station, on-wafer measurement setup. The measured maximum antenna power gain at 60 GHz is approximately –10 dBi, which is in good agreement with the simulation results. ***Table 2*** shows the performance summary of the antenna radiation characteristics.

CONCLUSION

This article discussed the design, fabrication and on-wafer measurement of a 60 GHz millimeter-wave CMOS RFIC-on-chip dipole antenna with an integrated microstrip via-hole balun. This is to realize an RF system-on-chip (SoC) for a 60 GHz radio with the antenna integrated with a low cost, monolithically integrated, CMOS RF front-end circuitry. The antenna chip is fabricated with a 0.18 μm CMOS process with a chip size of 0.75 × 0.66 mm. The HFSS FEM-based 3-D full-wave EM solver is used for design simulation. The input VSWR and the maximum antenna power gain of the RFIC-on-chip antenna were measured on-wafer. The measured antenna VSWR is less than 3 from 55 to 65 GHz. The simulated H-plane radiation pattern is close to an omni-directional pattern and the simulated antenna radiation efficiency is approximately 16 percent, which may be due to the CMOS substrate loss. The measured maximum antenna power gain at 60 GHz is approximately –10 dBi, which is in good agreement with the simulation results. The integration of the designed 60 GHz RFIC-on-chip antenna with a 60 GHz CMOS RF front-end circuit will be pursued. ■

ACKNOWLEDGMENTS

The authors would like to thank the Chip Implementation Center (CIC) of the National Science Council, Taiwan, ROC, for supporting the TSMC CMOS process.

References

1. Federal Communications Commission, *Amendment of Parts 2, 15 and 97 of the Commission's Rules to Permit Use of Radio Frequencies Above 40 GHz for New Radio Applications*, FCC 95-499, ET Docket No. 94-124, RM-8308, December 15, 1995; available via: ftp//ftp.fcc.gov./pub/Bureaus/Engineering_Technology/Orders/1995/fcc95499.txt.
2. C.H. Doan, S. Emami, A.M. Niknejad and R.W. Brodersen, "Design of CMOS for 60 GHz Applications," *2004 Proceedings of the IEEE Solid-State Circuits Conference*, pp. 440–449.
3. Y.P. Zhang, M. Sun and L.H. Guo, "On-chip Antennas for 60 GHz Radios in Silicon Technology," *IEEE Transactions on Electron Devices*, Vol. 52, No. 7, July 2005, pp. 1664–1668.
4. H.R. Chuang and L.C. Kuo, "3-D FDTD Design Analysis of a 2.4 GHz Polarization-diversity Printed Dipole Antenna with Integrated Balun and Polarization-switching Circuit for WLAN and Wireless Communication Applications," *IEEE Transactions on Microwave Theory and Techniques*, Vol. 51, No. 2, February 2003, pp. 374–381.
5. R.N. Simons and R.Q. Lee, "On-wafer Characterization of Millimeter-wave Antennas for Wireless Application," *IEEE Transactions on Microwave Theory and Techniques*, Vol. 47, No. 1, January 1999, pp. 92–96.

A LOW PROFILE MULTI-BAND U-SHAPED APERTURE-COUPLED MICROSTRIP ANTENNA WITH A COIL

In this article, an L-shaped probe-fed, U-slot patch antenna with a coil element is studied. The L-shaped probe feed is used to enhance the impedance matching, which is necessary because of a low radiation resistance in the usable band. The coil contributes to the size reduction of the antenna and acts also as a resonance device to create a multi-band response. The measured impedance bandwidths are approximately 795 to 962 MHz and 1825 to 2308 MHz for a S_{11} *less than –10 dB. This multi-band characteristic covers the cellular, PCS, IMT-2000 and WLL frequency bands. The measured results, for the radiation patterns, show relatively good characteristics.*

Microstrip patches are an attractive type of antenna because of their low cost, conformability and ease of manufacture. The aperture-coupled configuration[1] also provides the advantage of isolating spurious feed radiation by using a common ground plane. The primary barrier to the implementation of these antennas in many applications, however, is their limited bandwidth, which is only of the order of a few percent for a typical patch radiator. Because of this, much work has been devoted to increasing the bandwidth of microstrip antennas. One technique that has been used is a near resonance aperture, resulting in a bandwidth of the order of 20 percent.[2] Other techniques that have been used extensively are aperture-coupled stacked patch antennas with a bandwidth of 30 to 50 percent.[3,4] A broadband, air-filled, stacked U-slot patch antenna has been studied where a bandwidth of the order of 44 percent can be achieved.[5] A broadband, H-shaped, aperture-coupled, U-slot patch antenna[6] with an impedance bandwidth of 21.7 percent has also been presented. In addition, a wideband microstrip patch antenna, with a tilted L-probe feeding[7] and having an impedance bandwidth of 37.1 percent, has been described.

In this article, an alternative design technique that combines an L-shaped probe-fed, U-slot patch antenna with a coil is proposed. The L-shaped probe feed is used to enhance

YONG-WOONG JANG
Keukdong College
Chungbuk, Korea
HYUN-CHUL GO
AMC Centurion Korea Co. Ltd.
Seoul, Korea

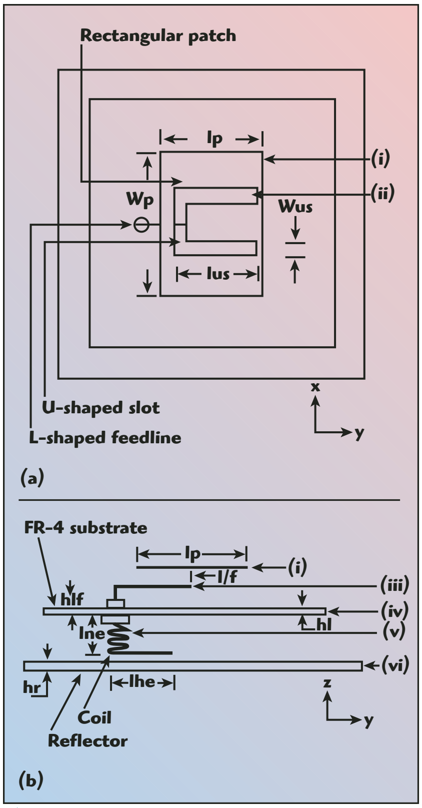

Fig. 1 *Structure of the proposed antenna; (a) top view and (b) side view.*

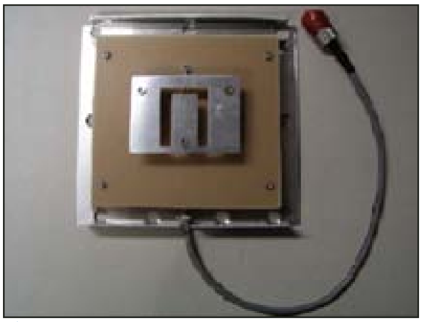

Fig. 2 *The fabricated antenna.*

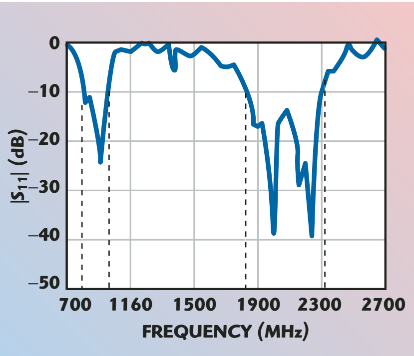

Fig. 3 *Measured return loss.*

the impedance matching, necessary because of a low radiation resistance in the usable band. In addition, the coil contributes to a reduction of the antenna size and acts as a resonance

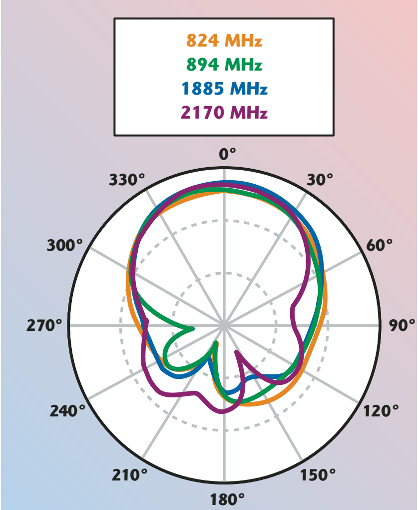

Fig. 4 *Measured x-z radiation pattern.*

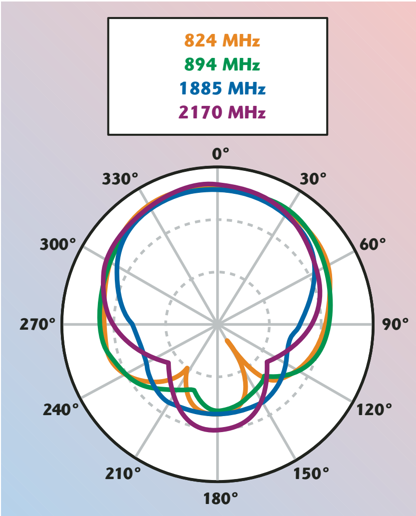

Fig. 5 *Measured y-z radiation pattern.*

device for the cellular band. A thick substrate is also used to enhance the bandwidth. The bandwidth characteristics of the proposed antenna depend highly on the thickness of the patch substrate as well as on the L-shaped feed line. The experimental impedance bandwidth is approximately 795 to 962 MHz and 1825 to 2308 MHz for a S_{11} less than –10 dB. Experimental results for the radiation patterns of the multi-band antenna are also presented.

ANTENNA STRUCTURE AND EXPERIMENTAL RESULTS

The geometry of an alternative design technique that combines an L-shaped probe-fed, U-slot patch antenna with a coil is shown in ***Figure 1***. The design parameters of the antenna are: For the patch (i), $l_p = 52$ mm, $W_p = 71$ mm; for the U-shaped slot (ii), $l_{us} = 33$ mm, $W_{us} = 40.5$ mm; for the L-shaped probe feed (iii), $l_{lf} = 38$ mm, $h_{lf} = 5.5$ mm; for the dielectric layer (iv), $\varepsilon_{rl} = 4.6$, $l = 21$ mm, $h_1 = 1.6$ mm, $\tan\delta_2 = 0.0009$; for the coil (v), $l_{he} = 16.5$ mm; and for the aluminum reflector (vi), $l_r = 148$ mm, $W_r = 160$ mm, $h_r = 1.3$ mm. The resonances of the coil and of the U-slot patch with probe feeding occur on either sides of the operating band. Since the U-slot patch is used as a radiator and a resonator, its length cannot be changed to control the impedance at the L-shaped feed line, as would be done ordinarily with an aperture-coupled patch. The L-shaped probe feeding is used to enhance the impedance matching. This is necessary because of the low radiation resistance in the usable band. In addition, a coil is used to reduce the size of the antenna and acts as a resonance device for the cellular band. A thick substrate is used to enhance the bandwidth. The bandwidth characteristics of the proposed antenna depend highly on the thickness of the substrate patch and the L-shaped feed line, which improve of the coupling and the impedance matching. A photograph of the fabricated antenna is shown in ***Figure 2***.

The return loss of the antenna was measured with an HP8510 network analyzer. The antenna size, including the reflector, is 160 × 148 × 34.5 mm. The measured impedance bandwidths, shown in ***Figure 3***, are approximately 795 to 962 MHz (19.8 percent at a center frequency of 880 MHz) and 1825 to 2308 MHz (24 percent at a center frequency of 2000 MHz), for a S_{11} of less than –10 dB. The experimental results for the return loss exhibit the dual-resonance characteristics of a multi-band of the antenna. After calibration using a horn antenna, the radiation patterns were measured. ***Figure 4*** shows the measured x-z radiation patterns as a function of frequency. The half-beam width is approximately 90°. ***Figure 5*** shows the measured y-z radiation patterns as a function of frequency. All the radiation patterns show good characteristics.

Figure 6 shows the measured gain versus frequency for the cellular and GSM bands. The gain is relatively high over most of the band, most probably because of the finite size of the antenna substrate, that is the power in the surface wave is not confined to the sub-

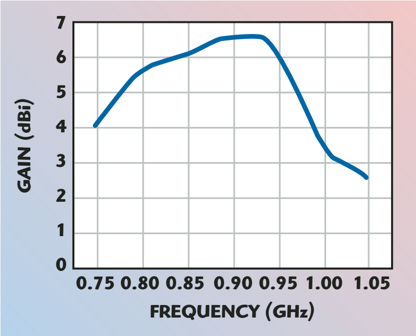

▲ *Fig. 6 Measured antenna gain in the cellular and GSM bands.*

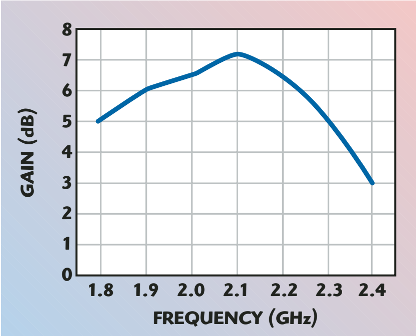

▲ *Fig. 7 Measured antenna gain in the PCS, IMT-2000 and WLL bands.*

strate but diffracted by the substrate edge, an effect which was not taken into account in the analysis. The measured gain is 5.5 dBi over the entire usable frequency band, but drops off rapidly past the band edges. The measured gain versus frequency in the PCS, IMT-2000 and WLL bands is shown in ***Figure 7***. The measured gain is also 5.0 dBi over the entire usable frequency band, but drops off rapidly past the band edges. This is due to impedance mismatch and pattern degradation, as the back radiation level increases rapidly at these frequencies.

CONCLUSION

In this article, an L-shaped probe-fed, U-slot patch antenna with a coil was described. The L-shaped probe feed is used to enhance the impedance matching necessary because of a low radiation resistance in the usable band. The coil contributes to the antenna size reduction and acts as a resonance device for the cellular band. The measured results on this antenna show a multi-band characteristic. The proposed reduced size antenna can be used in practical applications such as cellular, GSM, PCS, IMT-2000 and WLL. ■

References

1. D.M. Pozar, "A Microstrip Antenna Aperture Coupled to a Microstripline," *Electronics Letters*, Vol. 21, 1985, pp. 49–50.
2. F. Croq and A. Papiernik, "Large Bandwidth Aperture-coupled Microstrip Antenna," *Electronics Letters*, Vol. 26, No. 16, 1990, pp. 1293–1294.
3. F. Croq and D.M. Pozar, "Millimeter-wave Design of a Wideband Aperture-coupled Stacked Microstrip Antenna," *IEEE Transactions on Antennas and Propagation*, Vol. 39, 1996, pp. 1170–1176.
4. S.D. Targonski, R.B. Waterhouse and D.M. Pozar, "Wideband Aperture-coupled Stacked Patch Antenna Using Thick Substrates," *Electronics Letters*, Vol. 32, No. 21, 1996, pp. 1941–1942.
5. B.L. Ooi and C.L. Lee, "Broadband Air-filled Stacked U-slot Patch Antenna," *Electronics Letters*, Vol. 35, No. 7, 1999, pp. 515–516.
6. S.C. Gao, L.W. Li, M.S. Leong and T.S. Yeo, "Wideband Microstrip Antenna with an H-shaped Coupling Aperture," *IEEE Transactions on Vehicular Technology*, Vol. 51, No. 1, January 2002, pp. 17–27.
7. D.S. Qi, B.H. Li and H.T. Liu, "Wideband Microstrip Patch Antenna with Tilted L-probe Feeding," *Microwave and Optical Technology Letters*, Vol. 43, 2004, pp. 380–382.

Yong-Woong Jang *received his BS and MS degrees from Myongji University, Seoul, Korea, in 1989 and 1991, respectively, and his PhD degree from Ajou University, Suwon, Korea, in 1999, all in electronics engineering. He became a member of the faculty of the department of electronics communication engineering at the College of Keukdong, Chungbuk, Korea, where he is now an associate professor. His main research interests include antennas, RF systems and numerical methods in solving electromagnetic problems.*

Hyun-Chul Go *received his BS and MS degrees in electronics engineering from the Korea University of Technology and Education, Cheonan, Korea, in 1999 and 2001, respectively. He worked as a research engineer in the R&D center of Hankook Antenna Co. Ltd. from 2001 to 2004. Since 2004, he has been working as a research engineer at the R&D center of AMC Centurion Korea Ltd. His current research interests include internal antennas, wideband and high gain antennas for repeaters, and UWB antennas.*

6 × 6 MM QUAD-BAND RF TRANSMIT MODULES FOR HIGH EFFICIENCY EDGE OPERATION

In today's fast paced mobile handset market, design houses and manufacturers are challenged to meet a variety of targets to satisfy network provider's high expectations in cellular and multimedia phones. Design cycle time, performance, feature requirements, form factor, quality and cost targets remain dominant selection criteria for mobile phone designers.

Next generation mobile multimedia applications (combining GSM/GPRS/EDGE/WCDMA/WLAN/GPS in one phone, for example) put even more stringent requirements on the hardware architecture. Partitioning of the baseband and RF components are critical handset design decisions with respect to functionality, performance, integration level, size and cost.

In an effort to lead the market trend in RF front-end architecture, integration and form factor size reduction, TriQuint Semiconductor has recently introduced its latest RF transmit (TX) module, the TQM6M5001, which adds full linear EDGE functionality to its successful family of 6 × 6 × 1.1 mm^3 GSM/GPRS TX modules. This module family offers significant advantages in addressing these challenges using the TX module architecture already adopted with marketplace success by many GSM and EDGE phones.

TX modules in this family incorporate all of the critical RF transmit functions between the transceiver and the antenna into a single module offering a 60 percent size reduction compared to competing discrete solutions. EDGE operation has been added with no increase in size and has pin-out compatibility with the existing GSM/GPRS product, TQM6M4002, by re-using a ground pin as the EDGE (8PSK) mode pin. The high level integration needed

TRIQUINT SEMICONDUCTOR INC.
Hillsboro, OR

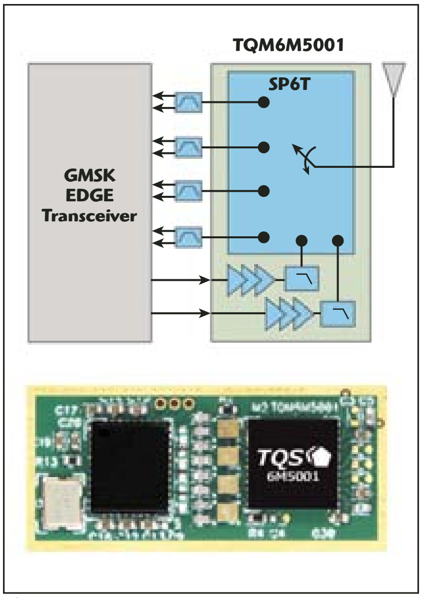

▲ *Fig. 1 The TQM6M5001-based GSM/EDGE RF reference design.*

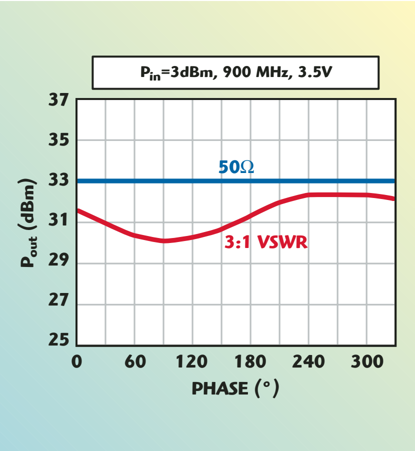

▲ *Fig. 2 TQM6M5001 GMSK output power performance vs. a 3:1 VSWR at the antenna.*

to develop such an advanced product—adding functionality while keeping to the previous generation's form factor—is possible by direct in-house control of key technologies including InGaP GaAs HBT and GaAs PHEMT circuits.

KEY DESIGN ADVANCES

The new TQM6M5001 EDGE-enabled TX module builds on the discrete GSM/EDGE 850/900 and DCS1800/PCS1900 PA blocks and integrated power control found in present generation power amplifier modules. It adds a low insertion loss, quad-band PHEMT transmit/receive SP6T switch with four RX-ports, harmonic and low pass filtering, integrated switch decoder, and full ESD protection—all in an unprecedented size of 36 mm^2. Full system level GSM/GPRS and EDGE compliance is assured when used with the latest generation of linear EDGE transceivers.

The TQM6M5001 EDGE TX module requires no external matching and eliminates the need to manage the PA-to-switch interface. This advancement in form factor and integration level was achieved in part by eliminating all surface-mount devices (SMD) inside the laminate-based module, resulting in clear size, cost and time-to-market advantages.

USER BENEFITS AND PROCESS TECHNOLOGY

The TQM6M5001 transmit module combines the functionality of a quad-band power amplifier (PA) with power control, a low pass transmit filter (LPF), a quad-band TX/RX switch including decoder and ESD protection into one module (see ***Figure 1***). A fundamental advantage of this transmit module is its built-in PA-to-front-end interface. By combining PA and antenna switch functionality into one module, the system bill of materials is significantly reduced, adding simplified supply chain management to an already lengthy list of advancements that benefit the mobile phone manufacturer.

In EDGE (8PSK) mode the module serves as a linear gain block with approximately 30 dB of gain in GSM850/900 and 34 dB of gain in the DCS/PCS bands, respectively. It provides a zero-bit, multi-bit or continuous bias feature for the lowest current consumption in 8PSK mode. The TQM6M5001 was designed utilizing in-house six-inch processes: InGaP GaAs HBT for the PA function and GaAs PHEMT for the LPF and switch components. All control functions for the PA and switch are incorporated into a proprietary CMOS design. A dedicated control pin toggles between GMSK and EDGE mode. All four switch RX ports are frequency independent allowing the user flexibility in handset phone-board layout.

Identical in size and pin-out to other GSM/GPRS TX module family members, the GMSK/EDGE-enabled TQM6M5001 is also laminate-based and uses bondwire inter-chip connections. All passive elements are integrated into the GaAs dies, thus eliminating the need for any SMDs inside the module. Full EDGE functionality could therefore be added to the module while maintaining a $6 \times 6 \times 1.1$ mm^3 footprint.

The TQM6M5001 transmit module architecture and interface is optimized for next generation multimode transceivers and baseband transceiver chip sets. By combining the TQM6M5001 GSM/EDGE TX module with TriQuint's small form factor RX SAW filters (1.4×1.2 mm^2 single filter series, or 2.0×1.5 mm^2 2-in-1 filter series, for example) a complete RF solution is achieved with the assurance of full interface alignment and best-in-class RF performance.

DESIGN GOALS AND PERFORMANCE HIGHLIGHTS

A primary design goal met by the TQM6M5001 transmit module is full EDGE functionality and ETSI specification compliance in all four frequency bands (GSM850/900 and DCS1800/PCS1900) without compromising critical DC and RF performance in GSM/GPRS mode.

In GMSK mode, the maximum output power in the GSM850/900 band is typically 33.5 dBm with a system power-added efficiency (PAE) of 42 percent. In DCS/PCS band, a maximum output power of 31.5 dBm is achieved with a system PAE of 38 percent. For maximum output power, the harmonic power is less than –36 dBm in all frequency bands. The input power level range between +1 and +5 dBm is aligned to most transceivers currently available on the market. Ruggedness of the new transmit module exceeds a VSWR of 30:1 and stability is guaranteed up to a VSWR of 20:1, with all spurious signals below –36 dBm.

Mobile handset designs are typically calibrated at an output power of 33 dBm in the GSM850/900 band and at 30.5 dBm in the DCS/PCS (high) band. Since the impedance of the antenna can deviate from the nominal 50 Ω value depending on operational environment (for example, metal plane vs. human ear), network providers are more and more focused on the total radiated output power at the antenna. For a typical mismatch

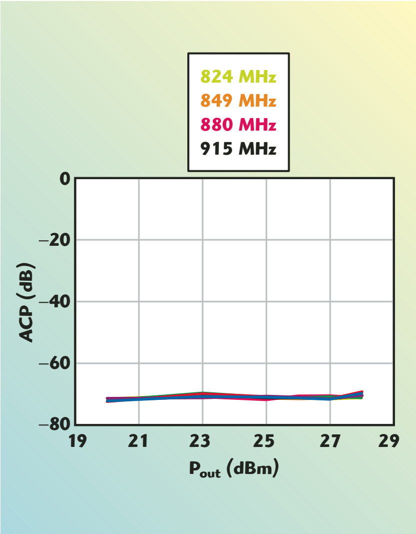

▲ *Fig. 3 Low band ACP400 performance vs. output power.*

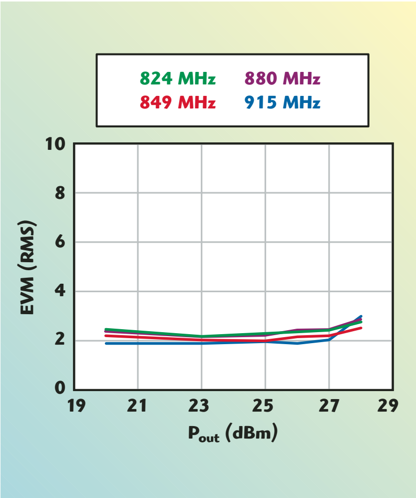

▲ *Fig. 4 EVM (RMS) vs. frequency.*

load (VSWR of 3:1), the peak-to-peak P_{out} variation of the TQM6M5001 vs. all phase angles is only 3 dB (see ***Figure 2***). Therefore, the device is able to provide sufficient radiated output power even under widely varying operational conditions that the mobile phone might conceivably experience in daily use.

EDGE PERFORMANCE

The TQM6M5001 transmit module behaves like a linear gain block in 8PSK mode. This means the output power of the TX module is controlled by the level of the input power. The transceiver provides the power setting and power ramp of the TX signal. For an output power of 27 dBm at the antenna pin, the ACPR at 400 kHz offset is typically lower than –65 dBc for nominal conditions (see ***Figure 3***), and lower than –60 dBc for a minimum battery voltage of 3.2 V. EVM (RMS) performance is < 3 percent at the same output power level of 27 dBm showing full specification compliance with good margin (see ***Figure 4***).

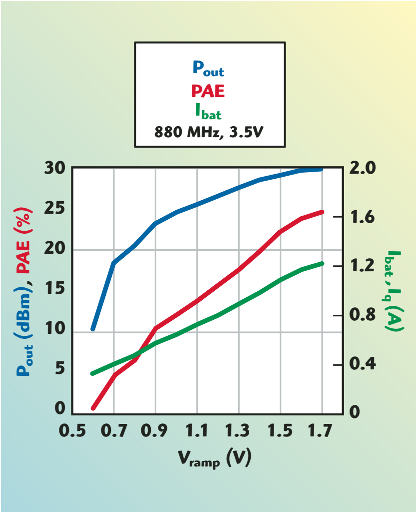

▲ *Fig. 5 EDGE mode current consumption improvement using continuous bias at ACP400 of –58 dBc (GSM900).*

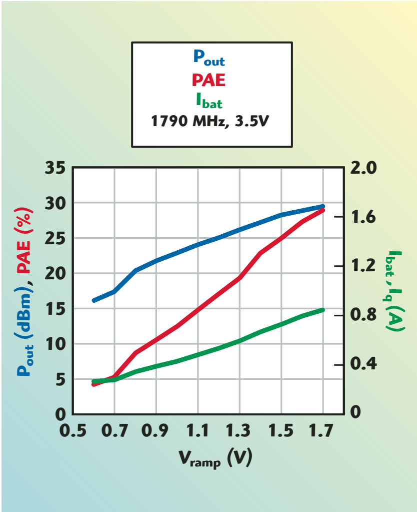

▲ *Fig. 6 EDGE mode current consumption improvement using continuous bias at ACP400 of –58 dBc (DCS).*

In EDGE (8PSK) mode the VRAMP pin is no longer used for setting the output power as was its function in GMSK mode. As previously noted the output power of the linear gain block is set by the input power as controlled by the transceiver. The V_{RAMP} pin now serves as a bias control input in EDGE mode, setting the idle current (continuous bias) depending on the output power. By varying the applied voltage between 0.6 and 1.7 V, operating current can be adjusted as a function of output power to benefit from improved PAE at low output power levels.

By utilizing this built-in feature of continuous bias in 8PSK mode, the current consumption at low output power can be improved significantly by re-adjusting the bias of the PA accordingly. The manufacturer has the option to use this feature in a multi-bit or continuous bias mode, or simply leave V_{RAMP} constant for zero-bit operation. For example, at 1790 MHz, with a V_{RAMP} voltage of 0.6 V, an output power up to 10 dBm can be achieved with an ACPR of < –58 dBc, thus resulting in an average operating current of 0.32A during an EDGE burst. With a control voltage of 1.7 V at the same P_{out} level the operating current would rise to approximately 0.75 A. More and more customers utilize this feature to their advantage as a current consumption benefit in next-generation handset designs.

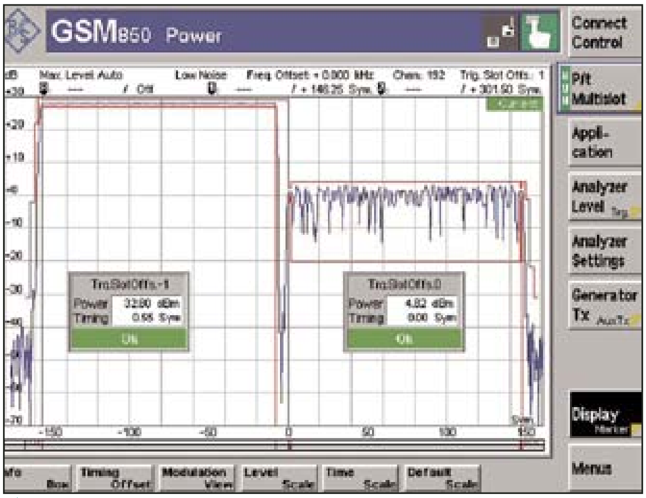

▲ *Fig. 7 TQM6M5001 behavior of two subsequent bursts with maximum P_{out} in GMSK mode and minimum P_{out} in EDGE mode.*

Plots in ***Figures 5*** and ***6*** illustrate PAE and I_{bat} as a function of V_{RAMP} when optimized for an ACP400 of –58 dBc and shown at various output power settings (controlled by input power from the transceiver).

By design, full multi-slot GMSK/EDGE capability is assured with the TQM6M5001 EDGE TX module as part of an RF system solution for today's CMOS-based EDGE transceivers. ***Figure 7*** shows full power vs. time specification compliance by the TQM6M5001 in the extreme case of a full power GMSK burst followed by the lowest power EDGE burst, as required by ETSI specifications.

SUMMARY AND OUTLOOK

High level integration continues to set the pattern for succeeding generations of mobile phone RF front-end modules. As more functionality is added to advanced phone devices and handset form factors continue to shrink or grow slimmer, manufacturers expect RF module solutions that not only meet specifications, but pay dividends such as enhanced PAE, greater platform design facilitation and ease in generational transitioning that is inevitable as phones migrate from GSM/GPRS mode to full GPRS/EDGE, and beyond.

TriQuint has reached the next integration milestone with its 6 × 6 × 1.1 mm^3 multi-mode GSM GPRS/EDGE quad-band transmit module, the TQM6M5001, which offers mobile handset designers size and cost advantages to satisfy the high performance RF needs of next generation mobile handsets. Leveraging sophisticated in-house InGaP GaAs HBT and PHEMT GaAs processes with design expertise in power amplifiers, switches, signal filtering and CMOS design, TriQuint has successfully applied key processes and engineering skill sets to produce an RF transmit module with highly competitive performance and features.

With its EDGE functionality the TQM6M5001 is a significant step in the move toward fulfilling 3G RF radio and chipset concepts, which will further optimize the interface between transceiver and transmit modules across various modulation schemes. The successful implementation of cost-effective multi-mode phones will only be achievable if the combination of performance, cost, quality and form factor can be met in all respects. While the TQM6M5001 represents a significant contribution to the manufacture of new EDGE mobile phones, the company's design engineers are already addressing the need for W-CDMA and EDGE (WEDGE) transmit modules that leverage existing experience in GSM, EDGE, W-CDMA and WLAN/WiMAX PA and front-end modules to enable the next generation of 3G multimedia mobile handsets.

TriQuint Semiconductor Inc., Hillsboro, OR (503) 615-9000, e-mail: info@tqs.com, www.triquint.com.

RS No. 301

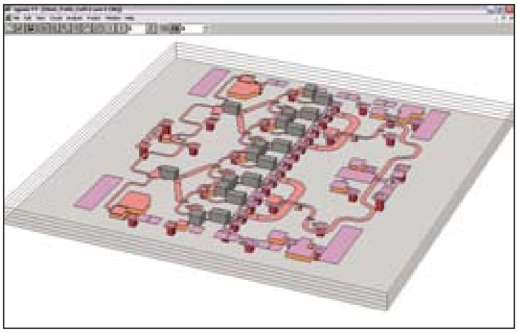

PERFECTLY CALIBRATED PORTS FOR EM ANALYSIS

Sonnet pioneered the high frequency EM (electromagnetic) market, shipping the first commercially viable product in 1989. Since then, the company has continued regularly introducing significant capability into this market. Sonnet's new Version 11 expands upon this tradition with multiple new features that fundamentally change high frequency design methodology in many areas, but especially in the field of radio frequency integrated circuit (RFIC) design.

Each of the new Sonnet Version 11 features deserves an entire article. However, following a brief description of the new features, this piece will focus on the most significant feature, the new "Co-calibrated™ ports," shown in ***Figure 1***. These are perfectly calibrated ports on the interior of a high frequency circuit, never before available in any EM tool. Perfect port calibration will completely change how high frequency design is accomplished, especially in the RFIC world.

Fig. 1 A 3-D planar circuit with numerous internal ports used for mounting surface-mount devices. ▼

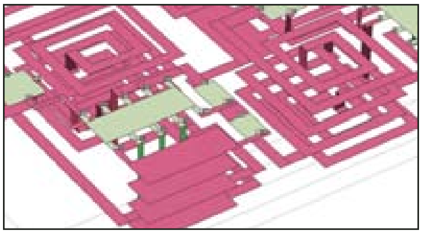

Prominent among Version 11's new features is a fully revised interface to the Agilent Advanced Design System (ADS) framework. Designed with the support of Agilent, the interface now easily installs as a design kit. In addition, a free ADS interface to the free SonnetLite EM analysis is available. Absolutely invaluable to ADS users who use Sonnet as their primary EM tool, the interface is also seeing wide use by ADS users using Sonnet to double check EM results from other sources, and by project teams using multiple EM tools. Two menu selections literally transfer an entire EM layout into Sonnet, including all analysis and substrate information. The interface is completely bi-directional, so users can confidently go back and forth as desired. Finally, one attractive new feature is that Sonnet can create the popular ADS "layout look-alike" symbols in the ADS schematic. The user can actually see in the ADS schematic where a port is in the layout, as shown in

SONNET SOFTWARE INC.
North Syracuse, NY

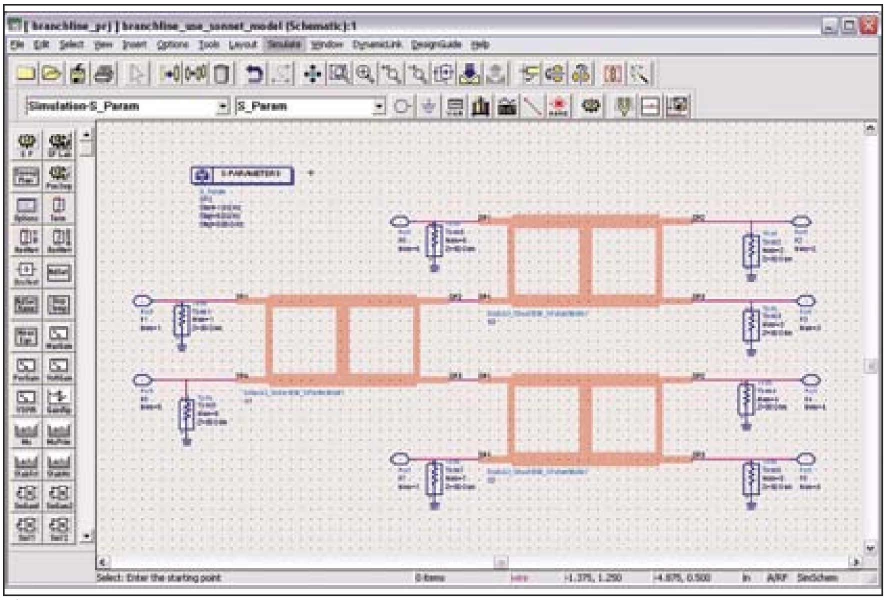

▲ *Fig. 2 Agilent ADS schematic with three "layout look-alike" schematic elements (pink) from Sonnet.*

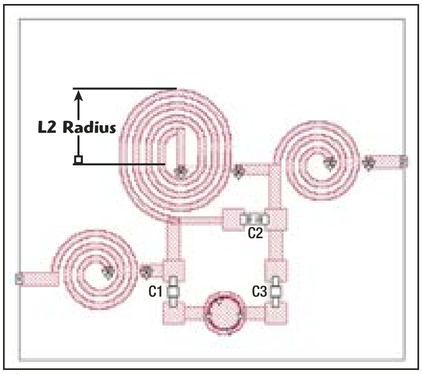

▲ *Fig. 3 Top view of an elliptic low pass filter with three pairs of Co-calibrated ports (C1, C2 and C3).*

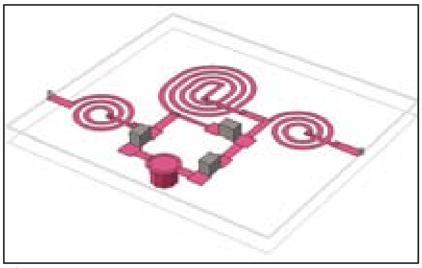

▲ *Fig. 4 3-D view of the same filter.*

Figure 2. This is useful if there are dozens, or even hundreds of ports, a situation expected to become common with the introduction of Co-calibrated ports.

The same easy bi-directional transfer also continues to be available in the AWR Microwave Office interface and in the Cadence Virtuoso interface. New with Version 11 is an interface to AWR's X-model capability, where users can create parameterized high frequency models based directly on Sonnet data.

New to all three interfaces (Agilent, AWR and Cadence) is the ability to specify use of Sonnet's thick metal model and Sonnet's patented conformal meshing. The thick metal model uses multiple sheets to model thick metal. Simpler "tube-like" models of thickness force all current to flow on the surface of the metal regardless of frequency. That model loses validity when metal thickness is less than several skin depths. This is not a problem with the Sonnet multi-sheet model, which is valid over the complete frequency range. Sonnet's conformal meshing lowers subsection count by a factor of up to 100 for curving transmission line structures, all the while still including the high edge current necessary for high accuracy.

To further enhance Sonnet's interoperability, there are procedures for bi-directional transfer and specification of the new Co-calibrated ports in all three frameworks, even though no framework is yet aware of this new concept. All three framework interfaces also now support direct use of Sonnet's remote execution and cluster computing capability. With remote execution, users set up and administer remote batch queues, easily submitting jobs to be performed anywhere on the network. With the addition of this capability to the interfaces, users may use these functions directly from the framework of their choice.

The cluster computing capability splits a multi-frequency job into multiple jobs for simultaneous execution. For example, if a job takes one hour per frequency and requires 10 frequencies, it is automatically split into 10 jobs with complete results (including interpolation capability) available in one hour. This means that what were previously overnight jobs now barely allow time for a cup of coffee and a chat with a friend.

A second cluster option is now available. Previously, cluster computing required use of third-party software. While that software is widely available in some large companies, availability is problematic elsewhere. Thus, cluster computing is now offered "for everyone else," that is, no third-party software is needed and it is easily administered.

Sonnet also now includes a 64-bit analysis engine. This means problem sizes over 2 Gbytes are now feasible. These analysis engines are available for Windows XP64, Redhat 64 Linux and SuSE 64 Linux, and are even included in the cluster computing solution.

Any and all of these features are major events by themselves, but the really major event in Version 11 is "Co-calibrated ports." This is a completely new concept in high frequency EM analysis, so a little background is in order.

Sonnet analyzes 3-D planar circuits. Planar means that much of the circuit is on the surface of one or more stacked substrates. Vias connect between circuitry on different levels. 3-D means that all coupling between metal in all three dimensions is included.

Sonnet is a "shielded" analysis, that is, it analyzes the circuit inside a conducting, shielding box. This shielding box allows a mathematical formulation that results in an extremely low numerical noise floor, typically 140 to 180 dB down. There is another subtle, but incredibly important result of analyzing with a shielding box: The shielding sidewalls form perfect short circuit reference planes.

Thus, from the very beginning, Sonnet has always had perfectly calibrated sidewall ports. What is new in

Version 11 is that a way has been discovered to perfectly calibrate all ports internal to the planar circuit. This allows perfectly calibrated, global ground referenced ports to be placed anywhere. All the tiny stray inductances and capacitances associated with (and between) all the internal ports in a group are now exactly removed.

This is a fundamental and brand new capability for high frequency EM design. Take, for example, a power FET amplifier, perhaps in the form of an RFIC. EM analysis cannot analyze the FET. Therefore, the FET is left out and internal ports are included in the EM analysis. Later, using a favorite framework, the nonlinear FET model is connected and a harmonic balance analysis is performed.

The problem with this old way is that the internal ports always include at least some tiny stray capacitances and inductances, electromagnetic artifacts of the way internal ports must be created and which are present in all EM analyses. These tiny port discontinuities cause large errors in certain situations, for example, at the inputs and outputs of power FETs, where they operate with impedances of only a couple ohms. Most EM analyses make no attempt at all to calibrate internal ports. Now, with Co-calibrated ports, exactly calibrated groups of internal ports are easily realized. The internal ports for the power FET are analyzed with absolutely all of the port discontinuities exactly removed.

The potential applications are limitless. For example, if the power FET is removed and perfectly calibrated ports substituted, why not take out all the resistors and capacitors in the RFIC and substitute Co-calibrated ports there, too? Now, with a single EM analysis, one may repeatedly populate the RFIC with different resistors, capacitors and transistors until an optimum design is achieved. ***Figures 3*** and ***4*** show a low pass elliptic filter designed in exactly this way.

With this design flow, design iterations are done at circuit theory analysis speed, hardly time enough for even a sip of coffee. In the old way, the designer would physically change one (or more, if you are desperate) components and then repeat the entire EM analysis. That approach can require weeks to complete a single design. In the new way, the best possible design can be determined in minutes. The old way of doing design is simply no longer viable.

The potential of perfectly calibrated internal ports is mind-boggling. Continuing with the power FET example, the power FET consists of an input manifold, gate fingers and an output manifold. Designers usually have a pretty good model for a single gate finger, but a model for the entire power FET can be elusive. Now the answer is simple. For the EM analysis, take out all the gate fingers and substitute a group of internal ports. If there are ten gate fingers, there are now 20 ports for the gate region. There is another port for the input to the gate manifold and one more port for the output manifold, for a total of 22 ports. Now simply connect 10 copies of the single gate finger model into the 20 internal ports.

Sonnet even includes the ability to automatically connect a user specified S-parameter data file or an ideal lumped component to the internal ports. There is no need to resort to a complicated schematic in the selected framework to do the connection. The S-parameter file can come from measurement, from a model in any design framework, from vendor supplied data (including models for surface-mount devices), or even from another Sonnet EM analysis. All this thanks to the box sidewalls providing perfect short circuit reference planes, critical in achieving Sonnet's perfect internal port calibration.

CONCLUSION

Sonnet's new Version 11 with 64-bit capability, an easy-to-administer cluster computing capability, significantly enhanced interfaces to Agilent, AWR and Cadence, and the new fundamentally significant Co-calibrated ports is simply going to change everything in planar microwave design.

Sonnet Software Inc.,
North Syracuse, NY
(315) 453-3096,
www.sonnetsoftware.com.

RS No. 300

Don't forget to check next month's issue for our software update, featuring the most recent design tools on the market.

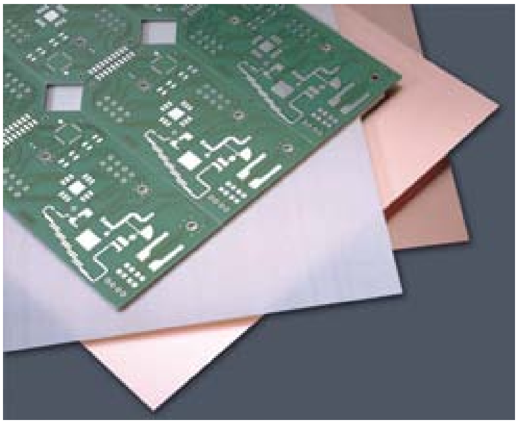

HIGH FREQUENCY CIRCUIT MATERIAL FOR BASE STATION APPLICATIONS

A replacement product for PTFE woven glass circuit material has been introduced that provides superior mechanical and thermal properties, uses the RO4000® resin system for ease of fabrication and is a cost competitive option for base station antenna applications (see ***Figure 1***).

Fig. 1 A typical base station antenna and installation.

The RO4230™ high frequency laminate extends the capabilities of the successful RO4000 product series into antenna applications. The ceramic-filled, glass-reinforced hydrocarbon-based material provides the controlled dielectric constant, low loss performance and excellent passive intermodulation response required for mobile infrastructure microstrip antenna applications.

One of the main advantages of the new RO4230 laminate is that it is fully compatible with conventional FR4 processing and does not require special treatments needed on PTFE-based laminates for plated-through-hole preparation. Thus, it is an affordable alternative to PTFE antenna materials, allowing designers to optimize performance/price benefits.

THERMAL CHARACTERISTICS

The resin system of the RO4230 dielectric material is designed to provide thermo-mechanical properties critical to antenna design. Its coefficient of thermal expansion (CTE) in both the X and Y directions is similar to that of copper, thus minimizing the thermal effects of environmental conditions by reducing the stresses that can lead to warpage of the printed circuit board antenna. RO4230 material's glass transition temperature exceeds 280°C; this, coupled with low Z-axis CTE, provides excellent plated-through-hole reliability. In addition, its increased thermal conductivity over equivalent PTFE woven glass materials (0.44 W/m/K) allows for antenna designs with increased power handling capability.

ROGERS CORP., ADVANCED CIRCUIT MATERIALS DIVISION
Chandler, AZ

ELECTRICAL PROPERTIES

To truly be an advantageous replacement for existing antenna circuit material requires that its electrical properties closely match the needs of antenna designers so existing antennas require minimal or no redesign. RO4230 laminate has a dielectric constant (Dk) of 2.98 ±0.05 and a loss tangent (Df) of 0.0020 measured at 2.5 GHz and 0.0023 at 10 GHz. These values allow antenna designers to realize desired gain while minimizing signal loss in the feed network. In addition, RO4230 material has demonstrated low PIM performance, with values better than –155 and up to –162 dBc using two 43 dBm swept tones at 1900 MHz. ***Figure 2*** shows an insertion loss comparison with PTFE/woven glass, RO4350 laminate and a competitive thermoset material. ***Figure 3*** shows the effect of the RO4230 material's improved thermal conductivity.

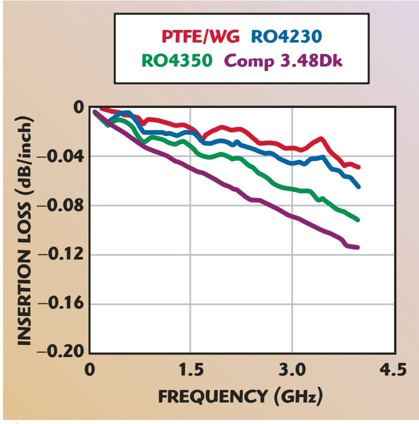

▲ *Fig. 2 A comparison of insertion loss of 0.030" RO4230 with RO4350B™ material and competitive thermoset materials.*

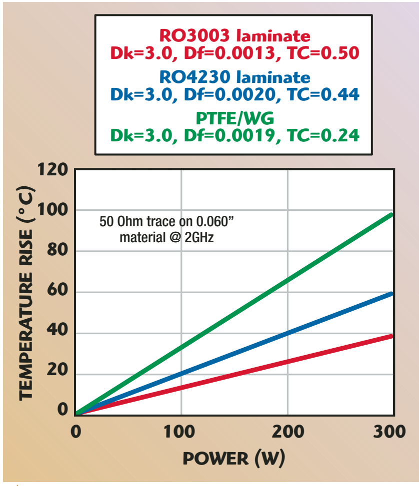

▲ *Fig. 3 The effect of thermal conductivity on power handling capability.*

CONCLUSION

The market has had a need for an improved material for use in cellular base station antennas, satellite radio applications and WiMAX antennas, as well as others. RO4230 laminate was designed to provide an enhanced price/performance benefit over Dk 3.0 PTFE/woven glass materials.

RO4230 laminate is available in standard thicknesses of 0.030", 0.040" and 0.060" with 1 oz. electrodeposited copper cladding. Standard panel sizes are 24" × 18", 24" × 36" and 48" × 36". Nonstandard panel sizes are available up to 48" × 108".

Rogers Corp., Chandler, AZ (480) 961-1382, www.rogerscorporation.com.

RS No. 302

RO4000 & R04230 are licensed trademarks of Rogers Corp.

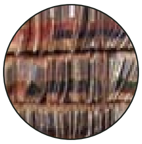

Application Note

This application note, "Preamplifiers and System Noise Figure," is designed to assist engineers in learning how to improve the accuracy of their measurements by using a low noise amplifier in front of a spectrum analyzer to reduce the effective noise figure of RF and microwave test systems. This paper discusses applications and characteristics of Agilent's latest amplifier technology. Highlighted are Agilent's 87405C portable preamplifiers that provide exceptional gain of 25 dB and a probe-power bias connection.

Agilent Technologies Inc.,
Palo Alto, CA (800) 829-4444, www.agilent.com.

RS No. 310

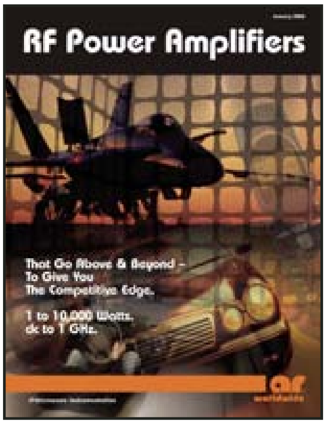

RF Power Amplifier Brochure

This RF power amplifier brochure from AR Worldwide RF/Microwave Instrumentation features the company's wide range of currently available RF power amplifiers. The brochure highlights the "A" and "W" series amplifiers that cover 1 to 10,000 W and DC to 1 GHz. Product photographs, descriptions, specifications and performance graphs are included for each model.

AR Worldwide RF/Microwave Instrumentation,
Souderton, PA (215) 723-8181, www.ar-worldwide.com.

RS No. 311

Multiphysics Introduction CDs

This suite of tutorial CDs introduces the viewer to different applications within FEA modeling: multiphysics modeling, RF simulations, AC/DC simulations, reaction engineering and acoustics simulations. Each CD contains a general introduction that illustrates how multiphysics modeling can be applied to the designated field. Following that is a series of audio-visual tutorials complete with detailed documentation explaining every step of the modeling process.

COMSOL Inc.,
Burlington, MA (781) 273-3322, www.comsol.com.

RS No. 312

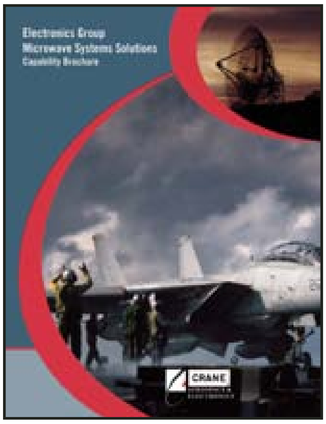

Capability Brochure

This newly revised capability brochure includes two new switch matrices and a new phase amplitude modulator in addition to numerous other products. Featuring the company's high reliability, high density products, ideal for military/defense, electronic warfare, space, aerospace and industrial application, the Microwave Systems Solutions Capability Brochure is available by e-mail: electronics@craneae.com.

Crane Aerospace & Electronics, Microwave Systems Solutions,
Chandler, AZ (480) 961-6269, www.craneae.com.

RS No. 313

Product Catalog

This product catalog highlights the company's Johnson® line of stainless steel SMA connectors. All designs are based on 50 Ω system impedance per MIL-STD-348 and operate at frequencies up to 26.5 GHz minimum. All contacts are plated with 50 microinches of gold for excellent durability and high frequency performance. The right angle PC mount jack features a rigid one-piece body and a one-piece swept contact.

Emerson Network Power Connectivity Solutions,
Waseca, MN (800) 247-8256,
www.emersonnetworkpower.com/connectivity.

RS No. 314

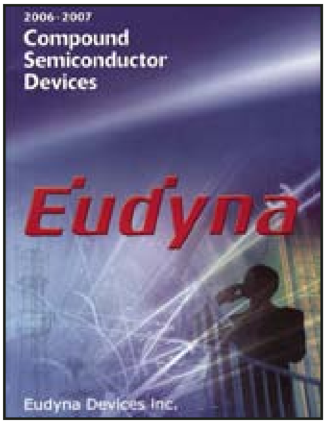

Product Catalog

This catalog features the company's compound semiconductor devices that include new products, wireless devices, fiber optics devices and foundry service. New information and telecommunications technology has resulted in the development of high speed mobile communications, subscriber/access lines and mobile computing at a very fast pace, one after another. The use of compound semiconductor products has been a key building block expanding and establishing the communications infrastructure.

Eudyna Devices Inc.,
Yokohama, Kanagawa, Japan +81-45-853-8151,
www.eudyna.com.

RS No. 315

Product Catalog

Focus Microwaves assists designers of power and low noise amplifiers in accelerating their design cycle and improving their products by providing accurate load pull and noise measurement systems. This catalog features the company's standard and customized solutions for R&D and production testing from 30 MHz to 110 GHz, as both stand-alone hardware and fully-integrated systems. Fields of use include: noise parameter testing; nonlinear load pull measurements; and harmonic load pull measurements.

Focus Microwaves,
Montreal, Canada (514) 684-4554, www.focus-microwaves.com.
RS No. 316

Product Selection Guide

The October 2006 product selection guide summarizes over 460 products including 40 new products. Newly redesigned are dedicated sections for connectorized modules, Designer's Kits, application circuits and a competitor cross reference table. This new selection guide contains over 71 new products released in 2006, which are not included in the 2006 Designer's Guide Catalog. In addition to the October selection guide, an updated version of Hittite's popular 2006 Designer's Guide CD-ROM is now available.

Hittite Microwave Corp.,
Chelmsford, MA (978) 250-3343, www.hittite.com.
RS No. 317

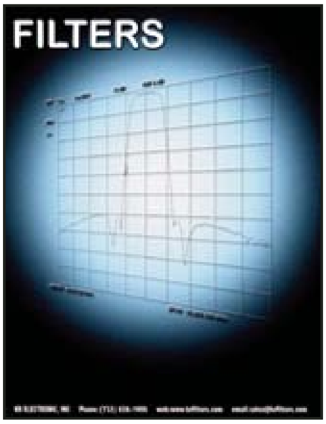

Filters Product Brochure

For over 34 years KR Electronics has designed and manufactured precision LC filters for the commercial and military markets. This brochure highlights the company's products that include low pass, bandpass, high pass and band reject filters. Custom filter specifications can be sent on the included request form for a prompt technical review and quotation.

KR Electronics Inc.,
Avenel, NJ (736) 636-1900, www.krfilters.com.
RS No. 318

Communications CD Catalog

This comprehensive Fall 2006 satellite communication and earth station equipment CD catalog features the company's up/downconverters, test translators, IF/video equalizers, redundancy switchover units, video modulators and modems. Specific products include synthesized converters with 1.0 kHz and 125 kHz step sizes, INMARSAT L- and C-band converters, pilot generators and receivers, crystal controlled converters, video exciters and custom designed products.

MITEQ Inc.,
Hauppauge, NY (631) 436-7400, www.miteq.com.
RS No. 319

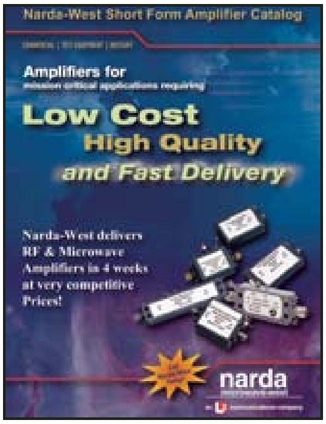

Short Form Amplifier Brochure

This brochure features the company's new amplifier product line that offers low cost, high quality and quick turnaround ("off the shelf" on some products and four weeks from time of order in most cases). These amplifiers are suitable for use in commercial, military, test equipment, prototype and laboratory applications. These new amplifiers broaden the already extensive line of amplifiers from Narda Microwave-West.

Narda Microwave-West,
Folsom, CA (916) 351-4500, www.nardamicrowave.com.
RS No. 320

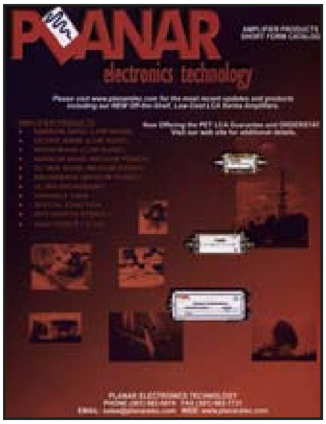

Short Form Catalog

This short form amplifier product catalog presents the company's full line of low noise and medium power amplifiers. Featured items highlight amplifier capabilities in narrow band, octave band, broadband and ultra-broadband, with low noise and medium power options. Also shown are higher power and variable gain amplifiers, as well as a section of new products.

Planar Electronics Technology,
Frederick, MD (301) 662-5019, www.planarelec.com.
RS No. 321

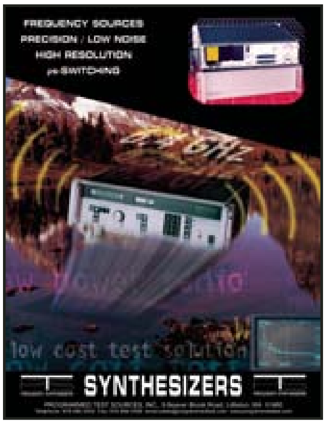

Product Catalog

This catalog describes the company's complete line of PTS frequency synthesizers. These synthesizers produce fast-switching, low phase-noise precision frequencies. With easy remote programming they are vital in advanced measurement or production systems and also serve as stand-alone test equipment. Numerous options and accessories that can be combined in a virtually limitless manner to provide a product that although not custom built, will closely match your specifications. Models range from 0.1 to 6400 MHz.

Programmed Test Sources Inc., Littleton, MA (978) 486-3400, www.programmedtest.com.

RS No. 322

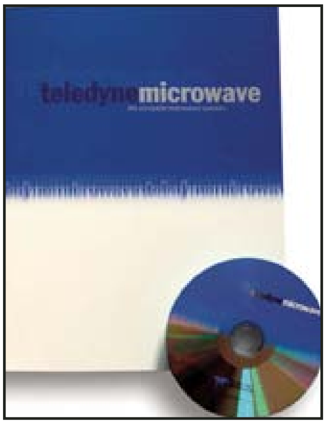

Product Catalog

This catalog features the company's product line that includes integrated microwave assemblies; transceiver subsystems; power and low noise amplifiers; BAW delay lines; isolators and circulators; filters: lumped element, combline and high power switched filters; YIG oscillators and filters; and frequency synthesizers. The catalog includes product descriptions, specifications, outline drawings, definitions, screening information, quality and reliability information, and ordering information.

Teledyne Microwave, Mountain View, CA (650) 962-6944, www.teledynemicrowave.com.

RS No. 323

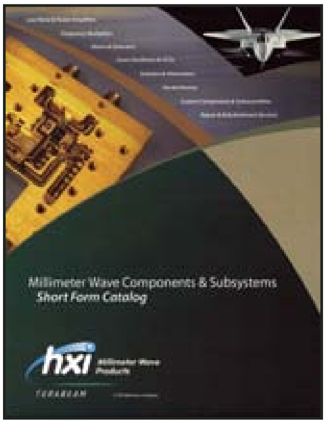

Short Form Catalog

This short form catalog highlights the company's millimeter-wave (MMW) products that include a complete line of components from 18 to 110 GHz. The millimeter-wave product availability includes low noise amplifiers, medium/high power amplifiers, mixers, detectors, Gunn oscillators and VCOs, frequency multipliers, PIN switches and attenuators, isolators and circulators, and custom subassemblies.

Terabeam/HXI, Haverhill, MA (978) 521-7300, www.terambeam-hxi.com.

RS No. 324

CD-ROM Catalogs

This CD-ROM includes several new and updated brochures and catalogs including the newest edition of the LMR® Wireless Products Catalog with the latest updates to the LMR product line, HeliFoil™ ultra low loss coaxial cable and connectors, and Phase-Track™ 210 phase stable coaxial cable assemblies. This CD-ROM features an easy-to-use menu for navigation within each catalog. Also included are valuable "how-to" installation videos to assist users of LMR low loss coaxial cable products.

Times Microwave Systems, Wallingford, CT (203) 949-8400, www.timesmicrowave.com.

RS No. 325

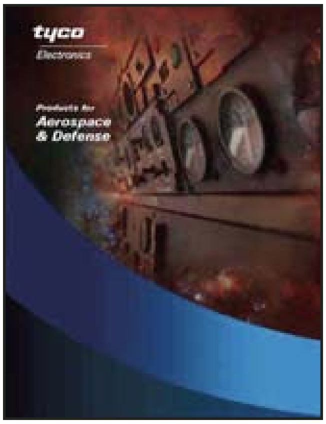

Product Catalog

The aerospace and defense product catalog combines the company's core product offering for space, commercial aircraft, aerospace electronics, defense electronics and in-flight networking applications. Also, the catalog provides nearly 700 pages of detailed information on products suitable for or specially designed for the aerospace and defense electronics industry. Products included in the catalog are AGASTAT timers and relays, AMP connectors and fiber optics, CII high performance, low power relays and power contactors.

Tyco Electronics Corp., Harrisburg, PA (800) 522-6752, www.tycoelectronics.com.

RS No. 326

Product Catalog

Weinschel Associates has a 40 year legacy as a supplier of high performance, high quality broadband passive components to the RF and microwave communities. This new full-line catalog provides a snapshot of product offerings in the company's fixed attenuator, termination, variable attenuator, DC block and coaxial adapter lines.

Weinschel Associates, Gaithersburg, MD (301) 963-4630, www.weinschelassociates.com.

RS No. 327

10 W Power Divider

This new line of 10 W power dividers is designed for antenna and test applications. The model 151-201-008 is an eight-way, 50 Ω power divider that operates in a frequency range from 800 to 2000 MHz. This unit offers 22 dB typical isolation, 1.5 dB maximum insertion loss, ±0.4 dB maximum amplitude tracking, 10 W average power at the common port and SMA female connectors. Other configurations are available.

BroadWave Technologies Inc., Franklin, IN (317) 346-6101, www.broadwavetech.com.

RS No. 216

Switch Matrix

This HF/UHF switch matrix offers combined frequency bands in a single rack-mount housing. Designed for advanced signal reception applications, the model 1517 switch matrix is configured with 16 inputs and 16 outputs and can be arranged with any combination of HF (1.5 to 32 MHz) and UHF inputs (20 to 1000 MHz). It is contained in a 4U (7 inches high) rack-mount chassis and is intended for small- to medium-sized antenna interfacing installations.

Crane Aerospace & Electronics, Electronics Group, Redmond, WA (425) 882-3100, www.craneae.com.

RS No. 218

EM Simulation

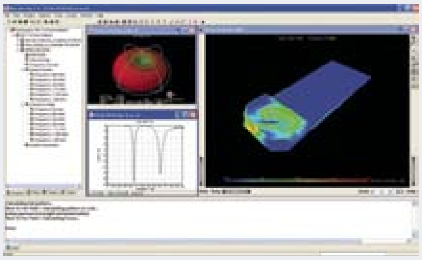

The MicroStripes 3D EM simulation solution for RF/microwave and antenna design which integrates with Applied Wave Research's Microwave Office® circuit design software has reached version 7.5. It enables users to import any desired excitation waveform during the modeling process, run the simulation, and evaluate the results without any additional post-processing. This makes it possible, for example, to simulate the effect of a lightning strike, electromagnetic pulse or electrostatic discharge on a system using a pre-computed, analytic or measured waveform. In version 7.5, ground planes can also be used for models without meshing all of the space between the system and ground plane. Version 7.5 also reduces the computational resources required to model ferrite tiles.

Flomerics Ltd., Hampton Court, Surrey, UK +44 (0) 20 8487 3000, www.flomerics.com.

RS No. 220

Portable Personal Antenna

The Freedom Antenna® is an all-in-one product with a completely redesigned look that is compatible with the top 10 selling cell phones sold in the US along with 200 other cell phone models. This antenna is a portable personal antenna with broadband capability to provide clearer reception for cellular phones and other wireless devices by extending the range and reducing dropped calls caused by hands-free and other demanding uses. Utilizing patented technology, the Freedom Antenna is compatible with all major wireless carriers and technologies and offers high performance in a slim package for both fixed and mobile hands-free use in vehicles, offices, homes and is ideal for travel. Price: $34.95.

ARC Wireless Solutions Inc., Wheat Ridge, CO (303) 421-4063, www.antennas.com.

RS No. 256

Two-way Power Divider

This two-way power divider operates in a frequency range from 350 to 6000 MHz. The broad frequency coverage allows multiple bands to share a common antenna or distributed antenna system. The design uses a multi-section microstrip design to achieve the bandwidth, offer adequate isolation and good input and output VSWR at a moderate price.

Microlab/FXR, Parsippany, NJ (973) 386-9696, www.microlab.fxr.com.

RS No. 254

Patch Antenna

The model MCR03-04-N is a reduced sized patch antenna that was designed for use with GOES satellites. mWAVE Industries was contracted to design a reduced sized rugged patch antenna for use in high wind and rough sea environments. The MCR03-04-N is only 9" across × 2.75" in height. This new antenna operates in the GOES 402 MHz band and is right hand circular polarized (RHCP). The recorded gain was 4 dBic, recorded return loss was 14 dB and the HPBW is 112 degrees.

mWAVE Industries LLC, Gorham, ME (207) 857-3083, www.mwavellc.com.

RS No. 221

2.45 GHz Antenna

The RH and RAH series 2.45 GHz antennas are ideal for products requiring an ultra-compact, aesthetically pleasing antenna in a straight (RH series) or right-angle (RAH series) form factor. These quarter-wave antennas feature a center frequency of 2.45 GHz and deliver a wide operational bandwidth and low VSWR. Despite their diminutive size, these antennas are able to resist shock and abuse. The antennas attach using a standard SMA or FCC-compliant Reverse Polarity SMA connector. Alternate connectors or custom colors are available for volume OEM customers. RH series and RAH series antennas are immediately available and priced under $2.50 in high volume.

Antenna Factor, Grants Pass, OR (800) 489-1634, www.antennafactor.com.

RS No. 255

Ultra-wideband Radar Sensors

These 24 GHz ultra-wideband (UWB) radar sensors are primarily for driver-assistance systems. The 24 GHz short-range radar sensor is a highly-integrated "smart sensor" designed to improve safety and comfort functions in automotive applications by providing object detection and tracking to further support drivers. The UWB radar sensors are designed to resist inclement weather and harsh environmental conditions more than other sensing technologies, such as infrared devices. Additionally, the radar sensors can be deployed in security, military and unmanned vehicle operations, as well as mining and industrial sensing applications.

M/A-COM, Lowell, MA (800) 366-2266, www.macom.com.

RS No. 257

COMPONENTS

Flange-mount SMA Adapter

The redesigned flange-mount, SMA in-series adapter has been made shorter and offers lower VSWR. This unit operates in the DC to 18 GHz frequency range with a 1.20 maximum VSWR. These adapters are shorter, model 5311A, male/female units 0.98" long compared with 1.13" in length for its predecessor; the model 5312A male/male is 0.95" compared to 1.00" and the model 5313A female/female is 1.01" compared with 1.25", respectively. The units are RoHS compliant and are ideal for panel-mounted applications.

Aeroflex/Inmet Inc.,
Ann Arbor, MI (734) 426-5553,
www.aeroflex-inmet.com.

RS No. 223

Digital Attenuator

This high speed, digitally-controlled attenuator operates in a frequency range from 2 to 19 GHz. This attenuator offers a maximum insertion loss of 4.5 dB and has a high speed driver offering switching between attenuation settings typically of less than 500 ns. The VSWR is 2.2 and the maximum operating RF input power is +20 dBm. The digital control is 8-bit true binary logic and the DC power supply on this model is ±12 VDC (other voltages are also available).

American Microwave Corp.,
Frederick, MD (301) 662-4700,
www.americanmicrowavecorp.com.

RS No. 224

Coaxial Isolators and Circulators

This new range of broadband coaxial isolators and circulators operate in a frequency range from 2 to 20 GHz. These isolators and circulators offer good isolation and losses and power of 20 W in a small package with SMA and N type connectors. Applications include military and commercial products such as VSAT, video transmitter/receiver and PCS cellular. Delivery: Lead time of one week.

Electronika International Inc.,
Cleveland, OH (440) 743-7034,
www.electronikainc.com.

RS No. 225

I and Q Vector Modulator

The model M2V-82N-5JX is a 360°, 50 dB high dynamic range PIN diode, I and Q vector modulator that operates in a frequency range from 18 to 21.5 GHz. This device offers simultaneous phase and amplitude control. Across the entire band the phase and amplitude flatness is ±10° and ±0.75 dB to 40 dB. The VSWR is better than 1.8. This device is capable of handling +15 dBm CW, 1 W maximum. With monotonic performance, this device is voltage-controlled via two (I and Q) inputs and switches in 350 ns. Size: 3.25" × 3" × 1".

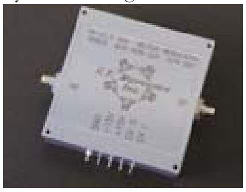

G.T. Microwave Inc.,
Randolph, NJ (973) 361-5700,
www.gtmicrowave.com.

RS No. 226

Bandpass Filter

The model D-462 is a space qualified bandpass filter that operates in a frequency range from 75 to 150 MHz. Typical features include: 3 dB bandwidth of 0.05 percent, 70 dB shape factor of 5:1, operating temperature of –45° to +80°C and package weight of < 25 grams. Comprehensive space environmental qualification performed in-house. Custom designs and package options are available (SMT, GPO, GPPO and SMA interfaces).

Networks International Corp.,
Overland Park, KS (913) 685-3400,
www.nickc.com.

RS No. 229

Directional Coupler

The model CS20-50-435/4 is a new 20 dB coupler that operates in a frequency range from 6 to 26.5 GHz with 0.9 dB insertion loss, 13 dB directivity and coupling, and flat within ±1 dB. The VSWR is a maximum of 1.55 and the unit can handle 20 W into a 1.2 VSWR. Connectors are 2.92 mm and outline dimensions are 1.060" × 0.625" × 0.4".

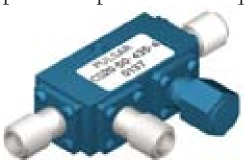

Pulsar Microwave Corp.,
Clifton, NJ (973) 779-6262,
www.pulsarmicrowave.com.

RS No. 230

Flange-mount Drop-in Isolator

The L-series of flange-mount drop-in isolators features up to 15 percent bandwidth in the 8 to 40 GHz frequency range. These products are ideal for military and space applications with a steel housing that is gold plated for better RF performance. This temperature stable device offers a typical loss of < 0.4 dB and VSWR and isolation > 20 dB. Size: 0.25" × 0.50" × 0.18".

Renaissance Electronics Corp.,
Harvard, MA
(978) 772-7774,
www.rec-usa.com.

RS No. 231

Phase Constant Attenuators

These PIN diode attenuators offer minimum phase variation with attenuation. The phase constant attenuators are available to cover the frequency range from 2 to 6 GHz and 6 to 18 GHz. The attenuators have an 8-bit digital control and offer an attenuation range in excess of 36 dB and a switching speed of less than 1.0 microsecond.

Rodelco Electronics,
Ronkonkoma, NY (631) 981-0900,
www.rodelcocorp.com.

RS No. 232

Miniature Coaxial Switch

The series CCR 33K miniature coaxial switch is designed to switch a microwave signal from a common input to either of two outputs and operates at frequencies from DC to 33.5 GHz. The latching single-pole, double-throw (SPDT) electromechanical switch offers an insertion loss repeatability of ±0.1 dB across the full bandwidth. On narrowband applications, the insertion loss repeatability can be as good as ±0.05 dB with ultra low passive intermodulation. The characteristic impedance is 50 Ω and switch life is characterized at 5 million cycles. The switches are small with connector spacing compatible with K connectors.

Teledyne Relays,
Hawthorne, CA
(323) 777-0077,
www.teledynerelays.com.

RS No. 233

Public Safety and SMR Filter

The model CFB6-815 filter features a passband of 806 to 824 MHz and is ideally suited for in-building bi-directional amplifier applications that require a compact mechanical package. Isolation is specified at 90 dB at F_c±36 MHz and the insertion loss is 1 dB. The design provides high "Q" and stable temperature performance and provides an excellent building block for compact diplexers and multiplexers. Size: 1.90" × 3.063" × 6.094".

Trilithic Inc.,
Indianapolis, IN
(317) 895-3600,
www.trilithic.com.

RS No. 234

3 dB Quadrature Combiner/Divider

The company's newly patented 3 dB quad coupler technology provides low insertion loss and exceptional amplitude balance. This bonded structure removes any air gaps within the circuit, insuring consistent unit-to-unit performance. The model QH7622 is a 500 to 3000 MHz, 40+ W CW unit with insertion loss of 0.5 dB maximum, VSWR of 1.30 maximum, isolation of 15 dB minimum, phase balance of 90° ±5° and amplitude balance of ±0.5 dB maximum. Size: 1.65" × 1.10" × 0.084".

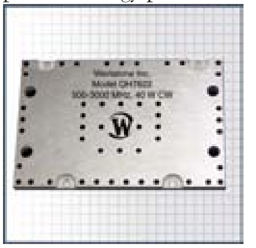

Werlatone Inc.,
Brewster, NY (845) 279-6187,
www.werlatone.com.

RS No. 235

AMPLIFIERS

Ultra-wideband Low Noise Amplifier

The APT4-00502000-2410-D4 is a SMA connectorized low noise amplifier (LNA) that operates in a frequency range from 0.5 to 20 GHz. This amplifier offers an ultra low noise figure of 2.4 dB maximum (2.1 typical), a minimum output power of +10 dBm (+20 dBm IP3), a minimum gain of 23 dB, with a gain flatness across the entire band of ±1.75 dB. Important for system integration is its VSWR, which is typically 2.0 for both the input and output. The amplifier comes with a three-year warranty and can be modified to cover down to 0.1 GHz with minor specification changes. Size: 1.4" × 0.7" × 0.29".

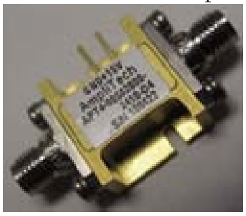

AmpliTech Inc.,
Hauppauge, NY (631) 435-0603,
www.amplitechinc.com.

RS No. 237

Solid-state Power Amplifier

The model BME27258-50 is a solid-state class AB linear amplifier that operates over the full frequency range from 20 to 2500 MHz in a single module. The typical P1dB is 40 W, with a saturated output power of 50 W. It has been designed for use in rugged military environments, and is capable of being produced at high rates of volume. The gain of this amplifier is 64 dB, ±4 dB. The input VSWR is 2:1 (maximum). The harmonic rejection is –15 dBc, and its spurious signal is –60 dBc. Size: 6.4" × 6.7" × 1.4". Weight: five pounds.

Comtech PST,
Melville, NY (631) 777-8900,
www.comtechpst.com.

RS No. 217

Connectorized Wideband Power Amplifiers

The model HMC-C037 is a GaAs PHEMT MMIC, 0.5 W wideband power amplifier that operates in a frequency range from 10 MHz to 15 GHz and features an integrated heat sink and EMI filtered DC terminals. The integrated heat sink allows for ease-of-use in a lab environment, since no heat sink has to be designed and specified. The HMC-C037 typically delivers flat 12 dB gain up to 12 GHz, making this device ideal for broadband instrumentation, lab and test equipment applications, as the need for band switching is eliminated. The HMC-C037 also provides up to +37 dBm output IP3 and up to +28 dBm of output power at 1 dB compression.

Hittite Microwave Corp.,
Chelmsford, MA (978) 250-3343,
www.hittite.com.

RS No. 238

Surface-mount Monolithic Amplifier

The Gali-74 (RoHS compliant) is a wideband amplifier that offers high dynamic range and operates from DC to 1 GHz. Lead finish is SnAgNi. This amplifier offers repeatable performance from lot to lot and is enclosed in a SOT-89 package. It uses patented Transient Protected Darlington configuration and is fabricated using InGaP HBT technology. Expected MTBF is 500 years at 85°C case temperature. Gali-74+ is designed to be rugged for ESD and supply switch-on transients. Price: $2.35 each (25).

Mini-Circuits,
Brooklyn, NY (718) 934-4500,
www.minicircuits.com.

RS No. 239

Successive Detection Log Video Amplifier

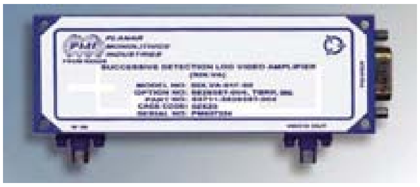

The model SDLVA-61F-80-582987-004 Option TBRK, MS is a matched set of successive detection log video amplifiers (SDLVA) in a compact stacked configuration. This unit operates over 61.25 MHz ±250 kHz and has been designed so that both modules share a common power terminal.

Planar Monolithics Industries,
Frederick, MD (301) 631-1579,
www.planarmonolithics.com.

RS No. 240

Ultra-linear Amplifier

The model SM2025-42LS is an ultra-linear GaAs FET amplifier designed for digital video broadcast applications. The unit operates from 2 to 2.5 GHz with a P1dB of +42 dBm and OIP3 of +61 dBm, allowing for +35 dBm (min.) of COFDM power output at < –40 dBc ACP. Small-signal gain is 52 dB with a flatness of ±0.5 dB across the band. Standard features include a single +12 VDC supply and thermal protection with auto reset. Size: 6" × 2.5" × 0.56".

Stealth Microwave Inc.,
Trenton, NJ (609) 538-8586,
www.stealthmicrowave.com.

RS No. 241

INTEGRATED CIRCUIT

GaAs Integrated Circuits

The first three members of this multi-function circuit (MFC) family of high performance GaAs ICs for point-to-point radio and satellite communications are the TG4402, TGC4403 and TGC4405. They address OEM needs for frequency upconversion in the transmit and local oscillator chains. The TGC4405 provides a high level of integration for designs that specify RF upconversion, a local oscillator frequency doubler and output RF signal amplification in a small, single product. The TGC4402 was created for designs that require upconversion without an integral LO doubler or output amplifier, while the TGC4403 is a millimeter-wave frequency doubler that includes an output buffer amplifier. Both the TGC4405 and TG4402 employ single-ended designs and therefore do not require external baluns.

TriQuint Semiconductor Inc.,
Hillsboro, OR (503) 615-8900,
www.triquint.com.

RS No. 222

SOURCES

Frequency Synthesizer

The WaveCor Dual frequency synthesizer is the latest addition to the WaveCor line of high performance DDS-based frequency synthesizers and features two independent microwave synthesizers in a single rack-mount enclosure. Each high performance synthesizer operates in a frequency range from 300 MHz to 18 GHz. At 9 GHz, the WaveCor Dual provides phase noise levels of –125 dBc/Hz at a 10 kHz offset and typical spurious levels of –65 dBc. Switching speeds are less than 300 ns maximum when tuning to any operating frequency. The WaveCor Dual's high reliability and performance are available in a 5U rack-mount chassis.

ITT Microwave Systems,
Lowell, MA (978) 441-0200,
www.ittmicrowave.com.

RS No. 244

High Performance VCOs

These ultra-wideband voltage-controlled oscillators (VCO) operate in a frequency range from 2 to 20 GHz. The VCOs feature an improved integrated voltage regulator, making them even more resistant to external power variations. By using the latest MMIC technology it has been possible to design a much smaller unit and also enhance uniform performance. The VCOs are available in two versions, drop-in (the VO3280 series) or in a SMA connector package (the VO4280 series). Other features include high power output directly from the oscillator, ultra broad bandwidth, with good phase noise density, high stability against load 'pulling' due to high isolation and a built-in low pass filter to reject harmonics. The range can be utilized in instruments and sensors and is suitable for all types of high performance microwave applications.

Sivers Ima,
Kista, Sweden +46 8 7036804,
www.siversima.com.

RS No. 245

Oven-controlled Crystal Oscillator

The C4550 oven-controlled crystal oscillator (OCXO) is a low cost, 25 by 25 mm package with a low profile packaged TO-8 crystal for better aging, g-sensitivity and temperature test performance. It has an available frequency range of 5 to 100 MHz and temperature stabilities down to 5 ppb from –40° to 85°C. The proven performance of the TO-8 crystal achieves typical aging rates of 30 ppb/year and g-sensitivities less than 1 ppb/g. Applications include the wireless infrastructure, military and test equipment sectors.

Vectron International,
Hudson, NH (603) 598-0070,
www.vectron.com.

RS No. 246

L-band Voltage-controlled Oscillator

The model V582ME20-LF is an L-band voltage-controlled oscillator (VCO) that operates in a frequency range from 1115 to 1285 MHz. This VCO is designed for applications that include base stations, portable radios and mobile communications. The V582ME20-LF offers a low phase noise performance of –107 dBc/Hz at 10 kHz offset away from carrier. It provides an average tuning sensitivity of 55 MHz/V and covers the entire band from 0.5 to 4.5 V. The typical harmonic suppression is –17 dBc. This product is lead free and RoHS compliant. Size: 0.50" × 0.50" × 0.22". Price: $18.95/VCO. Delivery: stock to four weeks.

Z-Communications Inc.,
San Diego, CA (858) 621-2700,
www.zcomm.com.

RS No. 247

SUBSYSTEM

44 GHz Multiplier

This 44 GHz frequency multiplier subsystem is designed for Milstar SATCOM uplink applications. The design is a frequency quadrupler (×4) that includes various buffer, driver and output power amplifier functionality into one integrated module. The multiplier module receives an X-band input signal and multiplies the frequency up to

fully cover the unclassified K-band Milstar uplink operating bandwidth. Typical performance specifications for the three output power options are: input F_{in} = X-band, 11 GHz center frequency, P_{in} = +14.25 to +18.25 dBm and input VSWR = 2.0.
Endwave Defense Systems,
Sunnyvale, CA (408) 522-3180,
www.endwave.com.
RS No. 219

TEST EQUIPMENT

USB Power Meters

The models 52012 and 52018 are the first two members of the new USB Power Meters series. Extending its product portfolio with the 52000 series family, the company is now providing reliable entry-level USB controlled CW power meters.

The new meters offer a frequency range from 10 MHz to 12.4/18.5 GHz and allow accurate power measurements between –50 dBm to +20 dBm. Its VSWR is better than 1:1.25 at 50 Ω impedance.
Boonton Electronics,
Parsippany, NJ (973) 386-9696,
www.boonton.com.
RS No. 248

Coaxial Noise Source

The model NW6G-26-CS is a coaxial noise source that sports a high 26 dB excess noise ratio (ENR). The NW6G-26-CS is ideal for noise figure measurements and built-in test applications. The unit features flatness better than ±1.75 dB, typically ±1 dB over the frequency range from 10 MHz to 6 GHz and comes with calibrated cardinal ENR frequencies. VSWR is excellent for a high output ENR source, at better than 1.35. Size: 0.75" × 0.5" × 1.25", excluding connectors.

NoiseWave Corp.,
East Hanover, NJ (973) 386-1119,
www.noisewave.com.
RS No. 250

Base Station Interface Tester

This base station interface tester can be used to emulate OBSAI RP3, RP3-01 and RP1 (timing) interfaces enabling the development and verification of individual RF or baseband modules without the presence of other base station parts. The tester supports simultaneous testing of up to four active RP3 or RP3-01 links at line rates 768, 1536 and 3072 Mbps defined by OBSAI. It can operate both in master and slave modes for RP1 synchronization and timing and interface analyzer features include BER measurements, analysis of RP1 timing and testing of synchronization capability. Received interface data can be captured according to user defined triggering rules and viewed as waveforms in a logic analyzer window with color-coding for erroneous data.
Elektrobit,
Oulu, Finland +358 40 344 2000,
www.elektrobit.com.
RS No. 249

Microwave Counters

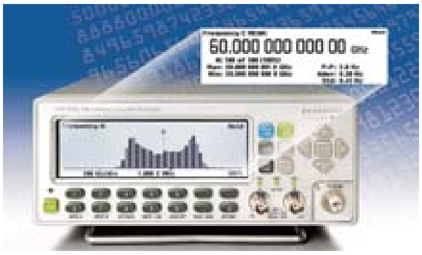

The CNT-90XL family of 27 to 60 GHz microwave counters offers high resolution and measurement speed, with the measurement speed for power and frequency up to 250,000 frequency samples/s. The graphical display shows frequency changes over time directly on-screen, for analysis of e.g. FM or AM, power or frequency switching, VCO settling and post-tuning drift. Built-in statistical processing presents numerical stability data and also frequency distribution histograms on-screen for analysis of frequency or power stability or modulation.
Pendulum Instruments AB,
Bromma, Sweden +46 8 598 51057,
www.pendulum-instruments.com.
RS No. 251

Baseband Analyzer

The FMU36 baseband analyzer is aimed at chipset development for mobile phones and base stations. With a frequency range up to 36 MHz it performs the measurement ahead of the RF signal and measures the I/Q signals in the baseband. For low frequency applications such as radio transmission via RFID or measurements on ADSL modems, the instrument features high sensitivity even at very low frequencies. The baseband analyzer combines all functions in one instrument and runs without an external PC, and for use in measurement systems it can be remote-controlled via GPIB or LAN.
Rohde & Schwarz GmbH & Co. KG,
Munich, Germany +49 89 4129-13779,
www.rohde-schwarz.com.
RS No. 253

2006 DSP THIRD QUARTER RESULTS

Although September DSP chip shipments were up a phenomenal 32.5% over the previous month (on a three-month rolling average basis), that was not enough to lift shipments for the third quarter beyond 2.2% (to the $2.2 B level). Of course, that is on a revenue basis. On a unit basis, quarterly shipments were up a more respectable 6.7%, but that means that ASPs were off by 4.3%, largely due to a severe (10%) drop in quarterly prices for DSPs in cellphones. Forward Concepts attributes most of that drop to a greater mix of low end cellphones for the third-world market, not a decrease in silicon area value. Computer and consumer segments had dramatic gains over Q2, while wireline (telecom) shipments were down almost 40%, as illustrated in the chart. In light of the lackluster Q3 growth and lower cellular forecasts for the fourth quarter by Nokia, Motorola and Texas Instruments, and problems at Infineon/BenQ, Forward Concepts believes that the touted projections (by others) of billion-unit cellphone shipments will not happen in 2006. Consequently, Forward Concepts is lowering its 2006 DSP chip revenue forecast from 15% to 10% (to the $8.4 B level).

DSP Shipments
Q3/2006: $2.2 B

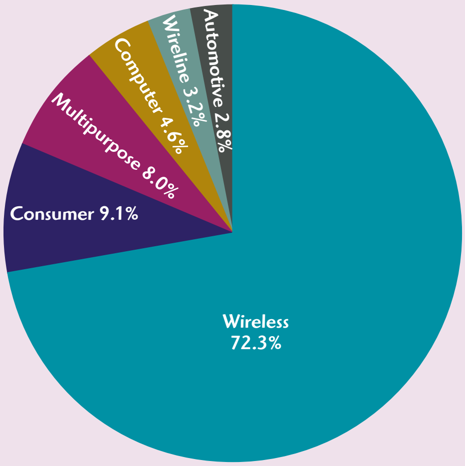

DSP Quarterly Shipment Change
Q3 2006/Q2 2006

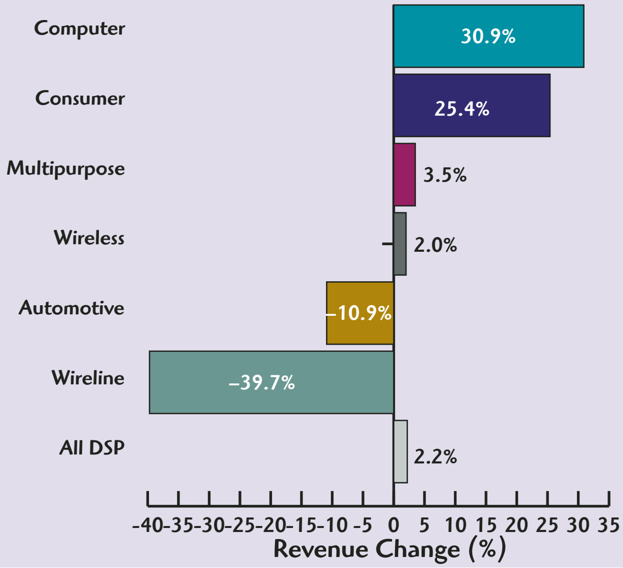

Source: Forward Concepts, 1575 W. University Dr., Suite 111, Tempe, AZ 85281-3283 (www.fwdconcepts.com)

Phased Array Antennas: Floquet Analysis, Synthesis, BFNs and Active Systems

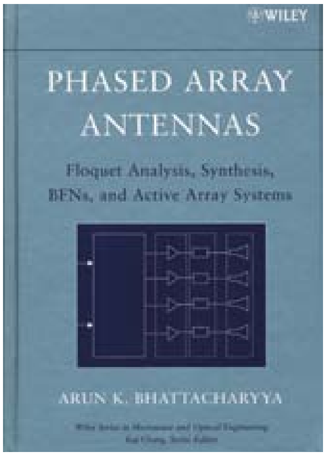

A.K. Bhattacharyya
Wiley Interscience • 514 pages; $125
ISBN: 0-471-72757-1

The purpose of this book is to present in a comprehensive manner the analysis and design of phased array antennas and systems. The book includes recent analytical developments in the phased array arena published in journals and conference proceedings. Efforts have been made to develop the concepts in a logical manner starting from fundamental principles. Detailed derivations of theorems and concepts are provided to make the book as self-contained as possible. Several design examples and design guidelines are included. It should be useful for antenna engineers and researchers, especially those involved in the detailed design of phased arrays. It can be used either as a text in an advanced graduate-level course or as a reference book for array professionals. The reader is assumed to have a basic knowledge of engineering mathematics and antenna engineering at a graduate level. The book contains 14 chapters that may be broadly divided into three sections. The first section, which includes Chapters 1 to 6, is mostly devoted to the development of the Floquet modal-based approach to phased array antennas, starting with an introductory chapter. The second section, which includes Chapters 7 to 10, presents applications of the approach to important array structures. The third section, which includes Chapters 11 to 14, is not directly related to the Floquet modal analysis as such; however, it covers several important aspects of phased array design. This section includes beam array synthesis, array beam forming networks, active phased array systems and statistical analysis of phased arrays, with respect to the amplitude and phase uncertainties of the amplifiers and phase shifters. Several practice problems are included at the end of each chapter to provide the reader with an interactive experience.

To order this book, contact:
John Wiley & Sons Inc.
One Wiley Drive
Somerset, NJ 08875
(800) 225-5945

Practical MMIC Design

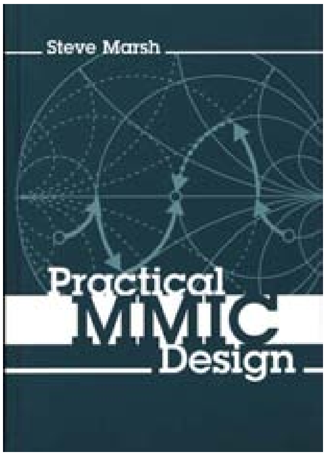

Steve Marsh
Artech House • 373 pages; $119, £72
ISBN: 1-59693-036-5

The aim of this book is to introduce the engineer to the basic technology of MMICs. Chapter 1 offers an introduction to MMICs and a history of their development. The first choice that must be made when designing a MMIC is the component technology that will be used and this choice will then lead to a decision as to which foundry process is required. This is the subject of Chapter 2. Because of the strong link between component technology and foundry suppliers, Chapter 3 describes the type of procedures the designer may go through when designing a MMIC with an external foundry. He must be able to take ideas for the circuit topology and accurately predict the performance of the circuit when implemented in MMIC form. Chapter 4 reviews the concept of S-parameter representation of components, discusses how a foundry typically goes about characterizing the individual components and describes the commonly used equivalent topologies for both active and passive components. Chapter 5 begins with the basic principles of impedance matching and shows how impedances may be plotted and transformed using the Smith chart and goes on to discuss the design of passive elements. Sections are then devoted to different functional types of chips that can be designed, including amplifiers, oscillators, mixers and digital circuits. Chapter 6 describes the format of layout data files and the type of CAD tools that create them. It continues by outlining the circuit array procedure and concludes with comments about mask manufacturing. Chapter 7 gives a brief overview of the typical processing steps involved in the fabrication of MMICs, while Chapter 8 is concerned with the test and measurements that are performed on whole wafers.

To order this book, contact:
Artech House
685 Canton St.
Norwood, MA 02062
(781) 769-9750 ext. 4030; or
46 Gillingham St.
London SW1V 1HH, UK
+44 (0) 207-8750

ADVERTISING INDEX

RS No.	Advertiser	Page No.	Phone	Fax	Web Address
1	Advanced Microwave, Inc.	138	408-739-4214		http://mwj.hotims.com/11712-1
2	Advanced Switch Technology	191	613-384-3939	613-384-5026	http://mwj.hotims.com/11712-2
4	Aeroflex/Inmet, Inc.	128	734-426-5553	734-426-5557	http://mwj.hotims.com/11712-4
5	Aeroflex/Weinschel, Inc.	107	800-638-2048	301-846-9116	http://mwj.hotims.com/11712-5
6,7,8,9, 10,11,12	Agilent Technologies, Inc.	75,81,83, 119, 131,145,171	800-829-4444	415-857-5518	http://mwj.hotims.com/11712-6
13	Allrizon-Tongguang Communications Equipment (Shanghai) Co., Ltd.	46	+86-21-5219-2719	+86-21-5218-6150	http://mwj.hotims.com/11712-13
14	American Technical Ceramics	125	631-622-4700	631-622-4748	http://mwj.hotims.com/11712-14
15	AML Communications Inc.	105	805-388-1345	805-484-2191	http://mwj.hotims.com/11712-15
16	Ansoft Corporation	143	412-261-3200	412-471-9427	http://mwj.hotims.com/11712-16
17	Applied Computational Sciences	158			http://mwj.hotims.com/11712-17
18	Applied Wave Research, Inc.	11	310-726-3000		http://mwj.hotims.com/11712-18
19,20	AR Worldwide	54,91	215-723-8181	215-723-5688	http://mwj.hotims.com/11712-19
21	Arlon-Materials for Electronics Division	127	800-635-9333	302-834-2574	http://mwj.hotims.com/11712-21
22	Bantam Instruments	188	866-371-6009		http://mwj.hotims.com/11712-22
23	CAP Wireless Inc.	124	805-499-1818		http://mwj.hotims.com/11712-23
24	Cernex, Inc.	187	408-541-9226	408-541-9229	http://mwj.hotims.com/11712-24
25	Channel Microwave Corporation	20	805-482-7280	805-987-8794	http://mwj.hotims.com/11712-25
26	Ciao Wireless, Inc.	36	805-389-3224	805-389-3629	http://mwj.hotims.com/11712-26
27	Cobham Defense Electronic Systems	22-23	603-775-5200	603-775-5201	http://mwj.hotims.com/11712-27
28	Coilcraft	14	800-322-2645	847-639-1469	http://mwj.hotims.com/11712-28
29	Comtech PST Corp.	39	631-777-8900	631-777-8877	http://mwj.hotims.com/11712-29
30	CPI Beverly Microwave Division	26	978-922-6000	978-922-2736	http://mwj.hotims.com/11712-30
31	Crane Aerospace & Electronics	52	480-961-6269		http://mwj.hotims.com/11712-31
32	CST of America, Inc.	29	781-416-2782	781-576-5702	http://mwj.hotims.com/11712-32
33	CTIA Wireless 2007	193	202-736-3664	202-785-0721	http://mwj.hotims.com/11712-33
34	CTT Inc.	79	408-541-0596	408-541-0794	http://mwj.hotims.com/11712-34
35	Daico Industries, Inc.	17	310-507-3242	310-507-5701	http://mwj.hotims.com/11712-35
36	dBm, LLC	179	973-709-0020	973-709-1346	http://mwj.hotims.com/11712-36
37	Dow-Key Microwave Corporation	6	805-650-0260	805-650-1734	http://mwj.hotims.com/11712-37
38	Eastern Wireless TeleComm, Inc.	102	410-749-3800	410-749-4852	http://mwj.hotims.com/11712-38
39	Elisra Electronic Systems Ltd. (Microwave Division)	71	972(3)6175655	972(3)6175299	http://mwj.hotims.com/11712-39
40	EM Research, Inc.	135	775-345-2411	775-345-1030	http://mwj.hotims.com/11712-40
41	EMC Technology Inc.	19	772-286-9300	772-283-5286	http://mwj.hotims.com/11712-41
42	Emerson Network Power	56	800-247-8256		http://mwj.hotims.com/11712-42
43	Emhiser Micro-Tech	98	775-345-0461	775-345-1152	http://mwj.hotims.com/11712-43
44	Endwave Defense Systems	27	408-522-3180	408-522-3181	http://mwj.hotims.com/11712-44
45	ES Microwave, LLC	191	301-519-9407	301-519-9418	http://mwj.hotims.com/11712-45
46	ET Industries	62	973-394-1719	973-394-1710	http://mwj.hotims.com/11712-46
47	ETS-Lindgren	101	512-531-6400		http://mwj.hotims.com/11712-47
48	Eudyna Devices Inc.	121	+81-45-853-8151	+81-45-853-8170	http://mwj.hotims.com/11712-48
49	EuMW 2007	177	+ 44 20 7596 8742	+ 44 20 7596 8749	http://mwj.hotims.com/11712-49
51	Feko	116	+27 21 880 1880		http://mwj.hotims.com/11712-50
52	Filtronic Compound Semiconductors, Ltd.	167	408-850-5740	831-621-8074	http://mwj.hotims.com/11712-51
41	Florida RF Labs Inc.	19	800-544-5594		http://mwj.hotims.com/11712-41
53	G.T. Microwave Inc.	28	973-361-5700	973-361-5722	http://mwj.hotims.com/11712-53
54	Herley New England	38	781-729-9450	781-729-9547	http://mwj.hotims.com/11712-54
55	Herotek, Inc.	126	408-941-8399	408-941-8388	http://mwj.hotims.com/11712-55
56,57, 58,59	Hittite Microwave Corporation	59,60-61, 63,64-65	978-250-3343	978-250-3373	http://mwj.hotims.com/11712-56
60	Huber + Suhner AG	104	+41 (0)71 353 41 11	+41 (0)71 353 45 90	http://mwj.hotims.com/11712-60
	IEEE MTT-S International Microwave Symposium - Hawaii	80,197	781-769-9750	781-769-5037	www.ims2007.org
61	Integra Technologies, Inc.	94	310-606-0855	310-606-0865	http://mwj.hotims.com/11712-61
62	Integrated Engineering Software	58	204-632-5636		http://mwj.hotims.com/11712-62
63	Interad Ltd.	62	757-787-7610	757-787-7740	http://mwj.hotims.com/11712-63
64,65,66	J microTechnology	191	503-614-9509	503-531-9325	http://mwj.hotims.com/11712-64
67	K&L Microwave, Inc.	7	410-749-2424	443-260-2268	http://mwj.hotims.com/11712-67

Advertising Index

RS No.	Advertiser	Page No.	Phone	Fax	Web Address
68	KOR Electronics	133	714-898-8200	714-895-7526	http://mwj.hotims.com/11712-68
69	KR Electronics, Inc.	191	732-636-1900	732-636-1982	http://mwj.hotims.com/11712-69
70	Logus Microwave Corporation	123	561-842-3550	561-842-2196	http://mwj.hotims.com/11712-70
71	Lorch Microwave	55	800-780-2169	410-860-1949	http://mwj.hotims.com/11712-71
72	M2 Global Technology, Ltd.	142	210-561-4800	210-561-4852	http://mwj.hotims.com/11712-72
3	Maury Microwave Corporation	9	909-987-4715	909-987-1112	http://mwj.hotims.com/11712-3
73	MECA Electronics, Inc.	139	973-625-0661	973-625-9277	http://mwj.hotims.com/11712-73
74	MFG Ratech	96	775-827-2222		http://mwj.hotims.com/11712-74
75	Micon Precise Corp.	176	886-2-2917-7528	886-2-2912-1659	http://mwj.hotims.com/11712-75
76	Microsemi	92	408-986-8031	408-986-8120	http://mwj.hotims.com/11712-76
77	Microwave Development Laboratories	111	781-292-6680/6684	781-453-8629	http://mwj.hotims.com/11712-77
	Microwave Journal	191	800-225-9977	781-769-5037	www.mwjournal.com
78	Mimix Broadband, Inc.	93	281-988-4600	281-988-4615	http://mwj.hotims.com/11712-78
79,80,81,82, 83,84,85,86,87, 88,89,90,91,92	Mini-Circuits	4-5,18,33,43,44, 57,77,97,108-109, 129,155,169,185,195	718-934-4500	718-332-4661	http://mwj.hotims.com/11712-79
93	Mini-Systems, Inc.	150	508-695-0203	508-695-6076	http://mwj.hotims.com/11712-93
94,95	MITEQ Inc.	3,84-85	631-436-7400	631-436-7430	http://mwj.hotims.com/11712-94
	Modelithics, Inc.	189			www.modelithics.com
96	Modular Components National, Inc.	73	410-879-6553	410-638-7356	http://mwj.hotims.com/11712-96
97	Molex RF/Microwave Connector Division	157	317-834-5600	317-834-5611	http://mwj.hotims.com/11712-97
98	Narda Microwave-East, an L3 Communications Co.	99	631-231-1700	631-231-1711	http://mwj.hotims.com/11712-98
99	Narda Microwave-West, an L3 Communications Co.	40	916-351-4500	916-351-4550	http://mwj.hotims.com/11712-99
100	Networks International Corporation	120	913-685-3400	913-685-3732	http://mwj.hotims.com/11712-100
101	Nexyn Corporation	15	408-982-9339	408-982-9275	http://mwj.hotims.com/11712-101
102	Noisecom	COV 2	973-386-9696	973-386-9191	http://mwj.hotims.com/11712-102
103	NoiseWave Corp.	8	973-386-1119	973-386-1131	http://mwj.hotims.com/11712-103
104,105	OML Inc.	141,161	408-779-2698	408-778-0491	http://mwj.hotims.com/11712-104
106	Piconics	114	978-649-7501	978-649-9643	http://mwj.hotims.com/11712-106
107	Picosecond Pulse Labs Inc.	117	303-209-8100	303-447-2236	http://mwj.hotims.com/11712-107
108	Planar Electronics Technology, Inc.	48-49	301-662-5019	301-662-1731	http://mwj.hotims.com/11712-108
109	Prewell Corporation	140	82-31-420-8362	82-31-420-8369	http://mwj.hotims.com/11712-109
110	Programmed Test Sources, Inc.	COV 3	978-486-3400	978-486-4495	http://mwj.hotims.com/11712-110
111	Pulsar Microwave Corporation	42	800-752-3043	973-779-2727	http://mwj.hotims.com/11712-111
112	QuinStar Technology, Inc.	147	310-320-1111	310-320-9968	http://mwj.hotims.com/11712-112
113	Radio Research Instrument Co., Inc.	190	203-753-5840	203-754-2567	http://mwj.hotims.com/11712-113
	Radio Waves, Inc.	189			www.radiowavesinc.com
114	Reactel, Incorporated	175	301-519-3660	301-519-2447	http://mwj.hotims.com/11712-114
115	Remcom	149	814-861-1299	814-353-1420	http://mwj.hotims.com/11712-115
116	REMEC Defense & Space	32	858-560-1301		http://mwj.hotims.com/11712-116
117	RF & Hyper Europe 2007	183	33 (0)1 49 68 51 00	33 (0)1 49 68 54 18	http://mwj.hotims.com/11712-117
118	RF Micro Devices	95	336-678-5570	336-931-7454	http://mwj.hotims.com/11712-118
119,120,121	RFHIC	74,76,78	82-31-250-5011	82-31-250-5088	http://mwj.hotims.com/11712-119
122	RLC Electronics, Inc.	25	914-241-1334	914-241-1753	http://mwj.hotims.com/11712-122
123	Rodelco Electronics Corp.	31	631-981-0900	631-981-1792	http://mwj.hotims.com/11712-123
124	Rogers Corporation	103	480-961-1382	480-961-4533	http://mwj.hotims.com/11712-124
125	Rohde & Schwarz GmbH	53	+49-1805-124242	+49-89-412913777	http://mwj.hotims.com/11712-125
126	Rosenberger	89	+49-8684-18-0	+49-8684-18-499	http://mwj.hotims.com/11712-126
127	Roswin Inc.	130	+82-41-621-4450	+82-41-621-4451	http://mwj.hotims.com/11712-127
128	Sector Microwave Industries, Inc.	191	631-242-2300	631-242-8158	http://mwj.hotims.com/11712-128
129	Sivers IMA AB	100	46 (0) 8 703 68 04	46-8-7519271	http://mwj.hotims.com/11712-129
130	Sirenza Microdevices	21	303-327-3030		http://mwj.hotims.com/11712-130
131	Skyworks Solutions, Inc.	47	781-376-3000		http://mwj.hotims.com/11712-131
132	Sonnet Software, Inc.	153	315-453-3096	315-451-1694	http://mwj.hotims.com/11712-132
133	Spectrum Elektrotechnik GmbH	173	+49-89-3548-040	+49-89-3548-0490	http://mwj.hotims.com/11712-133
134	Spinner GmbH	151	+49 89 12601-257	+49 89 12601-287	http://mwj.hotims.com/11712-134
135	Storm Products Company	115	630-754-3300	630-754-3500	http://mwj.hotims.com/11712-135
136	Symmetricom	90	978-232-1497		http://mwj.hotims.com/11712-136

Advertising Index

RS No.	Advertiser	Page No.	Phone	Fax	Web Address
137,138,139	Synergy Microwave Corporation	51,113,159	973-881-8800	973-881-8361	http://mwj.hotims.com/11712-137
140	Tecom Industries, Inc.	106	866-840-8550		http://mwj.hotims.com/11712-140
141	Tektronix, Inc.	87			http://mwj.hotims.com/11712-141
142	Teledyne Microwave	67	650-962-6944	650-962-6845	http://mwj.hotims.com/11712-142
143	Tensolite	13	800-458-9960	904-829-3447	http://mwj.hotims.com/11712-143
144	Tiger Micro-Electronics Institute	170	+86-28-66070208	+86-28-66070496	http://mwj.hotims.com/11712-144
145	TriQuint Semiconductor, Inc.	34-35	503-615-9000	503-615-8900	http://mwj.hotims.com/11712-145
146	Unique Broadband Systems Ltd.	152	877-669-8533		http://mwj.hotims.com/11712-146
147	Universal Microwave Components Corporation	190	703-642-6332	703-642-2568	http://mwj.hotims.com/11712-147
148	UTE Microwave Inc.	69	732-922-1009	732-922-1848	http://mwj.hotims.com/11712-148
149	ValueTronics International, Inc.	191	847-468-8258		http://mwj.hotims.com/11712-149
150	Waveline Inc.	148	973-226-9100	973-226-1565	http://mwj.hotims.com/11712-150
151	Weinschel Associates	132	877-948-8342	301-963-8640	http://mwj.hotims.com/11712-151
152	Werlatone, Inc.	COV 4	845-279-6187	845-279-7404	http://mwj.hotims.com/11712-152
153	Winchester Electronics Corporation	30	203-741-5400	203-741-5500	http://mwj.hotims.com/11712-153
154	Zeland Software, Inc.	137	510-623-7162	510-623-7135	http://mwj.hotims.com/11712-154

Visit Microwave Journal *on the Web at* **www.mwjournal.com**

Visit mwjournal.com/info and enter RS# to request information from our advertisers

Sales Representatives

microwave journal

Carl Sheffres, Publisher **Ed Johnson, Associate Publisher** **Ken Hernandez, Traffic Administrator**

Eastern and Central Time Zones
Chuck Curley
Eastern Reg. Sales Mgr.
685 Canton Street
Norwood, MA 02062
Tel: (781) 769-9750
FAX: (781) 769-5037
ccurley@mwjournal.com

Michael Hallman
Eastern Reg. Sales Mgr.
4 Valley View Court
Middletown, MD 21769
Tel: (301) 371-8830
FAX: (301) 371-8832
mhallman@mwjournal.com

Eastern and Central Time Zones
Ed Johnson
Associate Publisher
PO Box 5962
Ocala, FL 34478-5962
Tel: (352) 620-2442
FAX: (352) 620-2443
ejohnson@mwjournal.com

Pacific and Mountain Time Zones
Wynn Cook
Western Reg. Sales Mgr.
PO Box 23200
San Jose, CA 95153
Tel: (408) 224-9060
FAX: (408) 224-6106
wcook@mwjournal.com

International Sales
Richard Vaughan
International Sales Manager
Tel: +44 207 596 8742
rvaughan@horizonhouse.co.uk

Michel Zoghob
Deputy Publisher
Tel: +44 207 596 8741
mzoghob@horizonhouse.co.uk

46 Gillingham Street
London SW1V 1HH, England
Tel: +44 207 596 8740
FAX: +44 207 596 8749

Germany, Austria, and Switzerland (German-speaking)
Juergen Wissling
Wissling Marketing Services
Riedstrasse 5
72813 St. Johann-Wuertingen
Germany
Tel: +49 7122 828140
FAX: +49 7122 828145
jwissling@horizonhouse.com

Israel
Oreet Ben Yaacov
Oreet International Media
15 Kineret Street
51201 Bene-Berak, Israel
Tel: +972 3 570 6527
FAX: +972 3 570 6526
obenyaacov@horizonhouse.com

Korea
Young-Seoh Chinn
JES Media International
2nd Floor, ANA Bldg.
257-1, Myungil-Dong
Kangdong-Gu
Seoul, 134-070 Korea
Tel: +82 2 481-3411
FAX: +82 2 481-3414
yschinn@horizonhouse.com

Japan
Katsuhiro Ishii
Ace Media Service Inc.
12-6, 4-Chome,
Nishiiko, Adachi-Ku
Tokyo 121-0824, Japan
Tel: +81 3 5691 3335
FAX: +81 3 5691 3336
amskatsu@dream.com